University of Windsor

Scholarship at UWindsor

Electronic Theses and Dissertations

Theses, Dissertations, and Major Papers

2008

Identification and functional characterization of modulators of pro-apoptotic proteins Caspase 3 and Bax

Katrina McGonigal
University of Windsor

Follow this and additional works at: https://scholar.uwindsor.ca/etd

Recommended Citation

McGonigal, Katrina, "Identification and functional characterization of modulators of pro-apoptotic proteins Caspase 3 and Bax" (2008). *Electronic Theses and Dissertations*. 8078.
https://scholar.uwindsor.ca/etd/8078

NOTE TO USERS

Identification and Functional Characterization of Modulators of Pro-apoptotic Proteins
Caspase 3 and Bax

By: Katrina McGonigal

A thesis submitted to the Faculty of Graduate Studies through the Department of

Chemistry and Biochemistry in Partial Fulfillment of the Requirements for the Degree of

Master of Science at the University of Windsor

Windsor, Ontario, Canada

2008

Canada

I. Co-Authorship Declaration

I hereby declare that this thesis incorporates material that is result of joint research, as follows:

This thesis incorporates results of a joint research undertaken in collaboration with Deyzi Gueorguieva-Owens, Olena Kis, and Subitha Rajakumaran under the supervision of Dr. Siyaram Pandey. The results of this collaboration are covered in Chapter 4 of the thesis and include the competitive binding studies, Bax-induced ROS generation experiments, and previous work performed on anti-Bax sdAb5.2. Additionally, our work had collaborative aspects with the NRC in Ottawa under the supervision of Dr. Jamshid Tanha. The results of this collaboration are overviewed in Chapter 4 of the thesis and include isolation of the single domain antibodies, single domain antibody vectors, and labelling of anti-Bax single domain antibody 5.2. In each case, the main ideas, experimental designs, contributions, and analysis were performed by myself. The contribution of the co-authors was mainly through assistance with experiments and provision of both supplies the training to carry out said experiments.

I am aware of the University of Windsor Senate Policy on Authorship and I certify that I have properly acknowledged the contribution of other researchers to my thesis, and have obtained written permission from each of the co-author(s) to include the above material(s) in my thesis.

I certify that, with the above qualification, this thesis, and the research to which it refers, is the product of my own work.

II. Declaration of Previous Publication

This thesis includes 1 original paper that has been previously published in Applied Biochemistry and Biotechnology, as follows:

Thesis Chapter	Publication title/full citation	Publication status*
Chapters 3, 4 and, 5	Isolation and Functional Characterization of Single Domain Antibody Modulators of Caspase-3 and Apoptosis. Katrina McGonigal, Jamshid Tanha, Elitza Palazov, Shenghua Li, Deyzi Gueorguieva-Owens, Siyaram Pandey. Appl Biochem Biotechnol. 2008 Jun 14; : 18553063	Published

I certify that I have obtained a written permission from the copyright owner(s) to include the above published material(s) in my thesis. I certify that the above material describes work completed during my registration as graduate student at the University of Windsor.

I declare that, to the best of my knowledge, my thesis does not infringe upon anyone's copyright nor violate any proprietary rights and that any ideas, techniques, quotations, or any other material from the work of other people included in my thesis, published or otherwise, are fully acknowledged in accordance with the standard referencing practices. Furthermore, to the extent that I have included copyrighted material that surpasses the bounds of fair dealing within the meaning of the Canada Copyright Act, I certify that I have obtained a written permission from the copyright owner(s) to include such material(s) in my thesis.

I declare that this is a true copy of my thesis, including any final revisions, as approved by my thesis committee and the Graduate Studies office, and that this thesis has not been submitted for a higher degree to any other University of Institution.

Abstract

Oxidative-stress-induced neuronal apoptosis has been implicated in the development of neurodegenerative diseases such as ischemic stroke. Pro-apoptotic proteins including Caspase 3 and Bax are critical components of the apoptotic pathway. In this study we aimed to identify specific inhibitors of Caspase 3 and Bax. We isolated two single domain antibodies (sdAbs) against Caspase 3; one (VhhCasp31) capable of blocking Caspase 3 function *in vitro* and *in vivo,* and the other (VhhCasp32) acting oppositely. The genes and antibodies coded by them can be used as a platform for therapeutic development for neuroprotective or anti-cancer agents .

We also screened a pharmacaphore library of small molecular weight compounds capable of binding to Bax and blocking function in the same manner as a specific anti-Bax sdAb inhibitor previously found by our group. We found "compound 22," which was capable of competitive binding to Bax and blocked Bax function *in vitro* and *in vivo.*

Dedication

      I would like to dedicate this thesis to my parents and sister who have always been there to support me and encourage me to achieve my goals.

Acknowledgements

To begin with I would like to thank Dr. Pandey for his guidance, support, and enthusiasm in research over the last 3 years.

Additionally I would like to thank my fellow labmates past and present for their advice, friendship and animated discussions: Mallika Somayajulu-Niṭu, Carly Griffin, Danijela Domazet, Peter Siedlakowski, and Deyzi Gueorguieva-Owens. I would like to thank all the undergrads who have helped me with my project and wish you all the best in your future career paths: Olena Kis, Subitha Rajakumaran, Branden Gange, and Dennis Ma.

I would also like to extend a thank you to our collaborators in Ottawa, Dr. Jamshid Tanha, Shenghua Li, and colleagues for supplying the sdAbs, vectors, and labelled sdAb, as well as for their valued suggestions for the binding studies.

I would also like to express my gratitude to the Department of Biochemistry professors including Dr. Lee, Dr. Mutus, Dr. Ananvoranich, and Dr. Vacratsis for the generous sharing of lab equipment and guidance. In addition, I would like to especially thank Dr. Vacratsis for taking the time to be on my committee and Dr. Crawford for the use of his microscope and taking the time to be on my committee.

Lastly, I would like to acknowledge the Heart and Stroke Foundation of Ontario for the funding to support this project, as well as the University of Windsor for the graduate Tuition Scholarship.

Table of Contents

xi

Part 1

Part 2

List of Figures

List of Abbreviations

AIF   apoptosis inducing factor

ADP   adenosine diphosphate

ANT   adenine nucleotide translocase

AP-1   activator protein 1

APAF-1   Apoptosis-protease-activating factor 1

ATP   adenosine triphosphate

BDNF   brain-derived neurotrophic factor

BH(1-4)   Bcl-2 homology domains 1-4

BSA   bovine serum albumin

CAD	Caspase-activated dexyribonuclease
CARD	caspase recruitment domain
CDR	complementary determining region
CHAPS	3-[3-(Cholamidopropyl)dimethylammonio]-1-proanesulfonate
Cyp D	cyclophilin D
Cyt c	Cytochrome c
DISC	death inducing signaling complex
DMEM	Dulbecco's Modified Eagle's Medium
DMSO	dimethyl sulfoxide
DTT	Dithiothreitol
EDTA	ethylenediamine-tetraacetic acid
EGTA	Ethylene glycol-bis(2-aminoethylether)-N,N,N',N'-tetraacetic acid
EndoG	Endonuclease G
ER	Endoplasmic Reticulum
ERbB-2	erythroblastic leukemia viral oncogene homolog 2 (HER2 epidermal growth factor receptor)
FADD	Fas associated death domain
FasL	Fas Ligand
FBS	fetal bovine serum
Fv	variable region fragment (of an antibody)
Fc	constant region fragment (of an antibody)
GFP	green fluorescent protein
HEPES	N-(2-Hydroxyethyl)piperazine-N'-(2-ethanesulfonic acid)
His	histadine
HRP	horseradish peroxidase
ICAD	Inhibitor of caspase-activated deoxyribnuclease
IgG	immunoglobin

IMS	intermembrane space (referring to mitochondria)
IPTG	Isopropyl β-D-1-thiogalactopyranoside
MAPK	mitogen-activated protein kinase
MDA	malonaldehyde
MHC	major histocompatibilitycomplex
MIM	mitochondrial inner membrane
MOM	mitochondrial outer membrane
MOMP	mitochondrial outer membrane permealization
mtDNA	mitochondrial DNA
NF-κB	nuclear factor-kappa B
NMR	nuclear magnetic resonance
NOE	nuclear overhauser effect
NT-2	N Tera-2 (neuronally-committed teratocarcinoma cells)
OD	ocular density
PCR	polymerase chain reaction
PHPA	parahydroxy-phenylacetate
PMSF	phenylmethanesulphonylfluoride
PP2A	protein phosphatase 2A
PTP	permeability transition pore
Rev	Regulator of virion
RFP	red fluorescent protein
RNAi	RNA interference
ROS	reactive oxygen species
rTPA	recombinant tissue plasminogen activator
scFv	single chain variable fragment
sdAb	single domain antibody
SDS-PAGE	sodium diodecyl sulphate- polyacrilamide gel electrophoresis

Ser	serine
SHSY-5Y	human neuroblastoma cell line
siRNA	small interfering RNA
SOD	superoxide dismutase
Tat	trans-activator of transcription
TBST	Tris-Buffered Saline Tween-20
TNFR	tumor necrosis factor receptor
VDAC	voltage-dependent anion channel
V_H	heavy chain variable region (of antibody)
V_HH	variable chain of a heavy chain only antibody
V_HHs	variable chain of a heavy chain only antibodies
Vif	Viral infectivity factor
V_L	light chain variable region (of antibody)
$\Delta\Psi_m$	inner mitochondrial membrane potential

Chapter 1:   Introduction

1.1   Apoptosis

Apoptosis, or programmed cell death, is a tightly regulated process of cell removal and plays a fundamental role in the maintenance of tissue homeostasis in the adult organism and the developing fetus (Fadeel *et al.*, 2005). It is a necessary process that is crucial for not only the normal development of an organism, but in the removal of harmful or damaged cells. Apoptosis is an active, physiological process that is characterized by specific morphological and biochemical changes that distinguish it from necrotic or accidental cell death (Adhihetty *et al.*, 2003). Most of the recognizable events definitive of apoptosis were documented in the 1950's. Its role in embryonic development was understood then, but the importance of apoptosis in the daily maintenance of the adult organism was not recognized until the 1970's. Kerr *et al.* (1972) reported that the same type of cell death present during development also happens in mature organisms and continues throughout life. Additionally, they suggested that unlike necrotic cell death, where the cell is a passive victim, this form of cell death is active, meaning the cell expends energy toward its own destruction. They further proposed that inappropriate initiation or inhibition of apoptosis could contribute to many diseases such as neurodegeneration, and cancer (Kerr *et al.*, 1972).

1.2   Apoptosis vs. Necrosis

Apoptosis occurs in response to conditions such as DNA damage, oxidative stress, deprivation of growth factors and stimulation of specific death receptors, and is characterized by cell shrinkage, membrane blebbing, and chromatin condensation (Pollack *et al.*, 2001). Necrotic

cell death, on the other hand, is a passive, pathological form of cell death and occurs when a cell is severely injured, for example by oxygen deprivation or a physical stressor. It takes on morphological changes quite different from apoptotic cell death, including swelling of the cell, rupturing of the cell, leading to tissue inflammation and ultimately cell death (Pollack *et al*, 2001).

1.3 Apoptotic Pathways

Apoptosis can be induced by two different signalling pathways: an external route, where external factors bind to membrane bound death receptors on the outside of the cell, and an internal route, where internal cellular occurrences lead to the release of specific death inducing factors from the mitochondria or the endoplasmic reticulum (ER) (Adhihetty *et al.*, 2003). All apoptosis signalling pathways converge on a common pathway of cell destruction that involves activated caspases (Strasser *et al.*, 2000). In most cell types, the morphological characteristics of apoptosis remain consistent, whether the extrinsic or intrinsic pathway is followed.

1.3.1 Extrinsic: Receptor-mediated Apoptotic Pathway

Apoptosis can be induced by the binding of ligands to either one or more of the extracellular receptors belonging to the tumour necrosis factor (TNFR) superfamily. Important ligands involved in this cell death pathway are the cytokine TNF-α and the Fas ligand (FasL). Activation of the appropriate receptors by these ligands ultimately leads to the activation of a family of proteases collectively referred to as caspases (Adhihetty *et al.*, 2003). For example, binding of FasL to its receptor evokes oligomerization of Fas receptor and procaspase 8 recruitment to the Fas-Associated Death Domain (FADD) (Hsu *et al.*, 1996). This binding

recruits additional procaspase 8 molecules leading to formation of the Death-inducing Signalling Complex (DISC) which cleaves and activates Caspase 8 (Varadhachary *et al.*, 2001). Upon activation, Caspase 8 can mediate the cleavage of Caspase 3, which when active, DNA fragmentation occurs and ultimately causes apoptosis.

1.3.2 Intrinsic: Mitochondrial-mediated Apoptotic Pathway

Mitochondria are involved in many processes that are imperative for cell survival including: energy production, calcium homeostasis, redox control, and certain metabolic and biosynthetic pathways (Bouchier-Hayes, *et al.*, 2005). In addition, mitochondria frequently play an essential role in physiological cell death. Mitochondria are linked to several pathological conditions such as cancer, obesity, diabetes, ischemia/reperfusion injury, and neurodegenerative disorders such as Parkinson's Disease and Alzheimer's Disease (Kroemer *et al.*, 2007).

Most cell death in vertebrates proceeds via the mitochondrial intrinsic pathway of apoptosis (Green *et al.*, 2004). The key event in the mitochondrial pathway of apoptosis is mitochondrial outer membrane permealization (MOMP) and the subsequent leakage of proapoptotic proteins from the mitochondrial intermembrane space (IMS) into the cytosol. This leads to cytosolic caspase activation, loss of inner mitochondrial membrane potential ($\Delta\Psi_m$), cellular ATP depletion, and free radical production (Newmeyer *et al.*, 2003). There are two principal hypotheses as to the mechanism of MOMP, one of which is that MOMP is regulated by the Bcl-2 family of proteins; the other: MOMP is regulated by the permeability transition pore (PTP) (Bouchier-Hayes *et al.*, 2005). The first model focuses on MOMP as a process that involves only the outer membrane of the mitochondria and requires members of the Bcl-2 family of proteins to either promote or prevent the formation of pores. In a study

3

Extrinsic
Stimuli

FasL

Ligation

Fas Receptor

FADD

DISC

Procaspase 8

Active Caspase 8

Procaspase 3

Apoptosis

Active Caspase 3
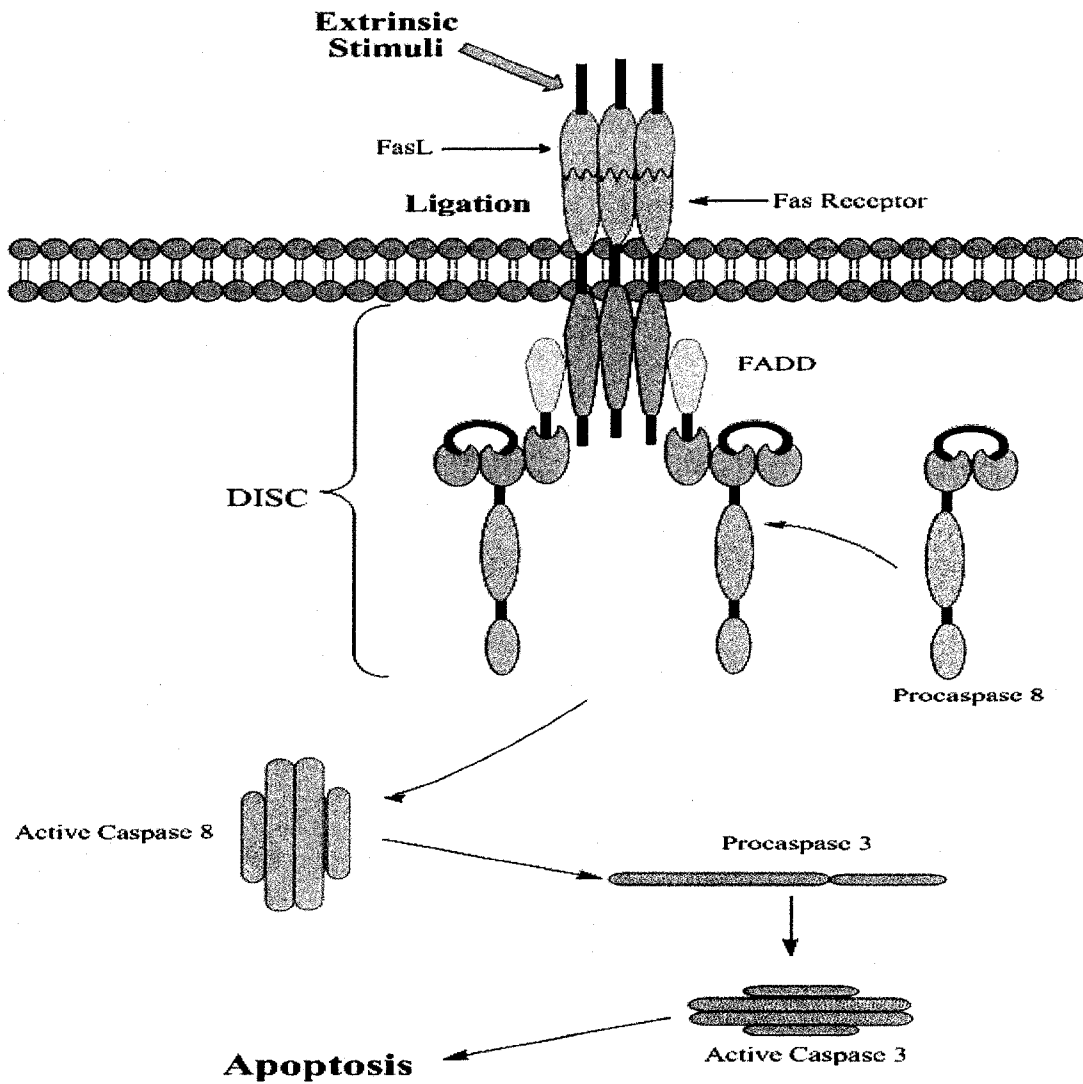
Figure 1.1 Extrinsic, Receptor-mediated Apoptotic Pathway

Overview of the receptor-mediated apoptotic pathway: Ligands (such as FasL) bind to extracellular receptors of the TNFR superfamily (TRAIL, CD95L). Binding of FasL induces oligomerization of Fas receptor and procaspase 8 recruitment to FADD. This binding recruits additional procaspase 8 molecules leading to the formation of the DISC with cleaves and activates Caspase 8. Upon activation, Caspase 8 can mediate the cleavage of Caspase 3, which when active, ultimately causes apoptosis.
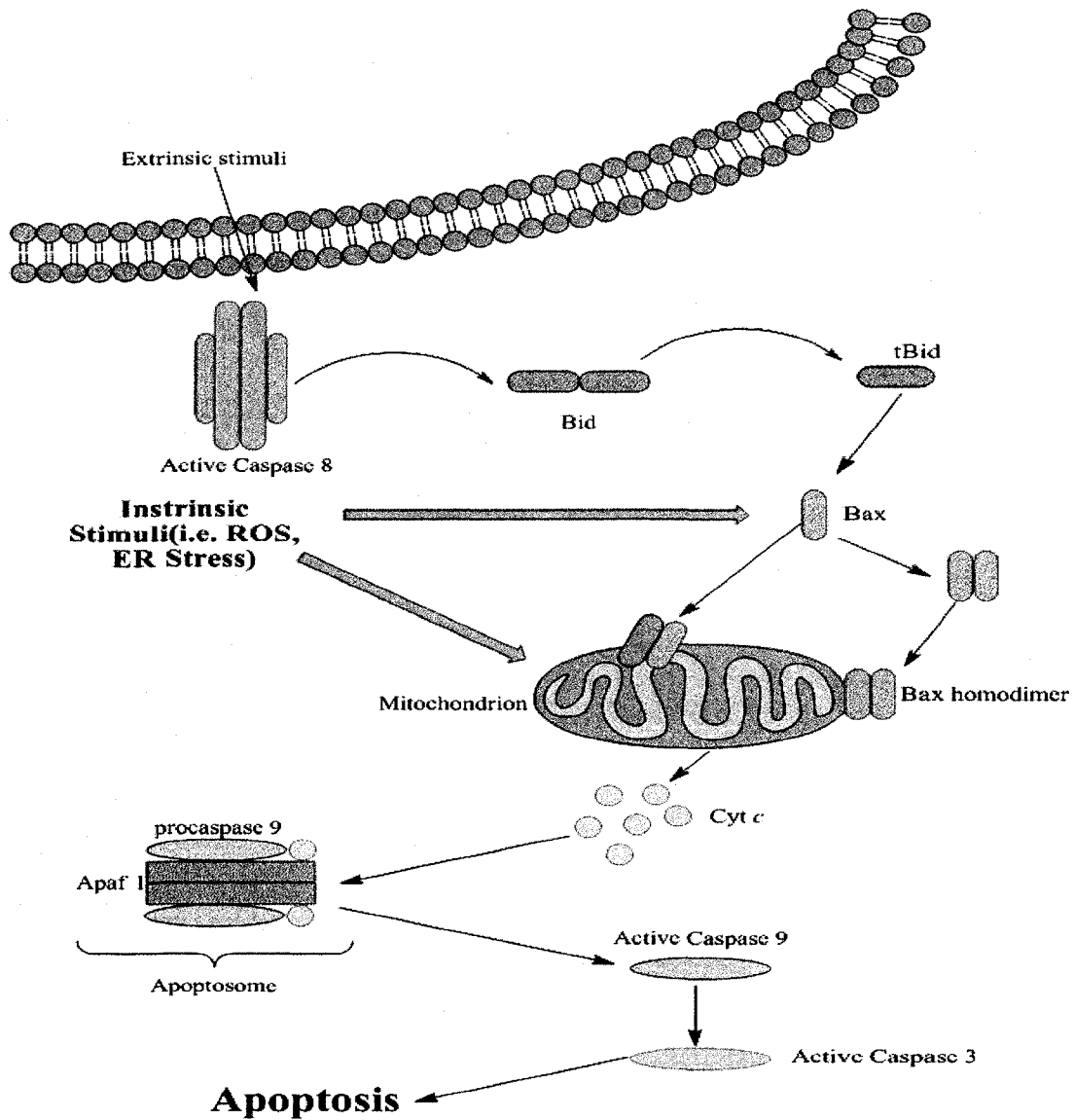
Figure 1.2 Intrinsic, mitochondrial-mediated apoptotic pathway

Upon appropriate apoptotic stimuli, pro-apoptotic proteins such as Bax will translocate to the mitochondria causing MOMP and subsequent release of Cyt *c*. Cyt *c* interacts with Caspase 9 and Apaf-1 forming the Apoptosome which leads to the activation of Caspase 9. Caspase 9 in turn activates effector Caspase 3 leading to apoptosis.

study by Kuwana *et al.* (2002) that used vesicles formed from isolated mitochondrial outer membranes (MOMs), showed that Bcl-2 family proteins can regulate the permeability of the MOM in the absence of the interior components of the mitochondria. In addition, many attributes of this process of membrane permealization could be reproduced using specific liposomes and recombinant Bcl-2 family proteins. However, a drawback of this cell-free system is that it probably does not represent the complete complexity of the permealization process as it happens *in vivo*. Other proteins of the MOM could be involved in either modulatng or potentiating the function of Bax and Bak proapoptotic Bcl-2 family proteins. Moreover, the release of specific IMS proteins in the cytosol could be influenced by the anchoring of these Bcl-2 proteins to internal mitochondrial components or involvement of the mitochondrial cristae (Scorrano *et al.*, 2002).

The second prominent model for MOMP is based on an event known as mitochondrial permeability transition pore (PTP) formation (Kroemer *et al.*, 2007). PTP formation allows for rapid permealization of the mitochondrial inner membrane (MIM) to solutes smaller than 1.5kDa. The PTP complex is known as a "megapore" that is thought to span the contact sites between the inner and outer mitochondrial membranes and is presumed to be composed of at least 3 main proteins. These three proteins are the voltage-dependent anion channel (VDAC) in the outer membrane, the soluble matrix protein cylcophilin D (Cyp D), and the adenine nucleotide translocase (ANT) in the inner membrane (Zamzani *et al.*, 2001).

During normal Ca^{2+} homeostasis, the PTP exists in a state of low conductance, however when excess Ca^{2+} is released from the ER and overloads the mitochondria, the pore transitions to a high-conductance state. This switch to high-conductance is irreversible and dependent on the

6

saturation of Ca^{2+} binding sites on the PTP (Ichas *et al.*, 1998). This high-conductance conformation of the PTP, which can be due to pro-apoptotic stimuli such as oxidative stress and ischemia/reperfusion (Crompton *et al.*, 1999), allows for the free diffusion of water and ions between the cytosol and the matrix, causing collapse of $\Delta\Psi_m$, swelling of the mitochondrial matrix, and uncoupling of oxidative phosphorylation. This ultimately results in the rupture of the MOM and subsequent release of IMS proteins (Bouchier-Hayes *et al.*, 2005). Rupturing of the MOM can also occur via Bax/Bak-mediated permealization and VDAC-mediated permealization. The expression of either Bax or Bak is required for MOMP, in several different models of apoptosis induction (Wei, *et al.*, 2001). Upon reception of apoptotic signals, Bax inserts into the OM (Wolter, *et al.*, 1997), where it is thought to form supramolecular openings, alone or in association with other pro-apoptotic members such as Bak or tBid. Bax and Bak have been shown function in coordination with PTP proteins, such as VDAC and ANT, to cause MOMP (DeGiorgi *et al.*, 2002; Precht *et al.*, 2005; Weaver *et al.*, 2005; Wigdal *et al.*, 2002). There has been much evidence that VDAC may exhibit some degree of specificity in the mitochondrial import/export of molecules (e.g. ATP, Ca^{2+}, and other ions). In 2000, Tsujimoto *et al.* showed that recombinant Bax and Bak accelerate the opening of VDAC in reconstituted proteoliposomes. This group presented evidence that VDAC1-deficent mitochondria isolated from a mutant yeast strain failed to exhibit the Bax/Bak-induced $\Delta\Psi_m$ loss and Cytochrome *c* (Cyt *c*) release that was observed with VDAC1-expressing control mitochondria. Lastly, it has been shown that microinjection of neutralizing anti-VDAC antibodies into cells prevented Bax-induced Cyt *c* release and $\Delta\Psi_m$ loss (Shimizu, *et al.*, 2001).

The release of IMS proteins is a pivotal component of both the caspase-dependent and caspase-independent pathways of mitochondria-mediated cell death. In the caspase-dependent

7
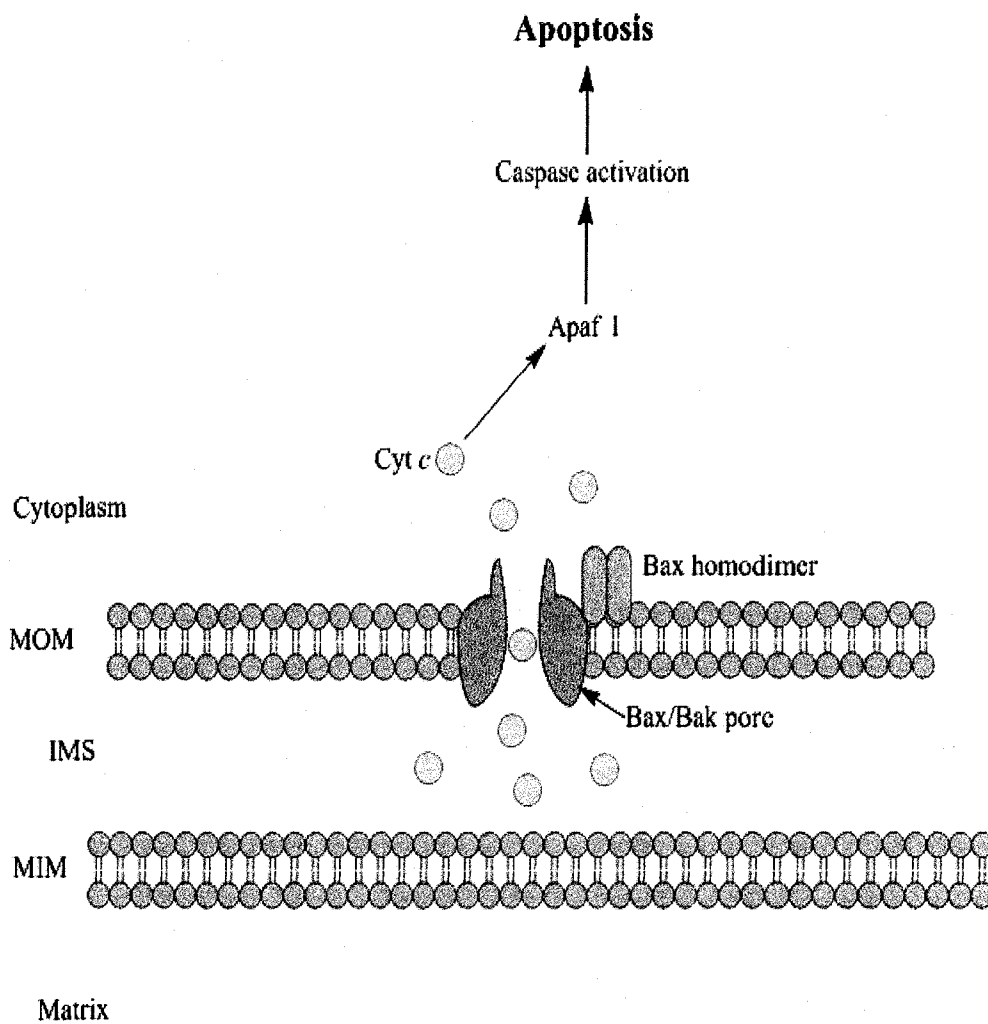
Figure 1.3A Mechanistic Model of MOMP

The first model focuses on MOMP as a process that involves only the outer membrane of the mitochondria and requires members of the Bcl-2 family of proteins, such as Bax, to either promote or prevent the formation of pores leading to the release of IMS proteins such as Cyt *c*.
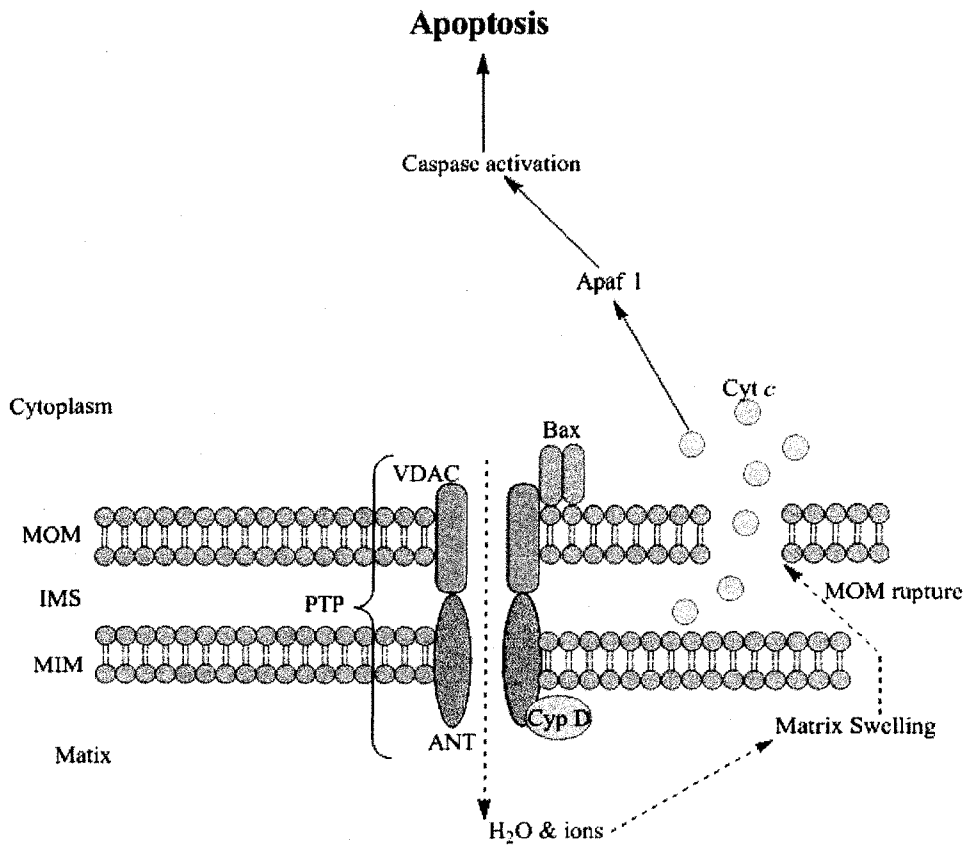
Figure 1.4: Model of MOMP

The second prominent model for MOMP is based on an event known as mitochondrial permeability transition pore (PTP) formation. The PTP complex is known as a "megapore" that is thought to span the inner and outer mitochondrial membranes and is presumed to be composed of at least 3 main proteins. These three proteins are the voltage-dependent anion channel (VDAC) in the outer membrane, the soluble matrix protein cylcophilin D (Cyp D), and the adenine nucleotide translocase (ANT) in the inner membrane. An influx of H_2O and other ions are believed to cause matrix swelling and MOM rupture leading to the release of Cyt c.

pathway, executioner caspases are cleaved and activated by the initiator Caspase 9. Caspase 9 is activated by multidimerization on the adapter molecule Apoptosis-Protease-Activating-Factor 1 (APAF-1) within a multidomain complex containing Cyt c called the apoptosome. APAF-1 pre-exists in the cytosol as a monomer, and its activation is dependent on the presence of Cyt c and ATP/ADP (Cain *et al.*, 2002). The release of Cyt c, which normally resides only in the IMS where it shuttles electrons in the respiratory chain, is required for the formation of the apoptosome. Activation of Caspase 9 leads to the activation of Caspase 3, which translocates to the nucleus to induce DNA fragmentation through the activation of DNases and deactivation of DNA repair machinery (Pollack *et al.*, 2001). Thus, MOMP is a crucial event responsible for caspase activation in the intrinsic pathway. MOMP can even commit a cell to die when caspases are not activated. This pathway, known as caspase-independent death, (Chipuk *et al.*, 2005, Kroemer *et al.*, 2005) occurs when there is irreversible loss of mitochondrial function as well as mitochondrial release of caspase-independent death effectors, such as apoptosis inducing factor (AIF) (Susin, *et al.*, 1999) and Endonuclease G (EndoG) (Li *et al.*, 2001). AIF and Endo G initiate apoptosis by directly translocating to the nucleus without the involvement of caspases (Adihihetty *et al.*, 2003).

1.4   The Bcl-2 Family of Proteins

The Bcl-2 family of proteins is comprised of over a dozen proteins that have been classified into three functional groups. These groups include both pro- and anti-apoptotic members, each containing one or more Bcl-2 homology domains (BH1 through BH4) (Adams *et al.*, 1998). Members of the first group are anti-apoptotic and have all four Bcl-2 homology (BH) domains (BH1-BH4). These proteins also have a C-terminal hydrophobic tail that allows them

10

to localize to the outer surface of the mitochondrial membrane. This group includes Bcl-2, Bcl-x_L, and Mcl-1. The members of the second group are similar in structure to the members of the first group; however they are pro-apoptotic and lack the BH4 domain. This group includes Bax, Bak, and Bok. Members of the third group, that are pro-apoptotic, are BH3-only proteins which include Bid, Bad, Puma, and several others (Hengartner, 2000).

Cell survival is determined by the balance between anti-apoptotic Bcl-2 family proteins such as Bcl-2, Bcl-x_L, and Mcl-1, and pro-apoptotic proteins such as Bax, Bak, and Bok proteins. Bax and Bak are effectors of MOMP, whereas their anti-apoptotic counterparts act as inhibitors of this permealization process, not as effectors of an independent survival mechanism (in regards to MOMP) (Kroemer *et al.*, 2007). In addition, MOMP mediated by Bax and Bak may be triggered by secondary modulator proteins, such as the BH3-only proteins Bim and Bid (Adams *et al.*, 1998) Pro- and anti-apoptotic Bcl-2 family members can heterodimerize and titrate one another's function, suggesting that their relative concentration may act as a rheostat for the cell suicide program (Oltavi, *et al.*, 1993). Studies using mutagenesis models have established that the BH1, BH2, and BH3 domains strongly influence homo- and hetero-dimerization within this family of proteins (Yin *et al.*, 1994). In the event of over-expression of pro-apoptotic members of the Bcl-2 family such as Bax, apoptosis is accelerated, as observed in tissues where cell death occurs as part of the normal maturation process (e.g. epidermis) (Oltvai, Z *et al.*, 1993). Conversely, over-expression of Bcl-2 (or related anti-apoptotic members) leads to heterodimerization (with Bax) and inhibition of death induction (Oltvai, Z *et al.*, 1993).

Bax, in particular, exists predominantly in the cytosol prior to apoptotic induction. Early during apoptosis, Bax translocates from the cytosol to the mitochondria where it participates in

mitochondrial disruption and the release of Cyt *c* (Hsu *et al.*, 1997 Wolter *et al.*, 1997; Green *et al.*, 1998). There are four different isoforms of Bax which are derived from the alternative gene splicing of *bax*: Bax γ (5kDa), β (24kDa), δ (16kDa), and α (21kDa). Of the four isoforms, only Bax α and β contain the BH3 domain necessary for pro-apoptotic function, and only α, the most prominent isoform of Bax, has the C-terminal transmembrane domain required for insertion into the mitochondrial membrane that leads to MOMP (Oltavai *et al*, 1993). By altering the insertion of Bax into the mitochondrial membrane, apoptosis can also be modulated. Several studies have examined the effects of alterations in the C-terminal transmembrane region of Bax on mitochondrial targeting and induction of apoptosis (Goping *et al.*, 1998; Gross *et al.*, 1998; Neuchushtan *et al.*, 1999).

It has been reported that the full-length cDNA of human Bax fused to GFP is diffuse in the cytosol in healthy cells, and becomes punctuate and localized in the mitochondria in cells undergoing apoptosis (Wolter *et al.*, 1997). Comparatively, Bax that is lacking its 21 amino acid hydrophobic C-terminal tail is found to be diffuse in the cytosol of healthy cells in addition to cells treated with staurosporine, a kinase inhibitor used extensively to trigger apoptosis (Weil *et al.*, 1996). In a study performed by Neuchuhstan *et al.* in 1999, it was noted that Ser184 is most important in the regulation of the subcellular location of Bax. Mutation of Ser184 can freeze Bax in either the cytosol or the mitochondria depending on the amino acid substitution. Altering Ser184 to Val or deleting it entirely causes Bax to localize with the mitochondria of healthy cells, whereas changing Ser184 to His, Glu, Lys, or Asp results in a cytosolic location in healthy cells (Neuchashtan *et al.*, 1999). The role of Ser184 has been further characterized by Xin *et al.* in 2006 where they identified the effect of nicotine induced post-translational phosphorylation of Bax at Ser 184 by protein kinase Akt. This post-translational modification has been shown to

12

inactivate Bax specifically in lung cancer cells. Additionally, protein phosphatase 2A (PP2A) was found to be an active regulator in this particular cell type, working to both dephosphorylate Bax and interfere with Bax-Bcl-2 heterodimerization, allowing Bax to homodimerize and permeate the mitochondria inducing apoptosis (Xin, M *et al.*, 2006).

In 2000, the solution structure of Bax was determined using NMR by Suzuki *et al.* It has been reported by this group (in addition to others) that the structure of Bax consists of nine α helices and its overall fold closely resembles that of anti-apoptotic protein Bcl-x_L (Muchmore *et al.*, 1996) which has eight amphipathic α helices clustered around one central hydrophobic helix (α5). Earlier studies have shown that a portion of helix α1 is hidden in the cytosolic form of Bax but becomes accessible to antibody binding after membrane insertion during apoptosis (Nechushtan *et al.*, 1999). In addition, helix α2 encompasses the BH3 domain that is the functionally important region for interaction between members of the Bcl-2 family. Particularly, this helix in Bcl-x_L and the Bcl-x_L-Bak complex is packed closer to the hydrophobic core of the protein than it is in Bax. This may be what makes the protein pro- or anti-apoptotic: the relative exposure of the BH3 domain. A portion of the C-terminal hydrophobic region of Bax, the putative transmembrane domain, contains helix α9. The helix α9 of Bax is located in the hydrophobic pocket in a similar manner to the way a Bak BH3 peptide binds to the Bcl-x_L, although the directional sense of the peptide is opposite to that of the C-terminal helix of Bax (Suzuki *et al.*, 2000). This demonstrates that although pro- and anti-apoptotic members of the Bcl-2 family both contain BH3 domains, the orientation and exposure of the domain to outside binding partners differs, allowing for the unique properties of members of the Bcl-2 family.

Studies utilizing various deletion mutants of Bax have demonstrated that Bax uses its BH3 domain (helix α2) for homodimerization and heterodimerization with other members of the Bcl-2 family (both pro- and anti-apoptotic), as a mutation in only this region rendered the protein unable to dimerize (Zha, H et al., 1995). Specifically, Bax is understood to bind to itself and other Bcl-2 members in a parallel tail-to-tail fashion using the BH3 domain. However, the anti-apoptotic Bcl-2 proteins dimerize to each other using an anti-parallel head-to-tail conformation that involves the BH4 domains of one protein and the BH1 and BH2 domains of the second. When heterodimerizing with a pro-apoptotic binding partner, BH1 and BH2 domains of the anti-apoptotic protein interact with the BH3 domain of the pro-apoptotic partner (Yin et al., 1994). Additionally, the Bax C-terminus (helix α9) has been shown to bind to its own BH3 binding pocket when present in the cytosol. This binding conformation would prevent dimer formation in the cytosol. It is unlikely that another Bcl-2 family member alone could compete with the C-terminal helix of Bax for binding to its BH3 pocket. This suggests that dimerization via this pocket cannot occur in the cytosol without the presence of an energy-driven process that would disengage helix α9 from helix α2 (Suzuki et al., 2000).

1.5   The Role of Caspases in Apoptosis

Caspases have been strongly implicated to play an essential role in apoptosis (Lee et al., 2000a). Caspases are cysteine aspartic acid proteases and in humans, they are synthesized as zymogens awaiting appropriate apoptotic stimuli, and upon stimulation, are protealitically cleaved to become activated. They are manufactured in the cell as single-chain precursors, where activation occurs by cleavage at the conserved Asp_{297} residue and a conformational change occurs, bringing it into the correct alignment for catalysis (Salvesen et al., 1999).

There are eleven human caspases that have been identified thus far (Humke *et al.,* 1998) and they can play an essential role in apoptosis as initiator proteins, such as Caspase 8/9, activating downstream caspases. As well, caspases can act as executioner or effector proteases (Caspase 3/7) resulting in DNA damage and apoptosis. Sequence analysis and x-ray crystallography data have suggested that all caspases share a common structure (Cohen, 1997; Humke *et al.,* 1998; Nicholson *et al.,* 1997; Shimin *et al.,* 1998; Van de Craen, *et al.,* 1997). Each zymogen contains an N-terminal prodomain, a large subunit containing the active site cysteine within a conserved QACXG motif, and a small C-terminal subunit. An aspartate cleavage site separates the prodomain from the large subunit, and an interdomain linker that contains one or two aspartate cleavage sites separates the large and small subunits (Wolf *et al.,* 1999). Activation of the caspase accompanies the cleavage of the interdomain linker, usually resulting in the removal of the prodomain. The active caspase enzyme functions as a tetramer, consisting of two large/small subunit heterodimers. The heterodimers each contain an active site comprised of residues from both the small and large subunits (Mittl, *et al.,* 1997; Walker *et al.,* 1994; Wilson *et al.,* 1994). Since caspases exist as latent zymogens, the question has often been raised as to how they are activated. Current evidence suggests that the activation may proceed via auto-activation, transactivation, or proteolysis by other proteinases (Wolf *et al.,* 1999).

Importantly, Caspase 3, one of the main executioner caspases of apoptosis, has been found to be activated in nearly every model of apoptosis and its substrates include many proteins involved in cell maintenance and/or repair (Nicholson *et al.,* 1997). For example, oligonucleosome fragmentation (DNA laddering) is a characteristic feature of apoptosis and is mediated by caspase-activated deoxyribonuclease (CAD), whose activation is modulated by the caspase-3-mediated cleavage of the CAD inhibitor ICAD (Enari *et al.,* 1998).

As previously mentioned, pathways to Caspase 3 activation have been identified that are either dependent on or independent of mitochondrial Cyt c release. It has been shown that microinjection of cytochrome c causes apoptosis of HeLa and Hek293 cells, but not of Caspase 3 defective MCF-7 (breast cancer) cells (Li, *et al.*, 1997). Once Caspase 3 is activated, downstream substrates of cell death are cleaved irrespective of the involvement of Cyt c (Cryns *et al.*, 1998; Nicholson *et al.*, 1997; Reed *et al.*, 1997). However, Caspase 3 may also amplify the upstream death cascade, including cytochrome c release, by cleaving Bcl-2 and Bcl-X_L, thus destroying the anti-apoptotic function of these proteins and releasing C-terminal fragments that are pro-apoptotic (Porter *et al.*, 1999; Wolf *et al.*, 1999).

However, Caspase 3 is important for survival, as Caspase 3-knockout mice are born at a low frequency and die after only a few weeks (Kuida *et al.*, 1996; Woo *et al.*, 1998). The mice that are born possess skull defects with masses of supernumary cells that represent the failure of programmed cell death during development of the brain. Additionally, insufficient apoptosis due to caspase inactivation may promote oncogenesis by allowing cell accumulation (Martin *et al.*, 1996). Alternatively, caspase over-reactivity promotes excessive cellular suicide, which may be the basis for such neurodegenerative disorders as Huntington's Disease (HD) and AD (Wellington *et al.*, 1998; Wolozin *et al.*, 1996). On the molecular level, an increase in expression/activity of caspases, adapters, apoptotic sensors, or diminished expression/activity of caspase inhibitors could increase caspase activity.

1.6   Oxidative Stress in Mammalian Cells: Mitochondria are the major site of ROS Production

Reactive oxygen species (ROS) such as superoxide anion (O_2^-.), hydrogen and organic peroxides, are produced in all aerobic cells as by-products of several metabolic reactions and in response to various stimuli (Fleury *et al*, 2001; Fridovich, 1998).   In particular, ROS are produced in the mitochondria by the partial reduction of molecular oxygen, where they play an important role as regulatory mediators in signalling processes (Dröge, 2002).   However, ER and the nuclear membrane also contain electron transport chains that can lose electrons and produce superoxide radicals.   Physiologically, the activity of the respiratory chain leads to the generation of semi-quinines, a potential source of ROS (Papa, *et al.,* 1997).   The respiratory chain produces ROS at complex I (NADH/ubiquinone oxidoreductase) and complex III (ubiquinol/cytochrome *c* oxido-reductase).   In particular, the ubiquinone site at complex III appears to be the major site of mitochondrial ROS production as this site catalyzes the conversion of molecular oxygen to the superoxide anion radical (O_2^-.) by the transfer of one electron to molecular oxygen (Papa *et al.,*1997; Turrens *et al.,* 1985).   Moreover, the inhibition of the respiratory chain, due to the lack of oxygen or an inhibitor such as cyanide or antimycin A, increases the ubisemiquinone free radical level in the normal catalytic mechanism of complex III (Turrens *et al.,* 1985).   The superoxide anion can generate other potent types of ROS such as H_2O_2.   A reductive homolytic cleavage of H_2O_2 yields the highly oxidative and cytotoxic hydroxyl radical (OH·).   This highly reactive radical is accountable for most of the oxidative damage leading to necrosis (Halliwell *et al.,* 1990).   Alternatively, mitochondrial superoxide may react with nitric oxide to produce peroxynitrite, a powerful oxidant, which causes irreversible inhibition of mitochondrial

respiration and damage to mitochondrial components such as complexes I, II, IV, and V, creatine kinase, membranes, mtDNA, and superoxide dismutase (SOD) (Groves, 1999). Nitric oxide (NO) can promote or inhibit apoptosis depending on the cell type (Chung *et al.*, 2001).

Cells have multiple sites for ROS production and few mechanisms for degradation. ROS are also involved in such physiological processes as mediation in signal transduction pathways, activation of proteins like tyrosine kinase or mitogen-activated protein kinases (MAPKs). Current evidence suggests that different stimuli use ROS as signalling messengers to activate such transcription factors as AP-1 and NF-κB, and to induce gene expression (Pinkus *et al.*, 1996).

An excess of ROS in the mitochondria causes oxidative stress, leading to enhanced activity of the antioxidant defence system and mitochondrial damage. Stresses, such as dysfunctional complex I, chemical poisoning, and ischemia followed by reperfusion, can subject tissues and cells to oxidative damage (Fleury *et al.*, 2001). The main targets of ROS in mitochondria are the protein components of the membranes and the polyunsaturated fatty acids. Oxidants increase the release of calcium from the mitochondria, thus stimulating enzymes that are calcium-dependent, such as proteases, nucleases, and phospholipases. Due to the absence of DNA-protecting proteins in the mitochondria, the low efficiency repair mechanism, and the proximity of the respiration chain, mtDNA is a prime target for ROS (Shoji *et al.*, 1995).

For prevention of oxidative damage, mammalian cells have established a complex antioxidant defence system that is composed of non-enzymatic antioxidants such as glutathione and thioredoxine, along with enzymatic components such as catalase and SOD (Sies, 1991). Importantly, mitochondria posses an antioxidant system of SOD, NADH, and a complete

18

glutathione redox system formed by glutathione reductase, reduced glutathione (GSH), and glutathione peroxidase. This system allows for the reduction of oxidants, such as hydroperoxide (Reed, 1990). When free radical generation exceeds the capacity of the cell to detoxify them, protein and DNA damage can occur, leading to cell death. The ability of oxidative stress to initiate necrotic cell death has been widely documented (Halliwell *et al.*, 1989); the possible involvement of ROS as signalling molecules in physiological cell death is a more recent concept. The first evidence suggesting the involvement of mitochondrial ROS in apoptotic cell death arose from the study of the TNF-α-induced cytotoxicity (Dröge, 2002; Fernández-Checa, 2003; Lanchaster *et al.*, 1989; Margaill *et al.*, 2005; Schulze-Osthoff *et al.*, 1992). Notably, ROS accumulation was found to precede alterations in the mitochondrial membrane, nuclear condensation, and other characteristic apoptotic events. Studies that utilized antioxidants displayed that ROS act upstream of mitochondrial membrane depolarization (Sidoti-de Fraisse *et al.*, 1998), Bax relocalization, Cyt *c* release, executioner caspase activation, and nuclear fragmentation.

1.7   Oxidative Stress and Neurodegenerative Disease

Acute and chronic neurodegenerative diseases are illnesses associated with high morbidity and mortality which have few or no effective options available for their treatment (Friedlander, 2003). One of the characteristics of many neurodegenerative diseases (which include, but are not limited to stroke, brain trauma, spinal cord injury, Alzheimer's Disease, Parkinson's Disease, amyotrophic lateral sclerosis, and Huntington's Disease) is neuronal cell death (Yuan *et al.*, 2000). Normally, apoptotic cell death plays a crucial role in the development of the nervous system, with both anti- and pro-apoptotic modulators being prominently featured

Single domain antibody libraries have been constructed from the RNA of naïve llama lymphocytes, which contain phages that display a specific sdAb on their surface and harbour the gene for this sdAb inside. Through a technique called panning, a specific sdAb along with its gene can be identified for a particular antigen of interest (Tanha *et al.*, 2002). Importantly, the gene itself can be transfected inside cells as intrabodies in order to understand the effects of the sdAb *in vivo*.

1.9   Intrabodies as Therapeutic Agents in Neurodegenerative Disease

Intrabodies, or intracellular antibodies, are known as antibody fragments that are expressed intracellularly and directed to specific subcellular compartments (Kontermann, 2004). For this study, the intrabodies are the product of the transfected genes for the sdAbs that had a high affinity for Caspase 3. The concept of using intrabodies as therapeutic agents is based on the ability of the intrabody to: directly inhibit the function of the subcellular molecule (i.e. by sterically preventing interactions of the target protein with its protein partners); to restore function to an intracellular molecule; or to divert the target molecule from its normal intracellular location or purpose (Miller *et al*, 2005). In contrast to the direct administration of a drug, this approach allows the cell to express the sdAb gene and use its own machinery to produce the therapeutic agent and since the intrabodies are produced only in cells, this yields the advantages of safety and efficacy (Kontermann, 2004).

Many neurodegenerative diseases such as Parkinson's Disease, Alzheimer's Disease, and stroke are mediated by abnormal intracellular protein expression, with intrabodies being a potential therapy for these diseases. The use of intrabodies may allow for the identification or validation of novel drug targets. As well, intrabodies are small in size, stable, specific, and may

27

prove less immunogenic than other protein therapies, important factors when treating neurodegenerative disease (Miller *et al*, 2005).

In the last few years much research has been done to discover ways in which these intrabodies can be used as therapeutics. Recently, expression of p21, erbB-2, huntingtin, and MHC have all been individually downregulated using intrabodies (Arafat *et al.,* 2000; Crochet *et al.,* 1998; Lecerf *et al.,* 2001; and Mhashilkar *et al.,* 2002). Additionally, intrabodies have been shown to have potent antiviral potential, particularly through targeting of the intracellular action of such mandatory HIV viral proteins as Vif, Tat, and Rev (Conclaves *et al.,* 2002).

Investigation has also been carried out on the ability of intrabodies to inhibit aggregation of proteins found in cases of Huntington's Disease. Work by Colby *et al.* in 2004, found a single domain intrabody capable of inhibiting toxic huntingtin (htt) aggregation in the brain. In this study, the group utilized a variable light chain intrabody against htt that prevented aggregation and rescued neurons from toxicity in a neuronal model (SHSY-5Y cells) of Huntington's Disease (Colby *et al.,* 2004).

Intrabodies have also been utilized in manipulating the subcellular location of proteins such as pro-apoptotic Caspase 7. In a study by Zhu *et al.* in 1999, a single chain scFv intrabody was genetically fused with known intracellular protein trafficking signals. They were able to direct Caspase 7 from its normal location in the cytosol to either the nuclei or peroxisomes, thus affecting its apoptotic function (Zhu *et al.,* 1999).

The use of intrabodies to obtain phenotypic knockouts has several advantages over other knockout models like RNA interference (RNAi) in understanding cellular functions and

developing therapeutic agents. RNAi has the risk of non-specific effects by binding to alternate mRNA sites, whereas intrabodies are tailored to manipulate specific antigens within the cell. It was reported by Persengiev *et al.* in 2004 that through use of a typical 21bp siRNA (small interfering RNA) on cells, over 1000 genes involved in many unrelated cellular functions were affected (Persengiev *et al.*, 2004). Moreover, many target complexes have multiple binding/interacting sites, and thus the modulation of the gene may lead to alteration of various functions, which may not be desired. Therefore, by developing and screening intrabodies that can bind to a specific site on multidomain complexes, this risk could be eliminated (Heng *et al.*, 2005).

Work by our group has demonstrated the use of single domain intrabodies against Bax protein to block its function under oxidative stress conditions, thereby inhibiting apoptosis (Gueorguieva *et al.*, 2006). These anti-Bax sdAbs can be used to study the role of Bax in oxidative-stress-induced-apoptosis intracellularly, and also as a platform from which to develop novel, small molecule therapies for neurodegenerative diseases involving oxidative stress.

1.10   Screening Pharmacaphore Libraries: Use of Small Molecule Inhibitors of Apoptosis

Small-molecule inhibitors are useful tools for the elucidation of many mechanisms of cellular processes (Schreiber *et al.*, 1998). They are more stable than peptide inhibitors and are often cell-permeable, thus making it easy to compare *in vivo* the activity of the analogues that have a variety of activities *in vitro*. Particularly, the use of small-molecule inhibitors of protein-protein interactions is extremely useful, as most intracellular pathways are controlled primarily by protein-protein interactions. Previously, most of the available cell-permeable inhibitors were mechanism-based enzyme inhibitors, and there were very few examples of small molecule-

29

inhibitors of protein-protein interactions acting inside cells. Presently, many researchers are focusing their studies in the field of inhibition of protein interaction making it an exciting new area of interest, especially when considering interactions of the Bcl-2 family of proteins (Young *et al.*, 1998).

There are two general approaches by which small-molecule, non-peptide modulators of protein-protein interaction can be identified. A number of studies have employed these approaches to identify modulators of protein-protein interactions with potential therapeutic use for the treatment of diseases such as cancer and degeneration (Berg *et al.*, 2003). One such approach is through screening combinatorial pharmacaphore libraries for modulators of protein-protein interaction. This approach does not require prior knowledge of the dimerization, although such information would be helpful when establishing assays for high-throughput screening of large chemical libraries.

A second approach involves *in silico* screening of chemical databases in order to preselect molecules most likely to bind to a region of protein-protein interaction, and thereby modulate it. The rate of success is much higher than that obtained screening untargeted libraries; however, this approach requires detailed structural information about the interface of the protein dimer from NMR spectroscopy or X-ray crystallography. Moreover, the plasticity of protein-protein interfaces makes the prediction of interactions, specifically those contributing to modulation, an even more challenging endeavour (Delano *et al.*, 2000).

Several studies have utilized these approaches to identify small molecule modulators of members of the Bcl-2 family in hopes of developing potential therapeutics for cancer and neurodegeneration. For example, Becattini *et al.* in 2006 identified two chemical fragments

using an NMR-based approach (structure-activity relationships by interligand NOE) that bind weakly to the surface of tBid, a pro-apoptotic protein. Covalent linkage of the two fragments led to a much higher affinity bidentate derivative. Through both *in vitro* and *in vivo* assays they were able to demonstrate that the compounds prevent tBid translocation to the mitochondrial membrane and subsequent release of pro-apoptotic stimuli, inhibiting neuronal apoptosis (Becattini *et al.*, 2006).

Two other studies performed independently by Wang *et al.* in 2000, and Oltersdorf *et al.* in 2005, examined the ability of two separate organic compounds to bind to anti-apoptotic Bcl-2 family proteins (Bcl-2 in the first study, and Bcl-2, Bcl-X_L, and Bcl-w in the second study) and induce apoptosis in tumour cells. Wang *et al.* examined through a computer binding strategy a small molecular weight compound, HA14-1, that was predicted to be a ligand of a Bcl-2 surface pocket. *In vitro* studies displayed the direct interaction of HA14-1 with this Bcl-2 surface pocket that is required for Bcl-2 biological function. HA14-1 was also shown to effectively induce apoptosis in human acute myeloid leukemia (HL-60) cells overexpressing Bcl-2 protein (Wang *et al.*, 2000).

In the study performed by Olsterdorf *et al.*, by utilizing NMR-based screening, parallel synthesis, and structure-based design, they found ABT-737, a small-molecule inhibitor of the anti-apoptotic proteins Bcl-2, Bcl-X_L, and Bcl-w. Importantly, ABT-737 was found to have an affinity of two to three orders of magnitude higher than previously reported compounds (Becattini *et al.*, 2004; Enyedy *et al.*, 2001, and Wang *et al.*, 2000). ABT-737 displayed the ability to induce apoptosis in cells from lymphoma and small-cell lung cancer carcinoma lines,

as well as primary-patient derived cells. In animal models, ABT-737 caused regression of established tumours and improved survival of the animal (Oltersdorf *et al.*, 2005).

Importantly, in a study performed by Degterev *et al.* in 2001, a commercially available library consisting of 16,320 chemicals was screened and three compounds BH3I-1 and BH3I-1´ (close homologues) and an unrelated BH3I-2 were identified as inhibitors of the Bcl-x$_L$/Bak-BH3 interaction. NMR spectroscopy experiments demonstrated that the inhibitor compounds targeted the BH3-binding pocket of Bcl-x$_L$. The Bcl-x$_L$/Bak-BH3 inhibitors restored the function of pro-apoptotic Bcl-2 family members in cell culture, and allowed previously resistant cancer cells to undergo apoptosis (Degterev *et al.*, 2001).

In our present study, the screening of pharmacaphore libraries for small molecular weight compounds that can bind to pro-apoptotic Bax and block its function was performed. We screened 34 small molecules from the same commercial library as Degterev *et al* (2001). One of these compounds is the BH3I-1 inhibitor itself, and the remaining 33 are derivatives of BH3I-1. Since all the members of the Bcl-2 family have a BH3 domain, and BH3I-1 disrupts the BH3 domain of Bak from interacting with the hydrophobic cleft formed by the BH1, BH2 and BH3 domains of Bcl-x$_L$, we proposed that perhaps one of these derivatives of BH3I-1 could preferentially bind to the BH3 domain of Bax, thus blocking its function/interaction with other proteins/mitochondria required for apoptotic induction (Degterev *et al.*, 2001).

1.11 Objectives

In this two-part study we plan examine two pro-apoptotic proteins, Bax and Caspase 3, which can become excessively activated during oxidative-stress-induced apoptosis and play

pivotal roles in the death of neurons in neurodegeneration. In order to prevent this inappropriate induction of apoptosis, we plan to investigate the use of single domain antibodies (sdAbs or V$_H$H) to inhibit the activity of Caspase 3, and small molecular weight organic compounds to inhibit the activity of Bax.

Part 1: Inhibition of Caspase 3 activity

The objectives of this study are as follows:

1) To isolate and purify recombinant Caspase 3 from a culture of *E. coli* harbouring the gene for said protein.

2) In collaboration with Dr. J. Tanha (NRC-IBS) to isolate Caspase 3 specific V$_H$Hs (sdAbs) by panning a llama phage display library and immobilized recombinant Caspase 3.

3) To evaluate and characterize the ability of isolated Caspase 3 specific V$_H$Hs to modulate the activity of active Caspase 3 *in vitro* by utilizing a Caspase 3 activity assay.

4) Lastly, to express the anti-Caspase 3 V$_H$H genes inside human neuroblastoma cells (SHSY-5Y) through transfection, and study their ability to block oxidative stress-induced-apoptosis.

Part 2: Inhibition of Bax activity

The objectives of this study are as follows:

1) To isolate and purify recombinant Bax from a culture of *E.coli* harbouring the gene for said protein

2) In collaboration with Dr. J. Tanha (NRC-IBS), to fluorescently label anti-Bax sdAb5.2 with cy5.5. This sdAb was previously found by Gueorguieva *et al.* in 2006 to confer the greatest resistance to oxidative-stress-induced apoptosis out of six screened sdAbs, and thus will be used in subsequent competitive binding assays.

3) To utilize the cy5.5-labelled sdAb5.2 in competitive binding assays with immobilized recombinant Bax to screen a 34-member pharmacaphore library in evaluating whether these small molecular weight compounds can competitively bind to Bax.

4) To evaluate *in vitro* the ability of the 34 compounds to lower the level of Bax-induced ROS in isolated mitochondria.

5) To study the efficacy of selected compounds to block oxidative stress induced apoptosis in neuroblastoma, differentiated neuroblastoma, and NT-2 neuronal precursor cells.

Chapter 2 Materials and Instrumentation

2.1 Chemicals and Supplies

Most of the chemicals were purchased from Sigma Aldrich Chemical Company, Mississauga, ON, Canada. These chemicals include: Bacto yeast extract, Bacto tryptone, chlormphenicol, kanamycin, arabinose, IPTG, lysozyme, DNase, imidazole, $NiSO_4$, BSA, CHAPS, HEPES, $MgCl_2$, H_2O_2, HRP, EDTA, EGTA, TRIS-HCl, Triton X-100, PHPA, PMSF succinate, trypsin-EDTA, KCl, mannitol, Tween, $CaCl_2$, Annexin V-FITC, collagen, retinoic acid, and horse radish peroxidise-conjugated anti-mouse and anti-rabbit.

NaH_2PO_4, Na_2HPO_4, DMSO, NaOH, NaCl, DTT, $NaHCO_3$, and sucrose were purchased from BDH, Toronto Canada. Protein assay reagent, protein marker, and acrylamide were obtained from Bio Rad, Ontario Canada. Glycine was purchased from EM Sciences, NJ, USA. Hoescht and Annexin V red were obtained from Molecular Probes, Eugene OR, USA. BDNF was obtained from Alomone Labs, Israel.

Monoclonal anti-Bax and polyclonal anti-Caspase 3 and VDAC antibodies were all purchased from Sigma, Mississauga, ON. ChemiGlow West kit was purchased from Alpha Innotech Corporation, San Leonardo CA, USA. JC-1 kit was purchased from Cell Technology, Mountain View. CA, USA. Fugene 6 Transfection Reagent was purchased from Hoffmann-La Roche Ltd., Mississauga, ON, Canada and DEVD-AFC was obtained from MP-Biomedicals, Aurora, OH.

2.2   Cell Culture Supplies

2.2.1   Cell Lines

Human   Neuroblastoma   (SHSY-5Y)   cells   and   neuronally-committed   human
teratocarcinoma (NT-2) cells were purchased from the American Type Culture Collection
(ATCC), Manassas, VA, USA.

2.2.2   Media

Dulbecco's Modified Eagles Medium (DMEM) F12 HAM was purchased from Sigma
Chemical Company, Mississauga, ON, Canada.   L-Glutamine, Gentamycin, and Fetal Bovine
Serum (FBS) were all purchased from Gibco BRL, VWR, Mississauga, ON, Canada.

2.3   Instrumentation

Fluorescence measurements were conducted in the SpectraMan Gemini XS multiplate
reader (Molecular Devices, Sunnyvale CA USA). Cell culture was performed under sterile
conditions in the class-II type A/B3 Biosafety cabinet (Nuaire).   Cells were maintained in an
incubator with 5% CO_2 which used a HEPA filter (Thermo Forma). A Dounce homogenizer
from Kontes Glass Company (NJ, USA) was used along with, freezer vials (VWR) and
Eppendorf pipettes (Fisher Scientific). Phase contrast and fluorescent pictures were taken using
an inverted stage fluorescent microscope (Leica DM IRB, Germany) and another fluorescence
microscope (Zeiss Axioskope 2 Mot plus, Gottingen, Germany) and fluorescence pictures were
taken using a camera (QImaging, Gottingen, Germany).   The images were processed using
Improvision Open*Lab* v3.1.2, and Adobe Photoshop v8.0. Cell culture supplies included culture

flasks and dishes, pipettes, freezer vials, and tubes were obtained from Sarstedt Inc, Montreal, Quebec, Canada.

A pH Meter model 8100 and buffer solutions (VWR) and an Adventurer balance (OHAUS) were used. Absorbance was measured by the Genesys 10 UV-Vis Spectrophotometer (Thermo Scientific, Waltham, MA, USA) and centrifugation was done using low speed centrifuge (Jouan) and DESAGA (Sarstedt-Gruppe). Vortex Jr. Mixer (Scientific Industries Inc), a heating block (Gibco BRL, VWR, Canada) and a rocking platform (VWR) were all used as well.

Chapter 3 Methods

3.1 Isolation of Recombinant Bax and Caspase 3

3.1.1 Expression of Recombinant Bax and Caspase 3

A culture of *E.coli* transformed with the gene for Bax protein harbouring a His_6-tag was obtained from Bruno Antonsson and used to inoculate a 100mL of a 1L stock of L.B. media (10g NaCl, 10g Bacto Tryptone, 5g Bacto Yeast Extract, 1L ddH_2O, and 30µg/mL Chlormphenicol). This was incubated on a shaker overnight at 37°C and then transferred to the remaining 900mL stock L.B. media. The culture was then placed in the 37°C shaker for an additional 3-4 hours, following which the OD_{280} was ensured to be between 0.40-0.75 using UV/VIS before induction with Arabinose (1g/L). This final culture was then incubated overnight on the shaker at 37°C before centrifugation at 12,500 x g for 15 minutes at 4°C. The supernatant was discarded and the pellets were stored at -20°C overnight for subsequent purification. A culture of *E. coli* transformed with the gene for Caspase 3 also containing a His_6-tag (ATCC, Manassas, Va) was used to inoculate an L.B. media stock in a similar manner as the Bax *E.coli* with the following differences: instead of 30µg/mL Chloramphenicol, 40µg/mL of Kanamycin was used in the LB. media, and instead of 1g/L of Arabinose, 0.24g/L of IPTG was used for induction.

3.1.2 Purification of Recombinant Bax and Caspase 3

Prior to purification, the *E. coli* pellets expressing either Bax or Caspase 3 were resuspended in a lysis/loading buffer (0.02M phosphate buffer (NaH_2PO_4, Na_2HPO_4), 100µg/mL lysozyme, 5µg/mL DNase, 350µg/mL PMSF, 1% Triton X-100, and 0.05M imidazole) and

incubated on ice for 45min. Following the incubation, the resupended pellets were sonicated at 4°C, centrifuged at 12,500 x g for 15min at 4°C and the supernatant was kept as it contained the protein of interest (either Bax or Caspase 3). Both cultures of Bax and Caspase 3 *E. coli* were purified using a Hi-Trap nickel chelating affinity column (GE Healthcare, Baie d'Urfé, QC, Canada). The column was prepared by running 20mL of ddH$_2$O, followed by 4mL of a 0.1M Nickel Sulfate solution, 20mL of ddH$_2$O, and lastly 30mL of the loading buffer to equilibrate the column. The supernatant was then loaded onto the column and washed with the loading buffer to elute any non-specific proteins that may be bound to the column. The fractions were collected (5mL/fraction) and the absorbance was determined using UV/VIS. This absorbance was monitored and once the values significantly decreased indicating the removal of the loosely-bound non-specific proteins, 10mL of the elution buffer (0.02 Phosphate buffer, 0.5M imidazole) was added. Fractions were collected in 1mL increments and the absorbance was read again to determine the fractions that contained the highest amounts of desired protein (Bax or Caspase 3). These fractions were placed in dialysis tubing overnight followed by lyopholization and resuspension in 5mL of ddH$_2$O and EDTA to a final concentration of 0.05mM. The purity of Bax or Caspase 3 was confirmed via Western Blot (described below).

3.2   Protein Estimation

The total protein estimation was done using the BioRad protein assay reagent and performed on isolated Caspase 3and the sdAbs to determine their concentrations. 2.5μL of the sample was added to 797.5μL of ddH$_2$O and 200μL of the BioRad protein assay dye reagent to obtain a final volume of 1mL in a plastic cuvette. The samples were then vortexed and incubated at room temperature for 10 minutes, following which the absorbance readings were taken using a

UV-Visible spectrophotometer at 595nm. A standard curve using 1.0mg/mL BSA solution was developed and the various unknown concentrations of the proteins could be determined from the standard curve.

3.3 Isolation of sdAbs (V_HHs) against recombinant Caspase 3 Through Panning a Llama Phage Display Library

The following work was carried out by Dr.J.Tanha and associates at the National Research Council of Ottawa (Institute for Biological Sciences) (NRC-IBS).

A llama V_HH phage display library described previously was used in panning experiments (Tanha, J et al., 2002). Panning against recombinant Caspase 3 protein was performed as described by Tanha et al. 2002, with the following changes. Phage elution in the second and third rounds additionally involved $MgCl_2$/HCl treatment. To begin with, the bound phages in the microtiter wells were eluted with 200µL and neutralized with 100µL 1M Tris-HCl pH 7.4. Then, emptied wells were incubated with 100µL of 4M $MgCl_2$ at room temperature for 15 min. The eluted phages were removed and the wells were incubated with 100µL of 100mM HCl for five min at room temperature. The $MgCl_2$/HCl-eluted phages were pooled, neutralized with 1.5mL of 1M Tris-HCl pH 7.4, and combined with the triethylamine-eluted phages. One mL of these combined phages was used to infect E. coli for overnight phage amplification and the remaining 1mL was stored at -80°C for future use. V_HH clones were identified from the plates by plaque-PCR and sequencing as described (Tanha, J et al., 2003). Following panning, phage clones from the plates were amplified in microtiter wells and screened for the ability to bind to Caspase 3 by ELISAs using a horse radish peroxidase/anti-M13 monoclonal antibody conjugate (GE Healthcare, Baie d'Urfe, QC, Canada) as the detection reagent.

3.3.1 Expression of V_HHs in *E. coli* and Purification

V_HH genes were cloned from the phage vector into the expression vectors by established cloning techniques. Expression of V_HHs in *E. coli*, followed by purification using immobilized metal affinity chromatography were performed as described (Tanha, J *et al.*, 2003). Protein concentrations were determined by A_{280} measurements using molar absorption coefficients calculated for each protein (Tanha, J *et al.*, 2002).

3.3.2 Formation of the V_HH Fusion Constructs

V_HH genes were inserted in the Hind III/BamH I sites of pEGFP-N1 (V_HH-green fluorescent protein (GFP) fusion) or pDsRed1-N1 (V_HH-red fluorescent protein (RFP) fusion) (BD Biosciences, Mississauga, ON, Canada). The V_HH recombinant vectors were propagated in *E. coli* and were purified using QIAprep® Spin Miniprep kit according to the manufacturer's instructions (QIAGEN, Mississauga, ON, Canada) by Dr.Tanha and associates in NRC-IBS Ottawa.

3.4 Competitive Binding Assay

3.4.1 Standardization of the Binding of cy5.5-labeled sdAb5.2 to Bax

Maxisorp 96 well fluorescence plates (Nalge Nunc, Edmonton, AB) were coated with 10μg/mL of purified Bax protein in PBS with protease inhibitors (10uL/mL PMSF, 1μL/mL Leupep, 1μL/mL Pep A) and incubated overnight at 4°C. The following day the Bax solution was removed and the wells were blocked with 5mg/mL of BSA for 30min. The BSA was removed and the wells were coated with varying concentrations of cy5.5-labeled sdAb5.2 and a saturation curve for the binding between Bax and the labelled sdAb was produced. This

saturation curve was used for the determination of the K_d of the binding between Bax and cy5.5-labeled sdAb, and subsequently the concentration of labelled sdAb used in the competitive binding assay.

3.4.2   Screening of Compounds 1-34 for Competitive binding to Bax

The Maxisorp 96 well plates were coated and incubated overnight with the 10μg/mL Bax solution as described above. This was followed with removal of the supernatant and blocking with 5mg/mL of BSA for 30min. The BSA solution was removed and replaced with the K_d concentration of cy5.5-labelled sdAb5.2 (0.677μM) and the predetermined concentration of compounds (1-34) in reaction buffer (0.25M Sucrose, 1mM $MgCl_2$, 10mM HEPES, 4mg/mL PHPA, 20mM Succinate). This was incubated for 30min after which the supernatant was removed (unbound fraction) and the plate containing the bound fraction was washed twice with reaction buffer. The fluorescence of the supernatant was then read at 675nm excitation and 694nm emission to determine the proportion of cy5.5-labelled sdAb5.2 that remained unbound, and the fluorescence of the plate (with fresh reaction buffer placed inside the wells) was read at the same excitation and emission to determine the proportion of cy5.5-labelled sdAb remained bound to the plate

3.5   Blot Binding Assay

In addition to the competitive binding assay, a blot binding assay was performed to confirm the results of the competitive binding assay. For this assay 1μg of purified recombinant Bax was run on an SDS gel and transferred to nitrocellulose. The nitrocellulose was stained with Ponseau for visualization of the Bax bands. These bands were excised and placed in the

bottom of the wells of a 96-well microtiter fluorescence plate. The wells containing the Bax bands were blocked with 5mg/mL of BSA solution for 30min, with the remainder of the assay performed as described above in "Competetive Binding Assay."

3.6   Cell Culture

3.6.1   Propagation of Cell Lines

SHSY-5Y (Human Neuroblastoma) Cells and NT-2 (Human Tetracarcinoma) Cells were grown in Dulbelco's Modified Eagles Medium (DMEM) F-12 Ham supplemented with 10% (v/v) Fetal Bovine Solution (FBS), 2mM L-glutamine, and 20μg/mL gentamycin. The FBS involved in the maintenance of the NT-2 Cell Line was inactivated at 60°C prior to its addition to the DMEM. The cells were incubated at 37°C, 5% CO_2, and 95% humidity.

3.6.2   Cell Line Subculturing

Cells were thawed and grown in 25cm^2 flasks sterile flasks and were subcultured by aspirating the media off and replacing with 1mL 0.15% Trypsin EDTA and incubating at 37°C for 5min until the cells were capable of detaching with minimal force from the bottom of the flask. Following this, a predetermined amount of fresh media was added to the flasks and the cell suspension was aliquoted into 6-well or 10cm^2 dishes as desired.

3.6.3   Differentiation of SHSY-5Y Neuroblastoma Cells

Plates that were to be used for culturing differentiated cells were first precoated with 0.05mg/mL of collagen diluted in serum-free DMEM F-12 Ham and incubated for 30min in a sterile environment. The collagen solution was then removed, and the cells were added to the

plate in complete DMEM F-12 Ham media supplemented with 10μM retinoic acid for 5 days. After 5 days the media was removed and the cells were washed 3 times with serum-free DMEM F-12 Ham. The media was replaced with 10ng/mL Brain Derived Neurotrophic Factor-supplemented serum-free media and incubated for an additional 5 days.

3.6.4 Transient Transfection of SHSY-5Y Cells

FuGENE 6 Transfection Reagent was used to introduce the anti-Caspase 3 V_HH constructs as well as the RFP constructs into SHSY-5Y cells that had been grown in 6-well plates using the ratio of 3μL of FuGENE reagent per 1μg of DNA as per manufacturer's protocol. The FuGENE was incubated for 10min in 100μL of serum-free media under sterile conditions in a laminar flow hood, following which, 1μg of DNA was added to the solution and incubated for 45min. The total mixture was then added to each well of a 6-well plate and incubated at 37°C with 5% CO_2 and 95% humidity for 24h.

3.7 Preparation of Post-nuclear Cytoplasmic Fraction

In order to isolate the post-nuclear cytoplasmic fraction, cells were first grown to 70% confluency and removed from their 10cm^2 plates by either mechanical dislodging or addition of 1mL of 0.15% Trypsin EDTA. Cells that were mechanically removed were centrifuged at 500xg for 5min. The media as aspirated off and the cells (pellet) were washed twice in 1% PBS (pH 7.4). After this, the pellet was resuspended in Hypotonic Buffer (10mM Tris HCl pH 7.2, 5mM KCl, 1mM $MgCl_2$, 1mM EGTA, 1% Triton X-100) and incubated on ice for 5min. The cell suspension was then mechanically homogenized and centrifuged for 5min at 800xg at 4°C,

following which the supernatant was removed and kept and the pellet was discarded as it consisted of the nuclear pellet.

3.8 Isolation of Mitochondria and Post-mitochondrial Cytosolic Fraction

The post-nuclear supernatant that was isolated as described above was centrifuged again 13,000 x g at 4°C for 10min with once difference being the hypotonic buffer that was used in its initial isolation consisted of 1mM EDTA, 5mM Tris HCl pH 7.2, 210mM Mannitol, and 70mM Sucrose. The pellet obtained consisted of the mitochondrial fraction and the supernatant consisted of the post-mitochondrial cytosolic fraction. The crude mitochondrial pellet was resuspended in isotonic buffer (250mM Sucrose, 1mM MgCl$_2$, 10mM HEPES, 20mM Succinate) and kept on ice and used within 2h for experimentation.

3.9 Monitoring Caspase 3 Activity: Measurement of the Effect the V$_H$Hs have on Caspase 3 Activity

A fluorescence assay was used to evaluate the activity of active Caspase 3 in the presence or absence of the different V$_H$Hs. DEVD-AFC was used as the fluorescent substrate in this assay. This substrate, in the presence of reaction buffer (0.1M HEPES, 2mM DTT, 0.1% CHAPS, 1% sucrose, pH 7.4) and active Caspase 3, was incubated at 37°C for 60min and fluorescence was measured at 400nm excitation and 505nm emission using the SpectraMax Gemini XS (Molecular Devices, Sunnyvale, CA). Caspase 3 activity was measured as relative to the level of fluorescence. For inhibition assays, the V$_H$Hs were incubated with the active Caspase 3 for 30min at 37°C prior to the addition of the DEVD-AFC in the reaction buffer. Following further

incubation for 60min, in a 96 well microtiter plate, fluorescence was measured as described above.

3.10 Measurement of ROS Production from Isolated Mitochondria

The effect each of the compounds has on the activity of Bax was estimated through incubation of Bax with isolated mitochondria in absence and in presence of the compound and subsequent measurement of the H_2O_2 (ROS) generation in each case. The amount of H_2O_2 generated was determined using a fluorometric assay based on a previously published protocol using para-hydroxyphenylacetate (PHPA) as the fluorescent reagent (Li, N et al., 2003). Horse-Radish Peroxidase (HRP) couples the oxidation of PHPA to the stoichiometric reduction of H_2O_2, allowing for a direct correlation. The isolated mitochondria were resuspended in reaction buffer (10mM HEPES (pH 7.4), 250mM Sucrose, 1mM $MgCl_2$, 20mM Succinate and 4mg/mL PHPA) and kept on ice while the protein estimation was performed on the suspensions.

There were four types of reactions performed in each experiment. The first group included three control reactions for the reaction buffer alone, for mitochondria suspended in the reaction buffer, and for mitochondria incubated with Bax. The other reaction types were analogous to the third control group, but with the addition of 20 µM of the compound tested. All reactions contained 4mg/mL PHPA, 10 µg/mL of Bax, 100 µg/mL of mitochondria, and 4U of HRP (added last), and the final volume in each well was kept constant, at 200µL. Each reaction was done in triplicate and read at 320nm excitation and 400nm emission using the Spectra Max Gemini XS immediately after the 30 min incubation at 37°C.

3.11   Western Blot

All the western blots that were conducted used the following protocol with variations in the primary and secondary antibody as needed (monoclonal anti-Bax, polyclonal anti-VDAC, monoclonal anti-caspase 3, and polyclonal anti-actin,). Protein samples were resolved using either 12% or 15% SDS-PAGE and loading between 1μg-50μg of protein per well. The protein was transferred from the gel onto a nitrocellulose membrane which was subsequently blocked using a non-fat milk solution (5% milk in TBST) for 1h on a shaker at room temperature. The membrane was then incubated with the required primary antibody at a dilution of either 1:1000 or 1:2000 (dependent on the antibody chosen) in 2% non-fat milk solution, overnight at 4°C (12-18h). After this incubation period, the membrane was washed with TBST for 15min, followed by three 5min washes and incubated with the secondary antibody (anti-mouse IgG (whole molecule) or anti-rabbit (whole molecule) peroxidase conjugate) at a dilution of 1:2000 in 2% milk solution and incubated at room temperature on a shaker for 1h. The blots were then developed using a ChemiGlow West kit according to manufacturer's protocol and recorded using an Alpha Innotech Corporation Imaging System.

3.12   Induction of Oxidative Stress

3.12.1 Hydrogen peroxide Method

Utilizing a stock H_2O_2 of 10M, a working stock solution of 100mM H_2O_2 was made by diluting with ddH_2O. The stock solution was refrigerated and stored out of light and checked periodically over its shelf life to ensure a lack of degradation. SHSY-5Y, differentiated SHSY-5Y, transiently transfected SHSY-5Y, or NT-2 cells were grown to 70% confluence and treated

with either 50μM or 100μM H_2O_2 for 1h at 37°C. Following this, the media was replaced with fresh, complete media and the cells were incubated for varying time periods and monitored for apoptotic features and protein expression.

3.12.2 Hypoxia/Hypoglycemia Model

SHSY-5Y cells were grown to70% confluence and placed in an oxygen free chamber in a salt solution (110mM NaCl, 5.4mM KCl, 0.8mM $MgCl_2$, 1.8mM $CaCl_2$, 15mM $NaHCO_3$ 15mM HEPES, 50mM Glycine pH 8) instead of the usual complete DMEM F-12 Ham media for 12-24h at 37°C. After this treatment, cells were removed from the chamber and the salt solution was replaced with fresh complete medium and cells were analyzed 24h later.

3.13   Monitoring Apoptosis

3.13.1 Cellular Staining Techniques

3.13.1.1 Nuclear Morphology: Hoechst 33342 Staining

Cells that were placed under oxidative stress conditions were monitored for signs of apoptotic nuclei via Hoechst 33342 staining. The Hoechst stain was added to a cellular suspension to achieve a final concentration of 10μM and incubated for 10min at room temperature in dark conditions. The cells were then examined using fluorescent microscopy and brightly stained, condensed nuclei were taken as apoptotic nuclei. The pictures were processed using Improvision Open*Lab* v3.1.2 and Adobe PhotoShop v8.0.

3.13.1.2 Monitoring Plasma Membrane Flipping: Annexin V Staining

Annexin V conjugate was used to monitor the plasma membrane flipping that occurs in cells undergoing apoptosis. Cells were removed from their plates by either trypsinization or mechanical dislodging and washed twice with PBS. The cellular pellets were resuspended in Annexin V Binding Buffer (10mM HEPES, 10mM NaOH pH 7.5, 140mM NaCl, 2.5mM CaCl$_2$, 50mM Sucrose) with the Annexin V Binding Dye was added to the suspension at a 1:1000 dilution. This suspension was incubated for 15min at room temperature in the dark and 10μL samples were pipetted onto slides and examined using fluorescent microscopy as described above.

3.13.1.3 Monitoring Mitochondrial Membrane Potential: JC-1 Staining

JC-1 staining was used to monitor the mitochondrial membrane potential which becomes disrupted in cells undergoing apoptosis. JC-1 dye was added to cellular suspensions to a final concentration of 10μM and incubated for 45min at 37°C in the dark. The cells were examined using fluorescent microscopy as described above.

3.13.2 Monitoring Intracellular ROS and Protease activity

3.13.2.1 Mitochondrial ROS

Cells that were treated under oxidative stress conditions were harvested and their mitochondria were isolated as described above. These mitochondria were analyzed for their levels of ROS using an Amplex Red assay. Isolated mitochondrial pellets were resuspended in the Amplex Red reaction buffer (2.5mM malate, 10mM succinate), Amplex reagent was added to a final concentration of 50μM, and HRP was added in the ratio of 6U/200μL. The mixture was

incubated at room temperature for 30min prior to reading the fluorescence at 560nm excitation and 590nm emission.

3.13.2.2 Caspase 3 Activity

Cells that had been subjected to oxidative stress treatment were harvested and their post-nuclear cytoplasm was isolated as described above. The Caspase 3 activity was monitored fluorometrically using a DEVD-AFC. This substrate, in the presence of reaction buffer (0.1M HEPES, 2mM DTT, 0.1% CHAPS, 1% sucrose, pH 7.4) and 100µg of post-nuclear cytoplasm sample, was incubated at 37°C for 60min and fluorescence was measured at 400nm excitation and 505nm emission using the SpectraMax Gemini. Caspase 3 activity was expressed as relative fluorescence per 100µg of protein.

3.13.2.3 Immunoprecipitation

Immunoprecipitation was performed to examine the effect of the compounds on the interaction between Bax and VDAC. Mitochondrial fractions were isolated as described above for cells that were completely untreated, placed under oxidative stress and either treated with/without compound. A solution of 1µL anti-VDAC polyclonal antibody with 10µL protein G-Sepharose beads was made in 300µL RIPA buffer (20mM Tris-OH, 150mM NaCl, 10mM KCl and 1% triton X-100) and incubated for 1h at 4°C. Approximately 60µg of mitochondrial protein from each cell type was added to the pre-incubated anti-VDAC solution described above, and both samples were incubated overnight (~18h) at 4°C on a shaker. The immunoprecipitates were collected by centrifugation at 500 x g for 2 min at 4°C followed by washing the pellet three times with RIPA buffer. After the final wash the pellet was resuspended in 30µL of RIPA buffer

and mixed with 10µL of SDS loading buffer and the samples were analyzed using SDS-PAGE

and Western Blot as previously described.

Chapter 4: Results[i]

<div align="center">

Part 1

</div>

4.1 Purification of Recombinant Caspase 3 for Identification of anti-Caspase 3 sdAbs (V_HHs) and Caspase 3 Activity Assay

Recombinant Caspase 3 was expressed in *E. coli*, in fusion with a His_6 tag and was subsequently purified by immobilized metal affinity chromatography. Purified protein was eluted by an imidazole buffer was confirmed to be Caspase 3 by Coomassie staining and Western blotting. It was shown that purified Caspase 3 was present in both active (15kDa) and inactive forms (35kDa) (figure 4.1). The recombinant Caspase 3 was subsequently used for panning experiments against a naïve llama V_HH phage display library (Tanha *et al.*, 2002) and for Caspase 3 activity assays.

4.2 Identification, Binding, and *In Vitro* Functional Analysis of anti-Caspase 3 sdAbs (V_HHs)

Pro/anti-apoptotic proteins are prime targets for selective modulation of apoptosis in treating neurodegeneration and cancer. Caspase 3 is a known universal executioner protein of apoptotic pathway and, thus, a key protein to modulate. In order to obtain apoptosis-modulating antibodies, we panned a naïve llama V_HH phage display library (Tanha, et al., 2002) against recombinant Caspase 3. Screening of 22 colonies gave two different V_HH sequences, VhhCasp31 and VhhCasp32, occurring at frequencies of 19 and 3, respectively (figure 4.2A). The V_HHs had the marker amino acids described previously (Harmsen, *et al.*, 2000). Both V_HHs bound strongly to Caspase 3 but not to a control protein, bovine serum albumin in phage ELISAs

<div align="center">

52

</div>

(figure 4.2B). V_HHs were expressed in fusion with C-terminal c-Myc-His$_5$ tag in *E. coli* and purified to homogeneity for subsequent functional studies.

Next, we performed Caspase 3 activity assays to determine if VhhCasp31 and VhhCasp32 alter the activity of Caspase 3. A tetra-peptide substrate (DEVD) conjugated to AFC was used in this assay. In the presence of active Caspase 3 the substrate is cleaved, releasing the fluorescent AFC which then gives a measure of activity of Caspase 3. Caspase 3 was pre-incubated with V_HHs prior to the addition of the reaction buffer and DEVD-AFC substrate and the activity of Caspase 3 was monitored for decreases or increases in comparison to the reaction without any V_HH or with an irrelevant V_HH. As can be seen in figure 4.2C in the presence of an equimolar concentration of VhhCasp31 (4.7μM), the activity of Caspase 3 (4.7μM) decreases to 61% compared to a non-treated control (100%). Conversely, VhhCasp32 treatment at the same concentration resulted in an increase in Caspase 3 activity of 22.5%. The effect of the V_HHs on Caspase 3 was also found to be concentration dependent: at VhhCasp31 concentrations three times that of Caspase 3 (14.1μM); Caspase 3 activity was decreased to as low as 14.5% of control. At the same concentration, VhhCasp32 treatment led to a 38% increase in Caspase 3 activity. When treated with an irrelevant V_HH, Vhh5.2, under both concentration conditions, Caspase 3 demonstrated negligible changes in activity (figure 4.2C), ruling out the possibility that the modulating effects of VhhCasp31 and VhhCasp32 might be non-specific.
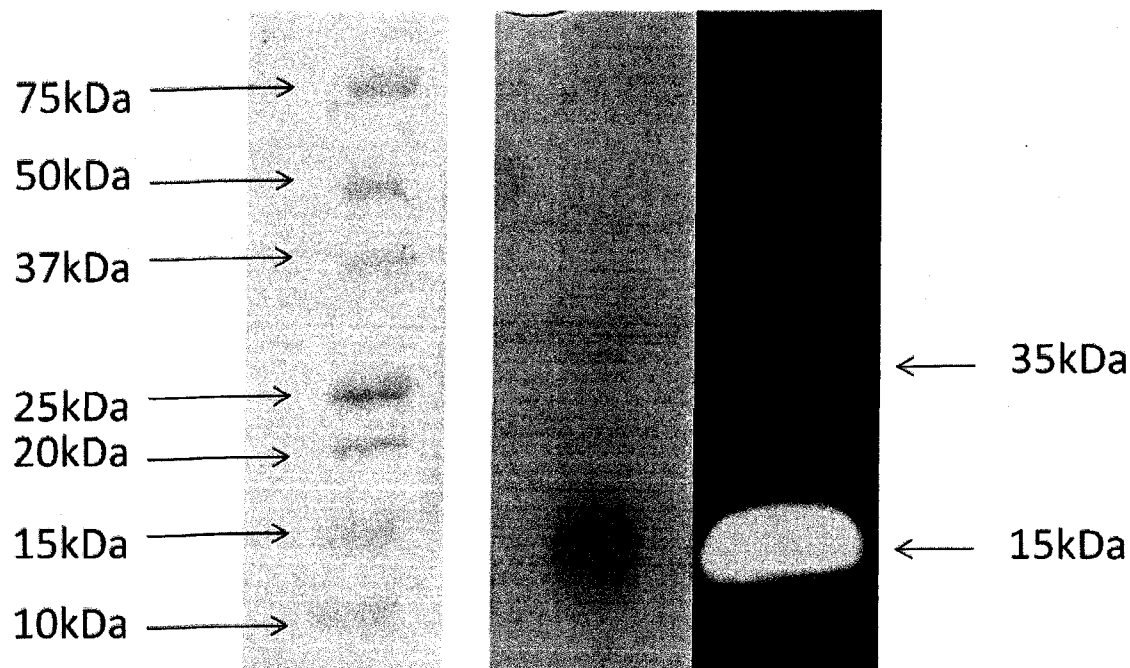
Figure 4.1: Coomassie gel and Western blot of purified recombinant Caspase 3

Coomassie staining and Western blot show bands reacting with anti-Caspase 3 antibodies of the expected size of active (15kDa) and inactive (35kDa) forms.

VhhCasp31	D V Q L Q A S G G G L V Q P G G S L R L S C A A S G S L S R
VhhCasp32	E V Q L Q A S G G G L V Q A G G S L R L S C A A S T N I F R
VhhCasp31	I T V M G W Y R Q A P G K Q R E L V A I I T S S G G - T N Y
VhhCasp32	D K F M A W Y R Q A P G K Q R E L V A S I T T G G R - T D Y
VhhCasp31	A D S V K G R F T I S R D N A K N T V Y L Q M N S L K P E D
VhhCasp32	A D S V K G R F T I S R D N T K D T M Y L Q M N S L K P E D
VhhCasp31	T A V Y Y C L A A R G Y D R Y W G R G T Q V T V S S
VhhCasp32	T A V Y Y C A G F L G - R T Y W G Q G T Q V T V S S

Figure 4.2A: Amino acid sequence of VhhCasp31 and VhhCasp32

Complementarity determining regions 1 (CDR1), CDR2 and CDR3 are underlined and appear sequentially. Dashes are included for sequence alignment.

54
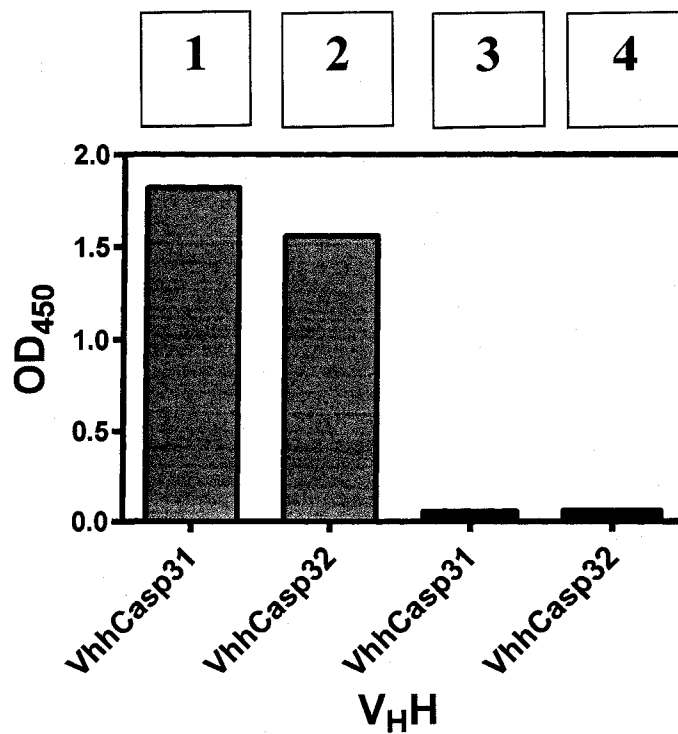
Figure 4.2B: Binding analysis of VhhCasp31 and VhhCasp32

The graph shows the binding, by ELISA, of V_HH-displayed phages VhhCasp31 and VhhCasp32 to immobilized Caspase 3 (columns 1 & 2). The V_HH-phages did not bind to non-specific bovine serum albumin (columns 3 &4).
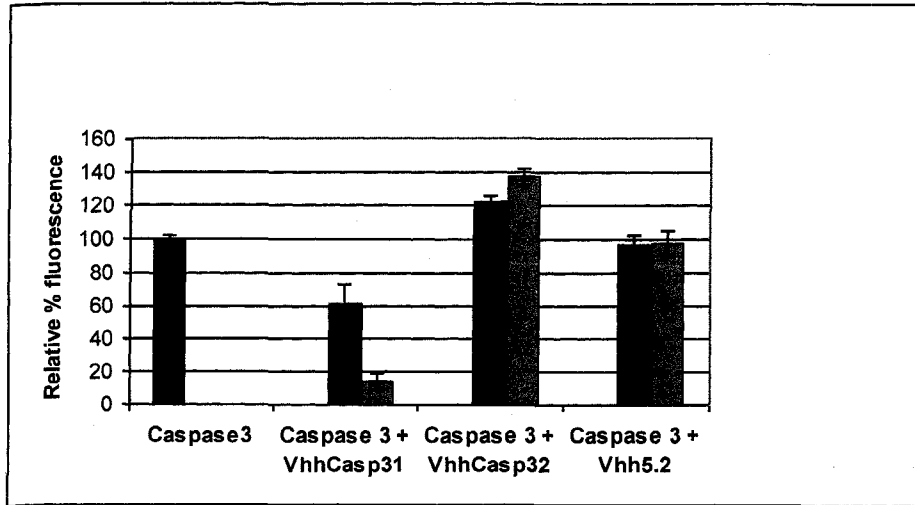
Figure 4.2C: Modulating effect of VhhCasp31 and VhhCasp32 on Caspase 3 activity

4.7μM of active recombinant Caspase 3 was treated with an equal (purple) or 3-fold (green) concentration of VhhCasp31, VhhCasp32 or Vhh5.2 V$_H$H control. The activity of the Caspase 3 was measured in terms of fluorescence release into solution relative to the fluorescence release observed with Caspase 3 alone as described in Materials and Methods. Experiments were performed in triplicates and standard errors were calculated using Microsoft Excel software.

4.3 Effects of Transiently-expressed VhhCasp31 and VhhCasp32 Intrabodies on Oxidative Stress induced Apoptosis in SHSY-5Y cells

Although the results described above indicated that V_HHs were capable of binding as well as modulating the *in vitro* activity of Caspase 3, it remained to be determined if they would affect Caspase 3 when expressed inside mammalian cells, and, thus, modulate apoptosis. We therefore set out to determine the effects of the V_HHs expressed intracellularly as intrabodies on apoptosis. In order to accomplish this, vectors for expression of VhhCasp31 and VhhCasp32 V_HHs as intrabodies in SHSY-5Y mammalian cells were constructed (Gueorguieva, *et al.*, 2006). Following transfection with VhhCasp31- and VhhCasp32-containing expression vectors, the cells were challenged with 50μM H_2O_2 and observed for physiological changes associated with apoptotic cell death by cellular staining with Hoecsht and Alexa Fluor 594-Annexin V. Hoechst dye intercalates with the DNA and thus, highly condensed nuclei like those associated with apoptosis, will fluoresce brightly when viewed under a fluorescent microscope. The Annexin V conjugate binds to phosphatidylserine, a marker for early apoptosis. Thus, cells that fluoresce red will be indicative of apoptosis. The V_HHs were expressed as a fusion protein conjugated to green fluorescent protein, so that a successful V_HH expression can be "visualized" as green fluorescence. It can be seen in figure 4.3A that non-transfected SHSY-5Y cells that were not challenged with H_2O_2 did not show apoptotic nuclei upon Hoechst staining. Also, no positive Annexin V staining indicated healthy, non-apoptotic cells.

Signs of apoptosis can be seen in non-transfected cells challenged with 50μM H_2O_2, indicated by brightly stained, condensed nuclei by Hoechst staining and positive red Annexin V staining (figure 4.3B). SHSY-5Y cells were also transfected with a vector expressing green

fluorescent protein (GFP) alone. These cells were also challenged with 50μM H$_2$O$_2$ and upon staining with Annexin V (red) it can be seen that the GFP does not offer any protection from apoptosis (figure 4.3C) . In contrast, the apoptosis modulating effects of VhhCasp31 and VhhCasp32 can be seen in cells expressing these V$_H$H intrabodies. Cells transfected with VhhCasp31 and challenged with 50μM H$_2$O$_2$ do not display morphology and staining indicative of apoptosis (figure 4.3E), just like the unchallenged VhhCasp31-transfected cells (figure 4.3D). Lastly, it can be noted in figure 4.3F and figure 4.3G that cells transfected with VhhCasp32 display signs of apoptosis even without H$_2$O$_2$ treatment. These results indicate that VhhCasp31 is an antagonist and VhhCasp32 is an agonist of apoptosis.

	(1) Hoechst	(2) Annexin V
A) Nontransfected, non-treated		
B) Nontransfected, treated		
C) Transfected GFP, treated		

	GFP/+ve transfected	Hoechst	Annexin V
D) VhhCasp31 transfected, untreated			
E) VhhCasp31 transfected, 50µM H$_2$O$_2$- treated			
F) VhhCasp32 transfected, untreated			
G) VhhCasp32 transfected, 50µM H$_2$O$_2$- treated			
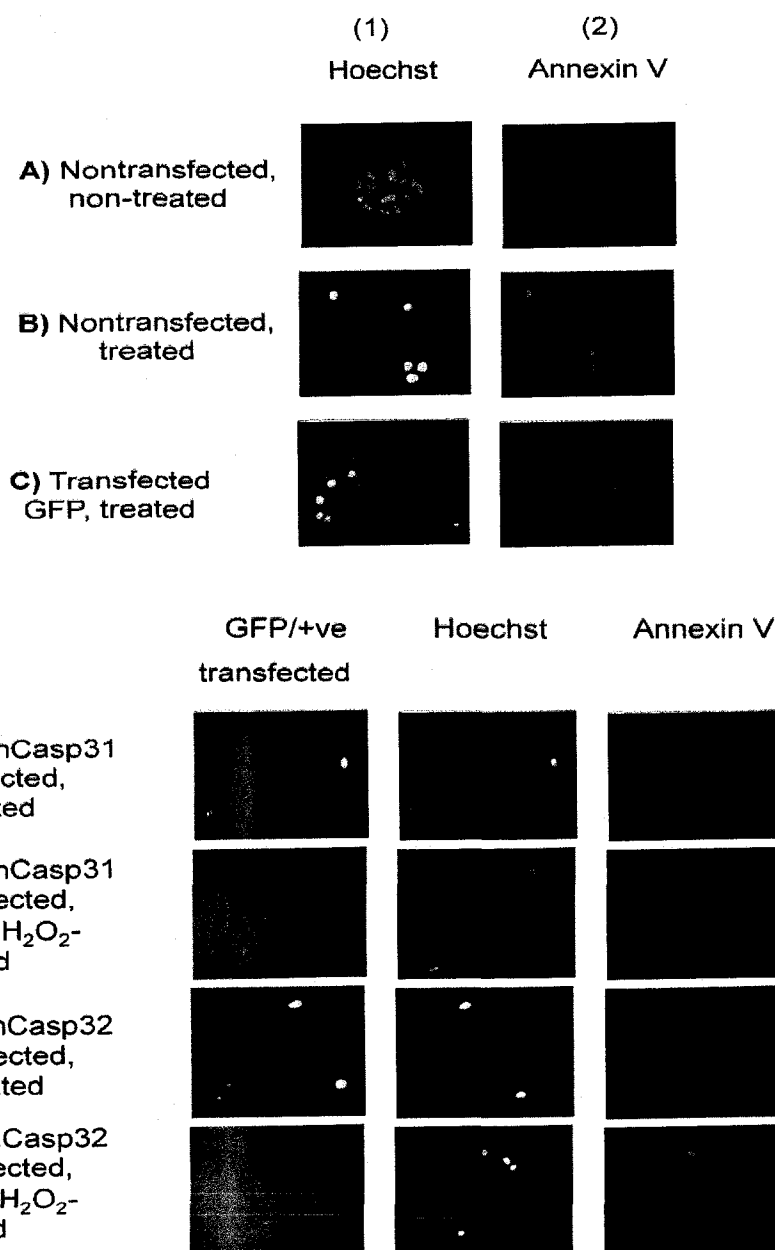
Figure 4.3: Cellular and nuclear morphology of VhhCasp31- and VhhCasp32-transfected SHSY-5Y cells.

Control (nontransfected) SHSY-5Y cells were passaged at the same point as the transfected SHSY-5Y cells and stained with cell permeable Hoechst dye to visualize healthy viable cells. Annexin V Fluor conjugate 594 was also used to visualize any apoptotic cells as described in Materials and Methods. The concentration of H$_2$O$_2$ used was 50µM. As seen in panels D-E, column "GFP", all the V$_H$H-tranfected cells are green indicating a successful expression of V$_H$H-GFP fusion proteins. All fluorescent pictures were taken using an inverted stage fluorescence microscope (Magnification: 400x).

Part 2

4.4 Purification of Recombinant Bax for Binding Assays and Mitochondrial ROS Generation

In order to carry out the competitive and blot binding assays, as well as mitochondrial ROS generation, pro-apoptotic protein Bax was isolated and purified from a culture of *E.coli* cells transformed with the *bax* gene harbouring an N-terminal polyhistidine-tag through affinity chromatography using a Ni^{2+} chelating column (as described in the methods of Chapter 3). The presence of the N-terminal polyhistidine-tagged protein allowed for the use of a metal affinity resin as a method for purifying recombinant Bax. The resin in the HiTrap column utilizes a tetradentate metal chelator to bind the Ni^{2+} ions by occupying four of the six coordination sites of the octahedral binding structure of the metal ion. The remaining two sites are left available for interactions with imidazole ring of the His tails on recombinant Bax. Using a low concentration of imidazole, non-specific proteins were eluted from the column, as imidazole alone has the potential to interact with Ni^{2+}. This was followed by elution of the recombinant Bax using a high concentration of imidazole.

Following purification, the Bax fraction obtained was analyzed using SDS-PAGE and Western blot to ensure purity. Bax is identified as the 40kDa band (figure 4.4) by Western blot, indicating that it was isolated in the homodimer form due to the presence of the non-ionic detergent Triton X-100 used during the purification process (Hsu, Y-T *et al.*, 1997). In this case, 20μg of protein was loaded into the SDS gel, which was subsequently transferred onto a nitrocellulose membrane. The membrane was then probed with monoclonal anti-Bax IgG (primary antibody) that has the recognition site N-terminus of Bax, common to isoforms α, δ,

and β in a 1:1000 dilution in 2% non-fat milk solution. The blot was further probed with a monoclonal anti-mouse HRP conjugate (secondary antibody) using a 1:2000 dilution and developed using ChemiGlow West kit, showing a positive band at 40kDa for Bax. The experiment was subsequently repeated for each individual purification with similar results.

4.5 Standardization of Binding of cy5.5-labeled sdAb5.2 to Bax

Prior to performing any analysis on the ability of the members of the pharmacaphore library to bind competitively to purified Bax in the presence of cy5.5-labeled sdAb5.2, a saturation curve characterizing the concentration-dependent binding of cy5.5-labeled sdAb5.2 to Bax was required (figure 4.5). SdAb5.2 was selected for fluorescent labelling with cy5.5 on its Lys residues, as it possessed the greatest ability to inhibit the function of Bax under oxidative stress conditions (Gueorguieva, *et al.*, 2006). Varying concentrations of cy5.5-labeled sdAb5.2 were added to wells that were precoated overnight with purified homodimer Bax (as described in Chapter 3) and incubated for 30min. Following this, it was determined relative to fluorescence how much was bound to Bax, up until its saturation point (at approximately 10μM). For the purpose of a competitive binding assay involving small molecular weight compounds, it was necessary to determine the concentration of cy5.5-labeled sdAb5.2 where half of the binding sites on Bax protein were occupied.
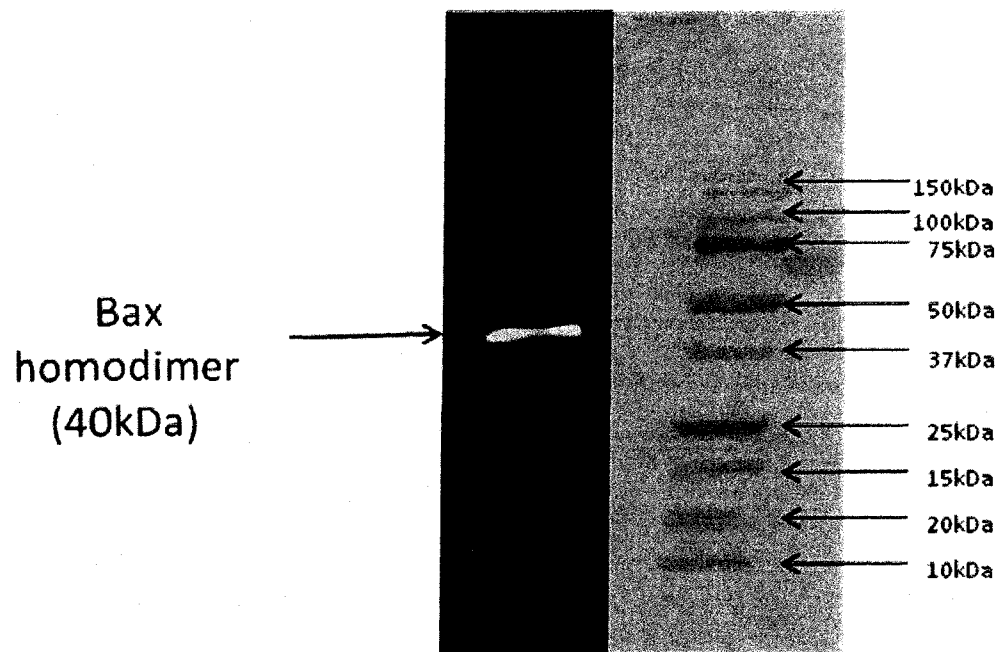
Figure 4.4: Western blot of recombinant purified Bax

...is were anaylyzed for purity through Western Blot using a monoclonal anti-Bax primary
...modimer (40kDa) was detected after incubation with secondary anti-body (anti-mouse IgG
...ijugate) and developed using a ChemiGlow West kit.
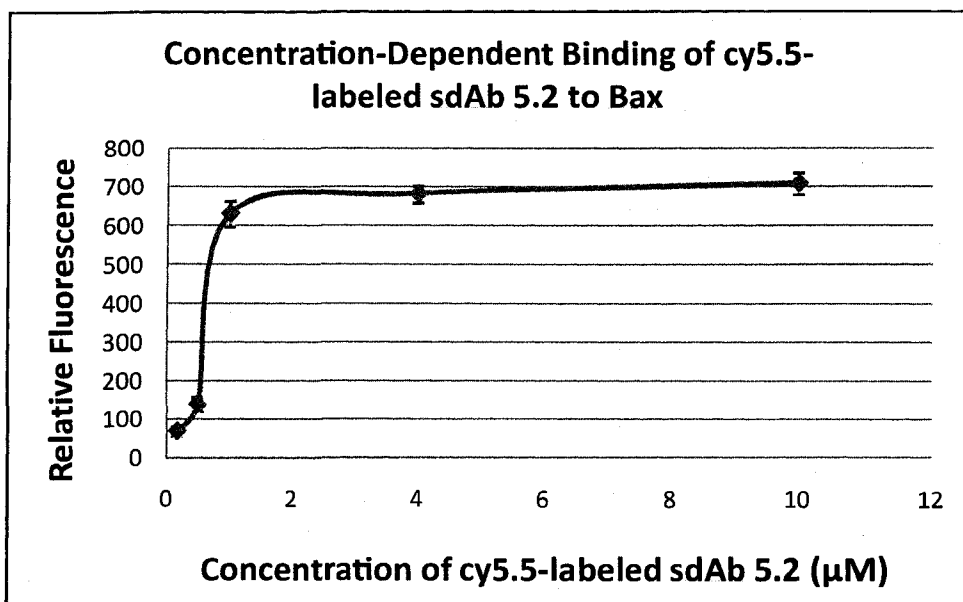
Figure 4.5: Binding curve of cy5.5-labelled sAb5.2 to Bax

Varying concentrations of labelled sdAb5.2 were added to immobilized Bax up to a saturation concentration of 10μM and fluorescence was measured using the SpectraMax Gemini XS fluorescence plate reader. The K_d of labelled sdAb5.2 was determined to be 0.67μM and was the concentration used for subsequent competitive binding assays.

This corresponds to the K_d of cy5.5-labeled sdAb5.2. If Bax were to be fully saturated with the labelled antibody, this would not afford the pharmacaphore the chance to properly compete for binding sites on Bax. The K_d was determined to be 0.67μM and this was the concentration of labelled antibody subsequently used in all competitive binding experiments.

4.6 Ability of Pharmacaphore Library Compounds (1-34) to Bind to Bax in the Presence of cy5.5-labeled SdAb: Competitive Binding Assay

Once the K_d of cy5.5-labeled sdAb5.2 was determined, the 34 small molecule members of the pharmacaphore library were tested for their ability to compete with the labelled antibody for binding sites on Bax. Immobilized Bax was incubated with 0.67μM of the labelled sdAb along with 10μM, 20μM, and 40μM of the pre-chosen compound. The results for 20μM concentration of compound are shown below, as this was the comparable concentration used for the ROS studies, which were performed in tandem with the binding studies. Following 30min of incubation of the labelled sdAb and the chosen compound with Bax, the supernatant was removed. This supernatant contained any unbound compound as well as any unbound labelled sdAb. This supernatant was compared with two control supernatants; one which was from a well with 0.67μM of labelled sdAb, but no immobilized Bax, and the other which contained immobilized Bax as well as labelled antibody. The wells which did not have any immobilized Bax should theoretically have no labelled sdAb binding, and thus have the maximum present in the supernatant, whereas wells with immobilized Bax and labelled sdAb, without any compound present should have the maximum amount of labelled antibody bound. The relative fluorescence of the supernatant from the wells lacking immobilized Bax, but incubated with the labelled sdAb was thus taken as 100% relative fluorescence. In fact, the wells containing labelled sdAb, but

without immobilized Bax displayed on average 4.249%-15.36% of labelled sdAb that remained bound to the plate. In the wells that contained immobilized Bax incubated with labelled sdAb alone, the percent relative fluorescence readings for the supernatant had values on average between 58.12-66.88%, and the percent relative fluorescence of the bound was between 30.61-50.2%. If a particular compound was capable of competing with the labelled sdAb for binding spots, then the displaced labelled sdAb should be present in the supernatant, thus increasing the fluorescence of the supernatant, giving a percent relative fluorescence value above 66.88%. The plate, that possessed the bound fractions, was washed to remove any loosely bound labelled antibody and compound. This plate was read to determine the amount of labelled sdAb that remained bound after incubation with the designated compound.

4.6.1 Compounds that did not display competitive binding specifically for Bax

Out of the 34 compounds that were screened, 25 did not show any ability to competitively bind to Bax in the presence of the labelled sdAb. This means that when compared to wells that contained only immobilized Bax and labelled sdAb, there should be a similar binding profile. This is what was seen for compounds 1-6 (figure 4.6.1A), compounds 7-12 (figure 4.6.1B), compounds 13-15, 18, and 20 (figure 4.6.1C), and compounds 21, 27-29, 32, and 34 (figure 4.6.1D). There was no change in the amount of labelled sdAb bound to immobilized Bax (it remains constant between 30.61-46.75%), meaning the compound did not compete for binding sites, and there was no increase in fluorescence in the supernatant (it remained between 50.89-68.71%).

Figure 4.6.1A: Compounds 1-6 do not compete with cy5.5-labeled sdAb5.2 for Bax binding sites

Following 30min of incubation with labeled sdAb5.2 and immobilized Bax, compounds 1-6 were not able to compete for binding sites on Bax. There was no change in unbound portion of labeled sdAb, as none was dislodged ᵣₒₘ Bax binding sites. The amount bound and unbound was measured relative to fluorescence, which was ᵤᵣₑd using the SpectraMax Gemini XS fluorescence plate reader.

Figure 4.6.1B: Compounds 7-12 do not compete with cy5.5-labeled sdAb5.2 for Bax binding sites

Following 30min of incubation with labeled sdAb5.2 and immobilized Bax, compounds 7-12 were not able to ⟨⟩mpete for binding sites on Bax. There was no change in unbound portion of labeled sdAb, as none was dislodged ⟨⟩ Bax binding sites. The amount bound and unbound was measured relative to fluorescence, which was measured using the SpectraMax Gemini XS fluorescence plate reader.
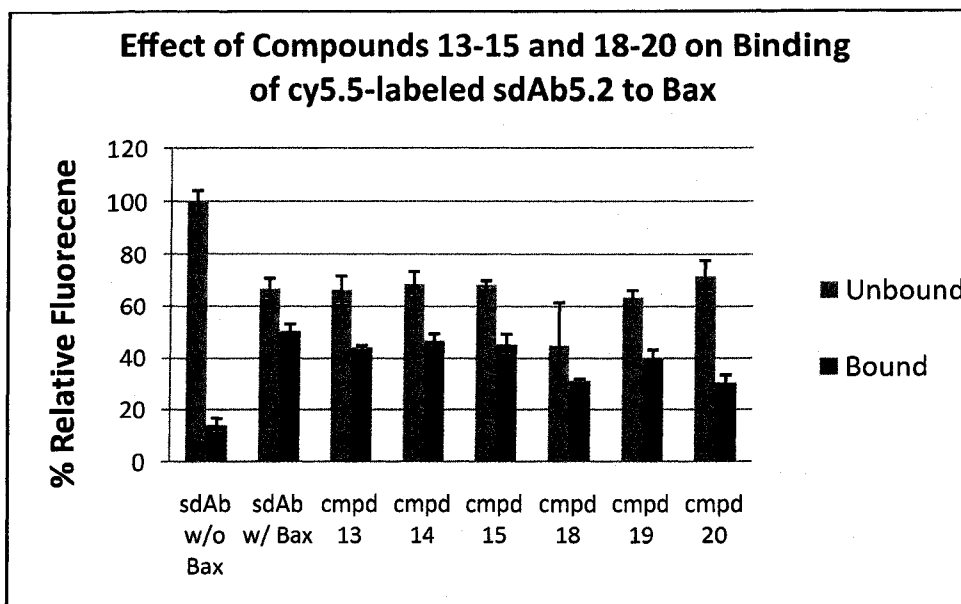
Figure 4.6.1C: Compounds 13-15, and 18-20 do not compete with cy5.5-labeled sdAb5.2 for Bax binding sites

Following 30min of incubation with labeled sdAb5.2 and immobilized Bax, compounds 13-15 and 18-20 were not able to compete for binding sites on Bax. There was no change in unbound portion of labeled sdAb, as none was dislodged from Bax binding sites. The amount bound and unbound was measured relative to fluorescence, which was measured using the SpectraMax Gemini XS fluorescence plate reader.

Effect of Compounds 21, 27-29, 32, and 34 on Binding of cy-5.5-labeled sdAb5.2 to Bax
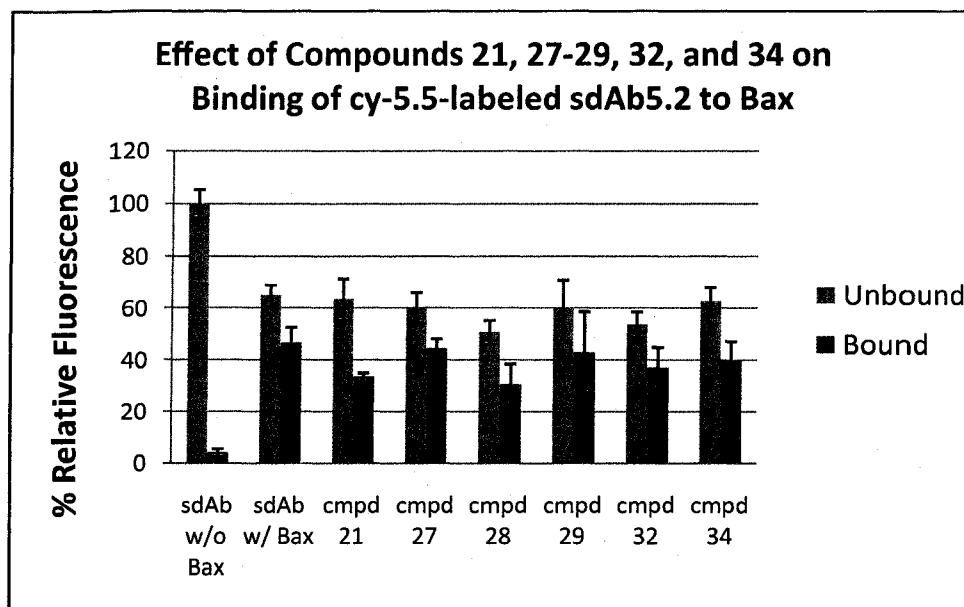
Figure 4.6.1D: Compounds 21, 27-29, 32, and 34 do not compete with cy5.5-labeled sdAb5.2 for Bax binding sites

Following 30min of incubation with labeled sdAb5.2 and immobilized Bax, compounds 21, 27-29, 32, and 34 were not able to compete for binding sites on Bax. There was no change in unbound portion of labeled sdAb, as none was dislodged from Bax binding sites. The amount bound and unbound was measured relative to fluorescence, which was measured using the SpectraMax Gemini XS fluorescence plate reader.

4.6.2 Compounds Displaying Competitive Binding Specifically for Bax

Out of the 34 compounds, there were 9 that appeared to competitively bind to immobilized Bax in the presence of the cy5.5-labelled sdAb5.2. When compared to the control well without immobilized Bax, containing labelled sdAb alone, there was a similar binding profile. This is what was seen for compounds 13-15 and 22-24 (figure 4.6.2A), and 25, 30, 31, and 33 (figure 4.6.2B). There was a difference in the amount of labelled sdAb bound to immobilized Bax (it decreased to between 8.214-38%), meaning the compound did compete for binding sites, and there was an increase in fluorescence in the supernatant (between 77.25-94.4%).

4.7 *In Vitro* Measurement of Mitochondrial ROS Due to Bax: Effect of Pharmacaphore Compounds on ROS Levels

The 34 compounds were initially tested to understand if binding to Bax would translate into inhibition of its function. Since there is no direct measure of Bax activity on mitochondria, we chose to measure the ROS production by mitochondria incubated with active Bax homodimer. Previous work in our laboratory has shown that in presence of isolated mitochondria, Bax is able to permealize the MOM and subsequently lead to increase in ROS production (Naderi, J *et al.*, 2006). ROS was detected fluorimetrically via measurement of the oxidation of PHPA coupled to the reduction of H_2O_2 by horseradish peroxidase (HRP). Thus, if by binding to Bax the 34 compounds were able to individually block the detrimental effect of Bax on the mitochondria, we would expect lowered fluorescence in samples containing isolated mitochondria, Bax, and compound in comparison to the positive control of mitochondria and Bax alone.

The data collected for this section represents a compilation of three to five independent experiments. In each individual experiment, the fluorescence detection for the negative control (mitochondrial alone) was subtracted from each subsequent fraction (e.g. the fractions containing mitochondria, Bax, and compounds). Additionally, the positive control fraction (mitochondria with Bax only) was taken as 100% fluorescence (or 100% ROS) and the fluorescence of all test samples (mitochondria, Bax, and compounds) were calculated relative to this control. The results were grouped together as either having no effect on Bax-induced ROS, an intermediate effect on Bax-induced ROS, or having a lowering effect on Bax-induced ROS.

4.7.1 Compounds Displaying no Effect on Bax-Induced Mitochondrial ROS at 20μM Concentration

Considering the 34 compounds, there were 4 compounds (compounds 9, 27, 32, and 34) that did not affect the level of Bax-induced mitochondrial ROS (figure 4.7.1). When compared to the positive control (Bax incubated with isolated mitochondria), which was designated as 100% relative fluorescence, the levels of percent relative fluorescence were all close to 100% (between 85-105% ± standard deviation). Interestingly, in the previous competitive binding studies, these compounds did not show any ability to competitively bind to Bax in the presence of cy5.5-labelled sdAb5.2.

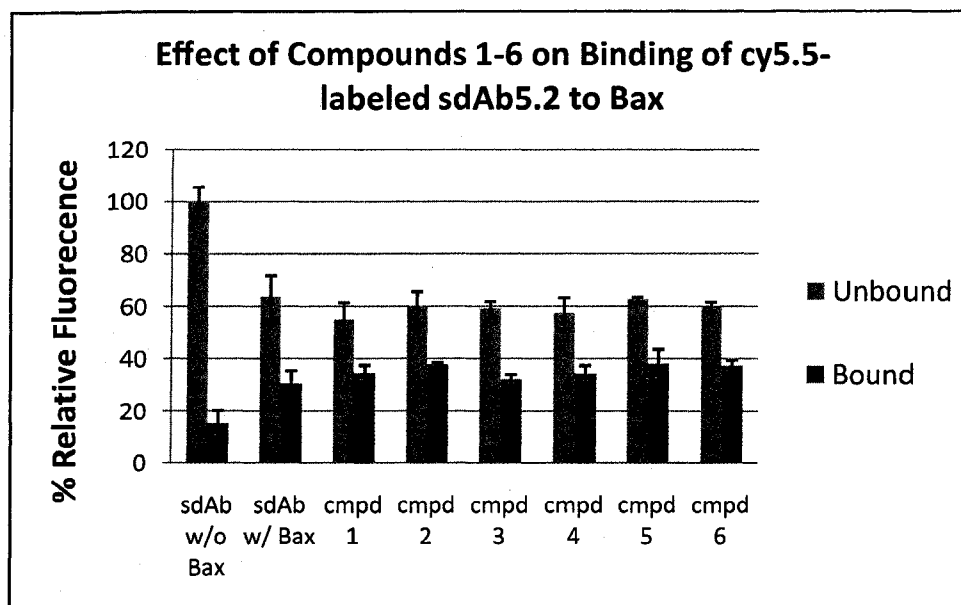**Effect of Compounds 16, 17, 22-24 on Binding of cy5.5-labeled sdAb5.2 to Bax**
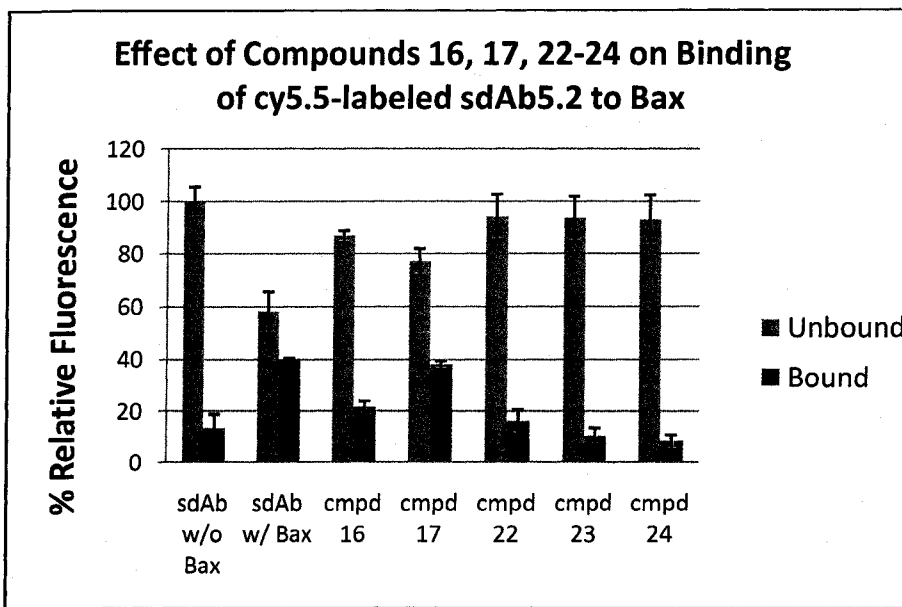
Figure 4.6.2A: Compounds 16, 17, and 22-24 compete with cy5.5-labeled sdAb5.2 for Bax binding sites

Following 30min of incubation with labeled sdAb5.2 and immobilized Bax, compounds 16, 17, and 22-24 were able to compete with the labeled sdAb for binding sites. This was reflected in the significant increase of fluorescence found in the unbound supernatant fractions, and the decrease in fluorescence of the bound fractions.
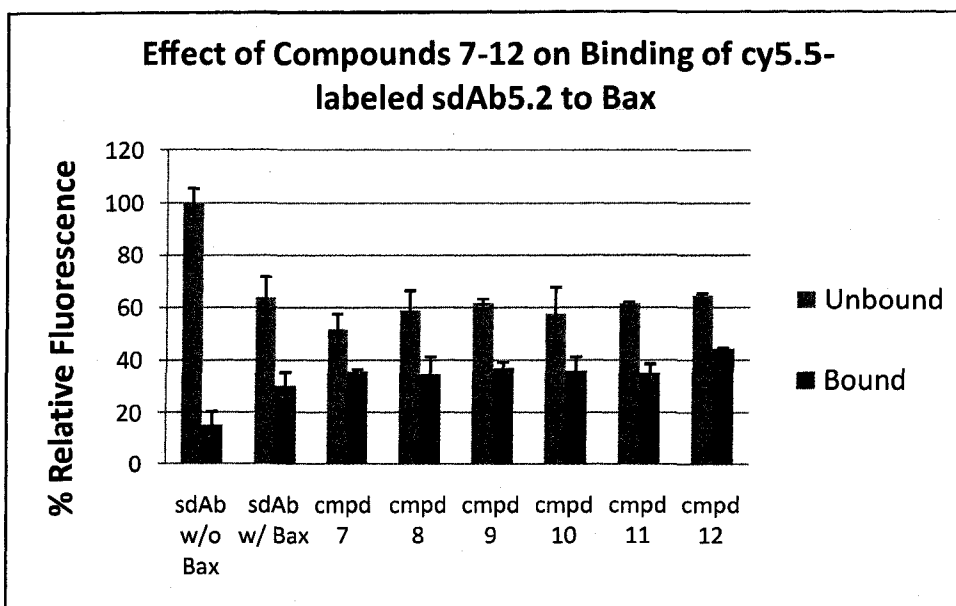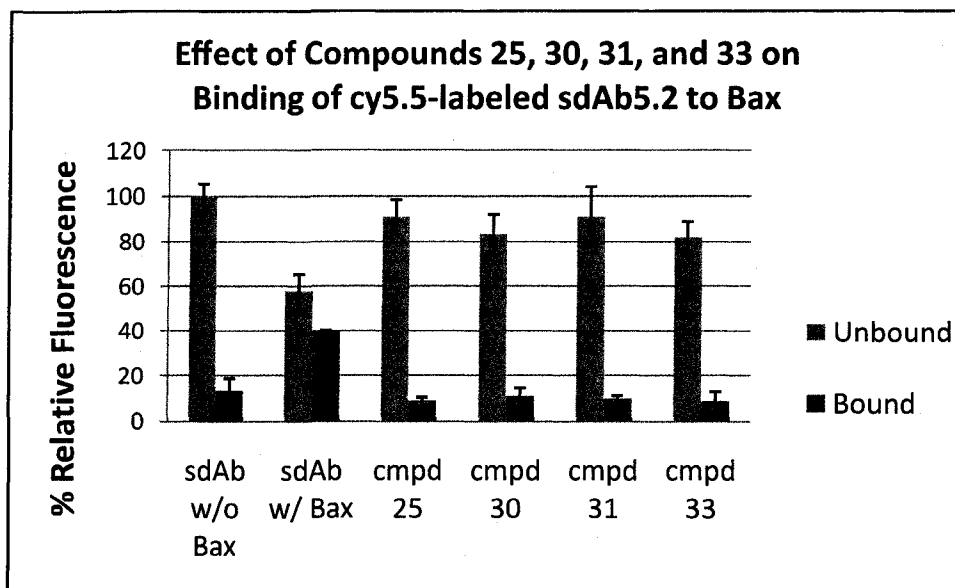
Figure 4.6.2B: Compounds 25, 30, 31, and 33 compete with cy5.5-labeled sdAb5.2 for Bax binding sites

Following 30min of incubation with labeled sdAb5.2 and immobilized Bax, compounds 25, 30, 31, and 33 were able to compete with the labeled sdAb for binding sites. This was reflected in the significant increase of fluorescence found in the unbound supernatant fractions, and the decrease in fluorescence of the bound fractions.

4.7.2 Compounds that had an Intermediate Effect on Lowering the Level of Bax-Induced Mitochondrial ROS

There were 17 compounds that had an intermediate effect on lowering the level of Bax-induced mitochondrial ROS which can be seen in figures 4.7.2A and 4.7.2B. The level of ROS was reduced to values between 40 and 80% relative fluorescence when compared to the positive control in this group of compounds. Out of these 17 compounds, only compounds 24 and 31 also displayed an ability to competitively bind to Bax in the presence of the labeled sdAb (see figure 4.6.2A).

4.7.3 Compound that increased the level of Bax-Induced Mitochondrial ROS

There was only one compound that increased the level of Bax-induced mitochondrial ROS, thus causing oxidative stress. Compound 25 increased the level of mitochondrial ROS by 30% when compared to the 100% relative fluorescence of the positive control (Bax incubated with mitochondria alone) (figure 4.7.3). Furthermore, compound 25 displayed an ability to competitively bind to Bax in the presence of the labeled sdAb (see figure 4.6.2B).
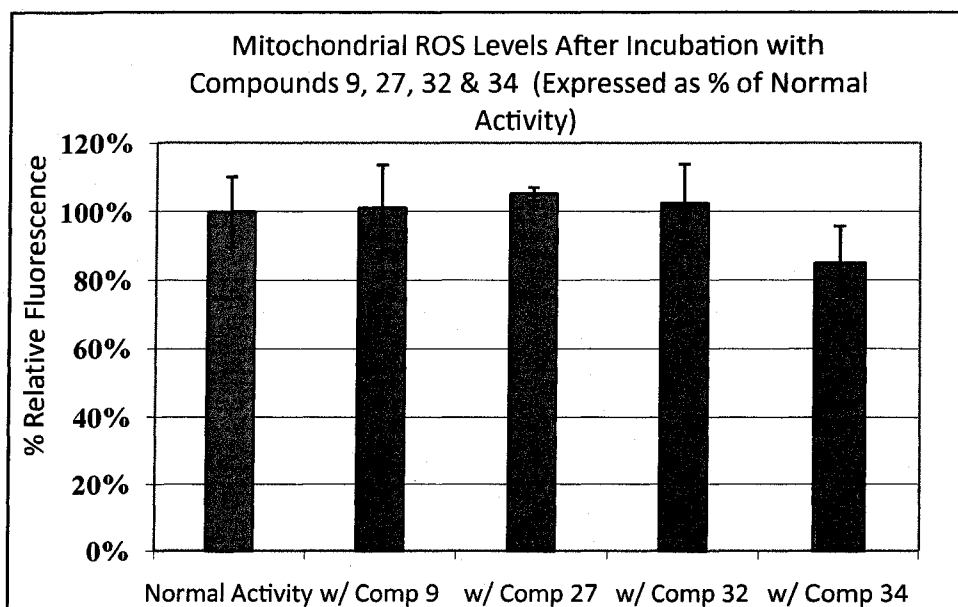
Figure 4.7.1: Compounds 9, 27, 32, and 34 have no effect on the level of Bax-induced mitochondrial ROS

Mitochondria (100µg/mL), isolated from SHSY-5Y, cells were incubated with 10µg/mL of Bax either in the presence or absence of compounds 9, 27, 32, or 34 in a reaction buffer and ROS generation was measured as described in Methods. ROS generated by Bax alone was taken as 100%. The compounds did not affect ROS generation and retained a percent relative fluorescence close to 100%. Fluorescence was monitored after 30min and red using the SpectraMax Gemini fluorescence plate reader and the standard error shown as error bars was calculated using Microsoft Excel program and the data obtained from six separate experiments.   .

Figure 4.7.2A: Compounds 1-7 and 10 have an intermediate effect on lowering Bax-induced mitochondrial ROS

Mitochondria ($100\mu g/mL$), isolated from SHSY-5Y, cells were incubated with $10\mu g/mL$ of Bax either in the presence or absence of compounds 1-7 or 10 in a reaction buffer and ROS generation was measured as described in Methods. ROS generated by Bax alone was taken as 100%. The compounds had an intermediate effect on ROS generation; lowering levels by approximately 40-60% relative fluorescence. Fluorescence was monitored after 30min and read using the SpectraMax Gemini fluorescence plate reader and the standard error shown as error bars was calculated using Microsoft Excel program and the data obtained from six separate experiments. .

Figure 4.7.2B: Compounds 23, 24, 26, and 29-33 have an intermediate effect on lowering Bax-induced mitochondrial ROS

Mitochondria (100μg/mL), isolated from SHSY-5Y, cells were incubated with 10μg/mL of Bax either in the presence or absence of compounds 23-26, 28-31, or 33 in a reaction buffer and ROS generation was measured as described in Methods. ROS generated by Bax alone was taken as 100%. The compounds had an intermediate effect on ROS generation; lowering levels by approximately 30-60% relative fluorescence. Fluorescence was monitored after 30min and read using the SpectraMax Gemini fluorescence plate reader and the standard error shown as error bars was calculated using Microsoft Excel program and the data obtained from six separate experiments.

4.7.4 Compounds that Significantly Lowered the Level of Bax-Induced Mitochondrial ROS

There were 5 compounds that demonstrated the ability to significantly lower Bax-induced mitochondrial ROS, thus offering some protection against oxidative stress. Compounds 8, 17, 18, 20, and 22 lowered mitochondrial ROS to 20-30% when compared to the positive control (100% relative fluorescence) as seen in figure 4.7.4. Out of these 5 compounds, compound 17 and 22 also displayed an ability to competitively bind to Bax in the presence of the labeled sdAb (see figure 4.6.2A). However, the competitive binding of compound 17 was shown to be very weak as seen in figure 4.6.2A, whereas the competitive binding of compound 22 was stronger, thus making compound 22 a desirable compound to study further in terms of its protective abilities. Compounds 8, 18, and 20 did not previously show any ability to competitively bind to Bax; however they could be protecting the mitochondria in another manner.

4.7.5 Effect of Varying Concentrations of Compound 22 on Mitochondrial ROS Levels

Since we observed that compound 22 was not only capable of competitive binding to Bax in the presence of the labelled sdAb, but was also able to significantly lower the levels of Bax-induced ROS at $20\mu M$ concentration, it was important to observe the effect of compound 22 at higher concentrations and in comparison to the known anti-oxidant Coenzyme Q_{10} (CoQ_{10}). CoQ_{10}, at a concentration of $230\mu M$, was shown to lower the relative ROS levels to 40%. Previous studies have shown that water-soluble CoQ_{10} has the ability to lower Bax-induced ROS, making it a valuable positive control (Naderi *et al.*, 2006). Furthermore, when the concentration of compound 22 was elevated to 30 and $40\mu M$, a reduction in relative ROS to 20% and 10% respectively was noted (figure 4.7.5). The next step would be to observe if this trend could be

translated to neuronal precursor (SHSY-5Y) cells. This *in vivo* model would allow us to monitor the effects of concentration of compound 22 on cell viability and toxicity, in addition to its protective abilities in oxidative stress conditions.

4.8   Blot Binding Assay: Confirmation of Binding of Compound 22 to Bax in the Presence of cy5.5-labeled sdAb5.2

Prior to commencement of the *in vivo* studies involving compound 22, confirmation via an alternative competitive binding assay was required. For this, a blot binding assay was utilized. In this assay, purified recombinant Bax was run on an SDS gel and transferred to nitrocellulose paper. This ensured that Bax was immobilized prior to incubation with the labelled sdAb and compound and was not lifting off, making it present in the supernatant. It can be seen in figure 4.8 that compound 22 does indeed competitively bind to Bax in the presence of labelled sdAb. This was compared with a compound that was found to be non-specific for Bax in the previous competitive binding assay (compound 9). In this blot binding assay, the fluorescence given by the bound fraction in the wells containing immobilized Bax with labelled sdAb alone was taken as 100% relative fluorescence, and all other fluorescent values were taken relative to this. It can be observed in figure 4.8 that when the immobilized Bax and labelled sdAb were incubated with compound 22, the relative fluorescence value of the bound fraction decreased to 45.58% ±12.39% and the unbound or supernatant fraction increased to 78.759% ±15.40%, indicating that there was competition for binding sites on Bax. In comparison, when incubated with the nonspecific compound 9, the relative fluorescence value of the bound fraction remained at nearly 100% with

79

Mitochondrial ROS Levels After Incubation with Compound 25 (Expressed as % of Normal Activity)
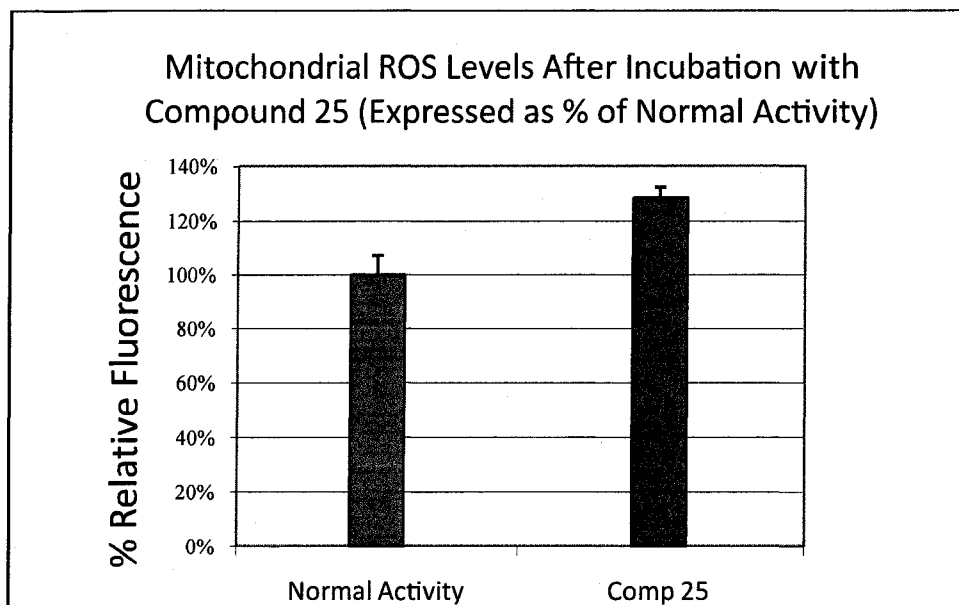
Figure 4.7.3: Compound 25 increases the level of Bax-induced mitochondrial ROS

Mitochondria ($100\mu g/mL$), isolated from SHSY-5Y, cells were incubated with $10\mu g/mL$ of Bax either in the presence or absence of compound 25 in a reaction buffer and ROS generation was measured as described in Methods. ROS generated by Bax alone was taken as 100%. Compound 25 increased ROS generation by approximately 30% relative to the control. Fluorescence was monitored after 30min and read using the SpectraMax Gemini fluorescence plate reader and the standard error shown as error bars was calculated using Microsoft Excel program and the data obtained from six separate experiments.
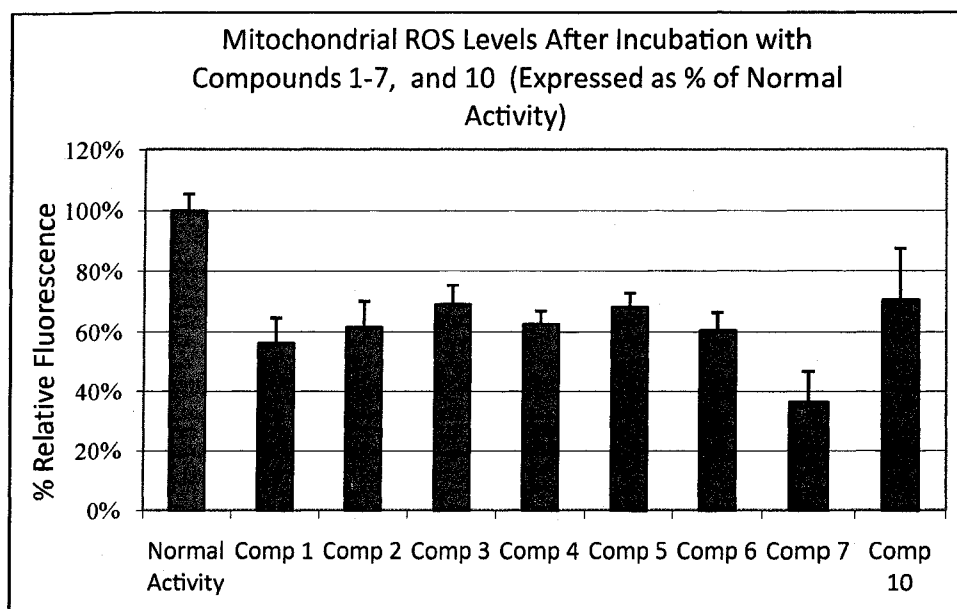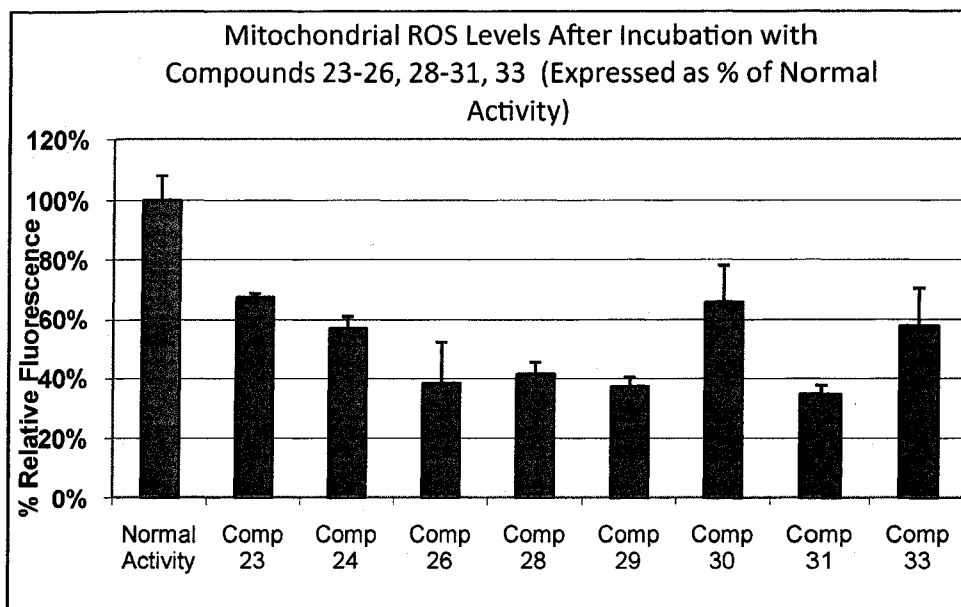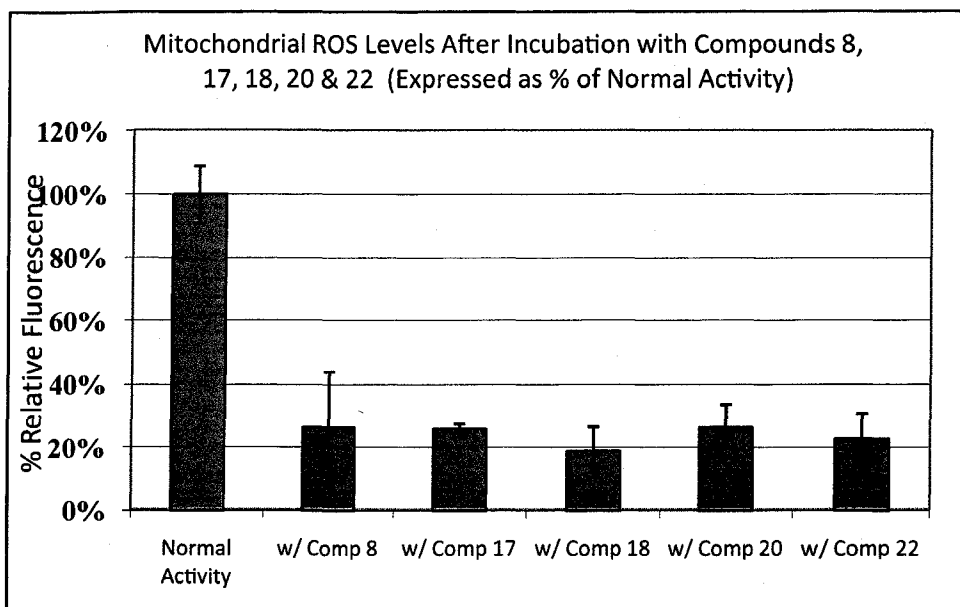
Figure 4.7.4: Compound 8, 17, 18, 20, and 22 significantly lower the level of Bax-induced mitochondrial ROS

Mitochondria (100μg/mL), isolated from SHSY-5Y, cells were incubated with 10μg/mL of Bax either in the presence or absence of compounds 8,17,18,20, or 22 in a reaction buffer and ROS generation was measured as described in Methods. ROS generated by Bax alone was taken as 100%. The compounds had a significant effect on lowering ROS generation; lowering levels by approximately 70-80% relative to the control. Fluorescence was monitored after 30min and read using the SpectraMax Gemini fluorescence plate reader and the standard error shown as error bars was calculated using Microsoft Excel program and the data obtained from six separate experiments.
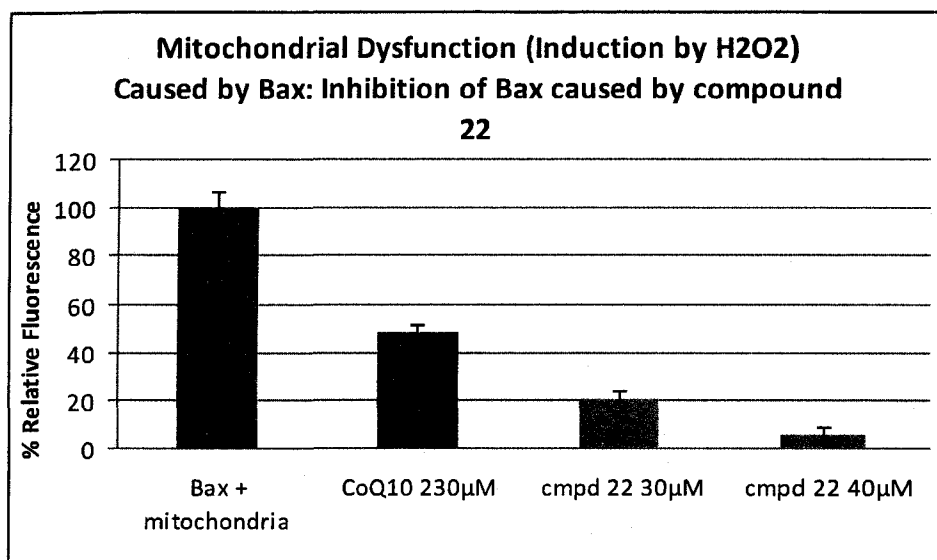
Figure 4.7.5: Effect of varying concentration of compound 22 on levels of Bax-induced mitochondrial ROS

Mitochondria (100μg/mL), isolated from SHSY-5Y, cells were incubated with 10μg/mL of Bax either in the presence or absence of compound 22 or CoQ$_{10}$ in a reaction buffer and ROS generation was measured as described in Methods. ROS generated by Bax alone was taken as 100%. Compound 22 had a significant effect on lowering ROS generation at varying concentrations. Compound 22 (40μM) lowered levels by nearly 90% relative to the control. Fluorescence was monitored after 30min and read using the SpectraMax Gemini fluorescence plate reader and the standard error shown as error bars was calculated using Microsoft Excel program and the data obtained from six separate experiments.
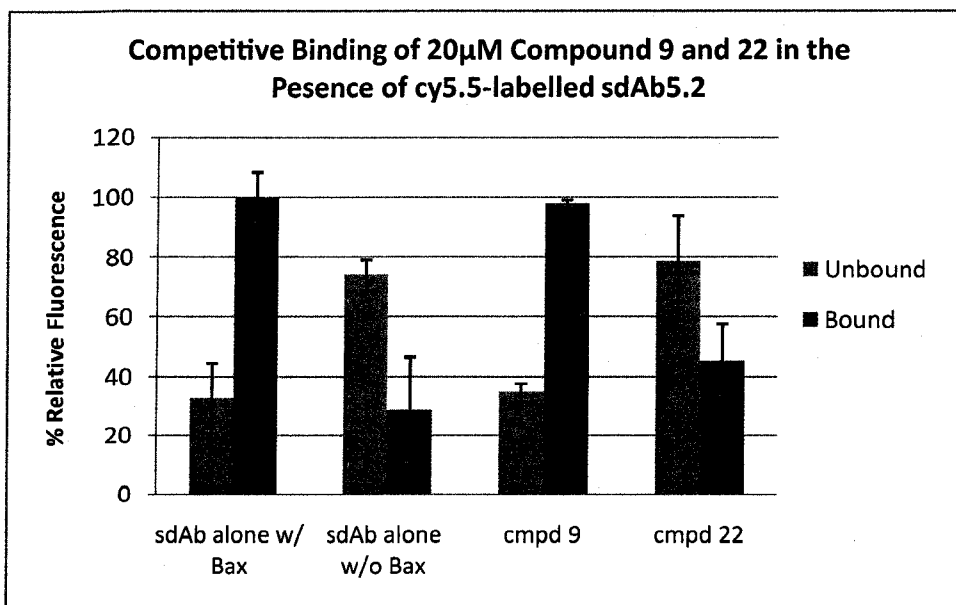
Figure 4.8: Blot binding assay: Compound 22 displays the ability to competitively bind to Bax in the presence of cy5.5-labeled sdAb5.2

Following 30min of incubation with immobilized Bax and labelled sdAb, compound 22 effectively competed for binding spots on Bax. This is seen by the decrease (by 50%) in the amount of bound labelled sdAb, and reflected in ~~ase (by 50%) in the unbound fraction of labelled sdAb. Compound 9 did not hav any effect on the amount ~~d, labelled sdAb (still at 100%), and there was no change reflected in unbound fraction. Fluorescence was measured using a SpectraMax Gemini fluorescence plate reader.

a value of 97.968% ±1.3315% and the unbound fraction (34.965% ±3.0117%) was comparable to the unbound fraction of the Bax incubated alone with labelled sdAb (33.0466% ±11.984%). This confirmed that compound 9 was indeed nonspecific and did not compete with labelled sdAb for binding sites on Bax and that compound 22 was indeed competitively binding to bax in the presence of the labelled sdAb.

4.9   *In vivo* Analysis of the Capability of Compound 22 to Prevent Apoptosis in Neuronal Cell Lines

Following the *in vitro* analysis of the ability of compound 22 to bind to Bax at various concentrations, and lower the levels of Bax-induced mitochondrial ROS, it was necessary to monitor the capability of compound 22 to halt apoptosis due to exogenous oxidative stress. The intracellular environment that encompasses the mitochondria is quite different than isolated mitochondria that are treated on their own with Bax and compound 22, and thus the effect of compound 22 could be quite different inside the cell. This involved tracking particular hallmarks of apoptosis such as apoptotic cellular and nuclear morphology, plasma membrane flipping, loss of MMP, and protease activation. Mammalian cell lines were pretreated with compound 22 and then subjected to external oxidative stress and monitored over a specified period of time for signs of apoptosis.

4.9.1   Monitoring Nuclear Morphology and Plasma Membrane Flipping 24h Following 100µM H_2O_2 Treatment in SHSY-5Y Cells

SHSY-5Y neuroblastoma cells were grown and treated with H_2O_2 treatment as described in the Methods section. As previously discussed, H_2O_2 causes oxidative stress leading to

apoptosis if the cell cannot act to detoxify it. Consequently, the cells were treated with $100\mu M$ H_2O_2, which has been used in previous studies, to initiate oxidative-stress-induced apoptosis. After 24h cells were monitored for two particular signs of apoptosis: brightly stained, condensed nuclei made visible by Hoechst 33342 staining, and plasma membrane flipping made visible by Annexin V-FITC binding. Hoechst 33342 labels DNA by preferentially binding to A-T base pairs, allowing nuclei to become visible under UV light. Early during apoptosis, the membrane phospholipid phosphatidylserine (PS) flips from the inner to the outer leaflet of the plasma membrane. Once exposed to the extracellular environment, binding sites on PS become available for Annexin V, a phospholipid binding protein with a high affinity for PS. Annexin V can be conjugated to a fluorochrome such as FITC which allows for visualization under UV light. It can be seen in figure 4.9.1A that the untreated control cells display both healthy nuclei and minimal Annexin V staining, which is typical for untreated cells. Control cells that were challenged with $100\mu M$ H_2O_2 display a significant amount of cells with brightly stained condensed nuclei indicative of apoptosis, in addition to a considerable amount of plasma membrane flipping observed by the green stain of the Annexin V-FITC congugate. SHSY-5Y cells exposed to $100\mu M$ H_2O_2 and $20\mu M$ of nonspecific compound 9, displayed similar apoptotic features (brightly stained condensed nuclei and plasma membrane flipping) as cells treated with $100\mu M$ H_2O_2 alone. This indicated that compound 9 did not offer any protection against H_2O_2-induced apoptosis 24h-post treatment. Conversely, cells that were treated with $100\mu M$ H_2O_2 and $20\mu M$ of compound 22 remained resistant to apoptosis as indicated by the healthy nuclear morphology of the Hoechst stained cells, and the lack of plasma membrane flipping apparent in the Annexin V figures.

Quantitatively, cell counting (healthy vs. apoptotic nuclei) provided us with an idea of the percent cell viability in the different treatment groups 24h post-100μM H_2O_2. Five different fields were taken, and the percent cell viability was an average of the five different fields. It can be noted in figure 4.9.1B that untreated SHSY-5Y cells had a cell viability of 84.93%, whereas cells that were treated with 100μM H_2O_2, and those treated with 100μM H_2O_2 and compound 9 possessed cell viability percentages of 52.74%, and 53.27% respectively. In contrast, cells that were challenged with 100μM H_2O_2 and treated with compound 22 had a cell viability of 80.98%, which is comparable to the untreated cell population.

4.9.2 Monitoring Nuclear Morphology and Plasma Membrane Flipping 48h Following 100μM H_2O_2 Treatment in SHSY-5Y Cells

SHSY-5Y cells were grown and treated in an identical manner as above, except the nuclear morphology and signs of membrane flipping were monitored 48h post-100μM H_2O_2, as opposed to 24h. Similar results, both qualitatively, and quantitatively were observed at the 48h time point when compared to the 24h time point. SHSY-5Y cells that were treated with 100μM H_2O_2 and non-specific compound 9 displayed brightly stained, condensed nuclei in addition to plasma membrane flipping 48h post treatment (comparable to cells challenged with 100μM H_2O_2 alone) (figure 4.9.2A). Cells that were treated with 100μM H_2O_2 and compound 22 had healthy nuclear morphology and no apparent plasma membrane flipping 48h post treatment as seen in figure 4.9.2A.

Quantitatively, the cell viability that was observed 48h post-100μM H_2O_2 was similar to that of the 24h treatment as noted in figure 4.9.2B. However, the cell viabilities of the cells

treated with 100μM H₂O₂, and those treated with 100μM H₂O₂ and compound 9 possessed slightly lower cell viabilities of 46.52%, and 47.64% respectively.

4.9.3   Mitochondrial ROS is Lowered by Compound 22 24h Post-100μM H₂O₂ Treatment

Since we observed that cells challenged with 100μM H₂O₂ could be rescued from apoptosis by treatment with compound 22 (seen by the healthy nuclear morphology and absence of plasma membrane flipping), we wanted to examine the mitochondria for any change in levels of ROS. As discussed previously, excessive levels of mitochondrial ROS can lead to oxidative stress in the cell, leading to initiation of the apoptotic pathway. Increased levels of ROS can lead to DNA damage, p53 activation, followed by activation of Bax. Cells that were treated with 100μM H₂O₂ have an increase in mitochondrial ROS and thus it was important to see if compound 22 was able to protect the cell from apoptosis by lowering the levels of mitochondrial ROS by inhibiting Bax. It is seen in figure 4.9.3 that mitochondria harvested from SHSY-5Y cells challenged with 100μM H₂O₂ display a 40% increase in ROS when compared to the untreated control cells. Mitochondria isolated from cells that were treated with 100μM H₂O₂ and a nonspecific compound (compound 9) display the same levels of ROS as cells challenged with 100μM H₂O₂ alone, thus showing that it is not capable of diminishing the levels of ROS. Conversely, mitochondria harvested from cells that were treated with 100μM H₂O₂ and compound 22 show levels of ROS comparable to the untreated control mitochondria alone (between 80-100 % relative fluorescence).
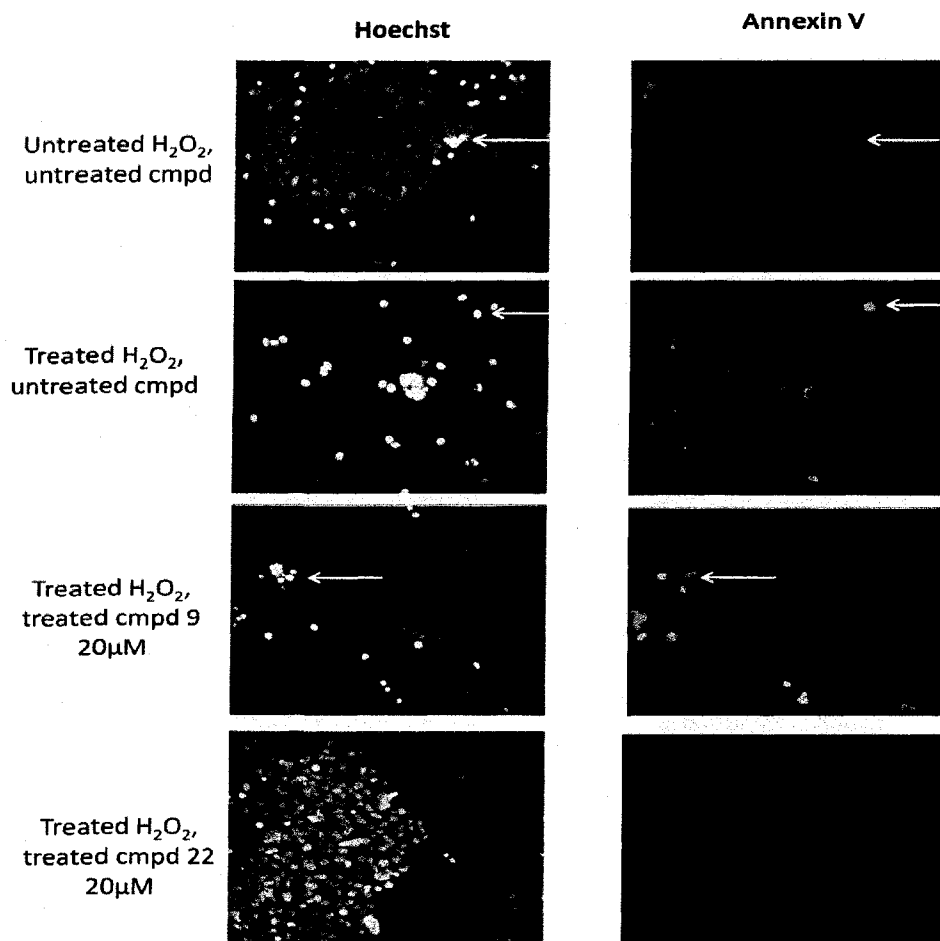
Figure 4.9.1A: Nuclear morphology and plasma membrane flipping of SHSY-5Y cells 24h post 100μM H₂O₂ treatment

Control cell lines that were untreated show predominantly healthy nuclear morphology, with minimal plasma – membrane flipping that reflected only normal amount of apoptosis. Control cell lines treated with 100μM H₂O₂ show many brightly stained condensed nuclei made visible by Hoechst staining (white arrow) and significant plasma membrane flipping (Annexin V staining) indicated by the white arrow. Cells treated additionally with compound 9 still display apoptotic nuclei and plasma membrane flipping, whereas cells treated additionally with compound 22 do not and are comparable to control untreated cells. All fluorescent pictures were taken using an inverted stage fluorescence microscope (Magnification: 400x).

Figure 4.9.1B: Viability of SHSY-5Y cells 24h post-100μM H₂O₂ treatment

24h following 100μM H₂O₂ treatment, cultures were stained with Hoechst. Healthy and apoptotic nuclei from three separate experiments were counted using 5 fields/cell line/experiment, and the number of healthy cells was plotted as a percentage of all the cells counted as Cell Viability. SHSY-5Y cells that were treated with compound 22 show strong resistance to apoptosis, with cell viability values close to those of the untreated control cells (~80% cell viability).

Hoechst   **Annexin V**

Untreated H₂O₂, untreated cmpd

Treated H₂O₂, untreated cmpd

Treated H₂O₂, treated cmpd 9 20uM

Treated H₂O₂, treated cmpd 22 20uM
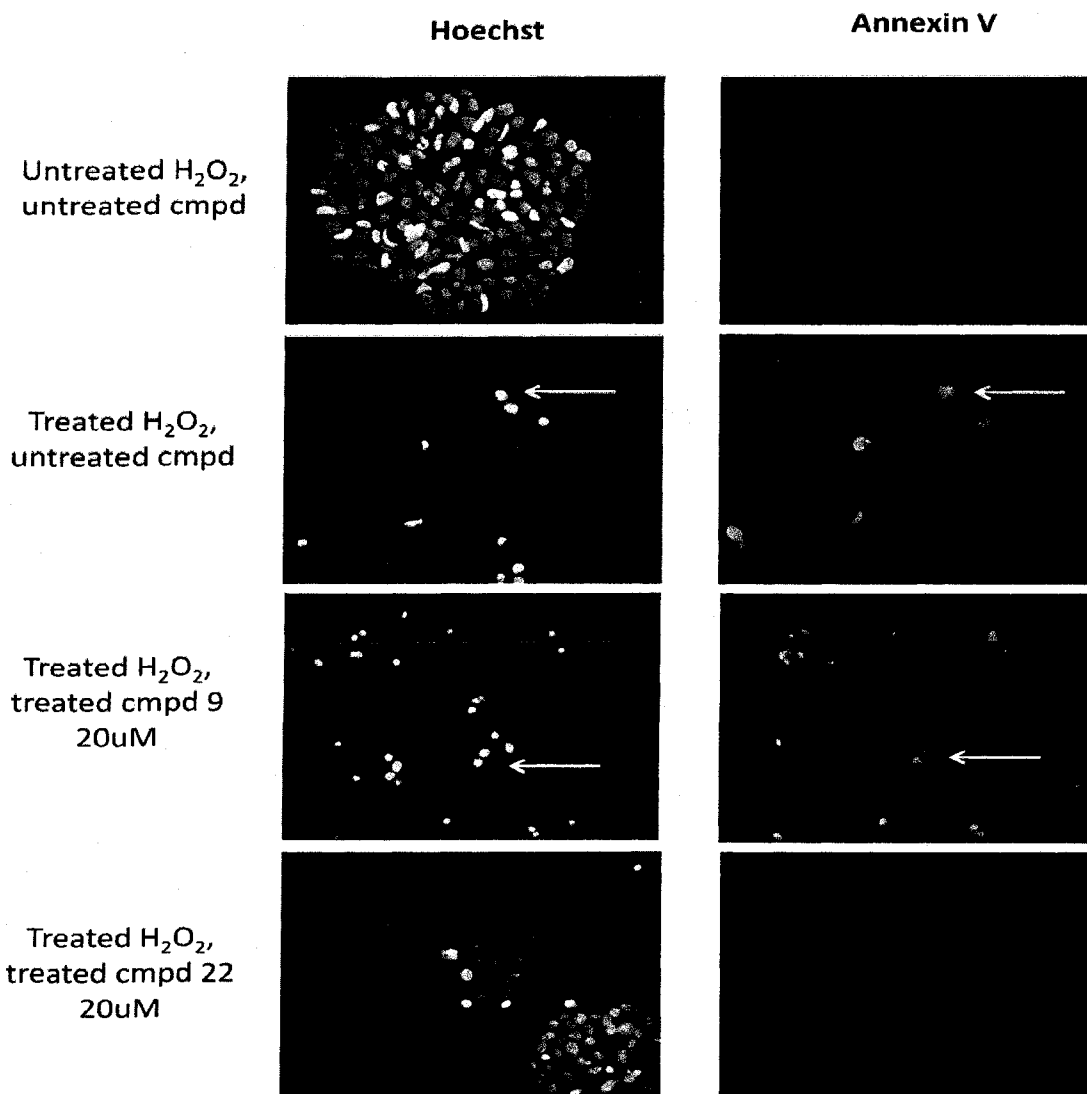
Figure 4.9.2A: Nuclear morphology and plasma membrane flipping of SHSY-5Y Cells 48h post-100μM H₂O₂ treatment

Control cell lines that were untreated show predominantly healthy nuclear morphology, with no plasma membrane flipping. Control cell lines treated with 100μM H₂O₂ show many brightly stained condensed nuclei made visible by Hoechst staining (white arrow) and significant plasma membrane flipping (Annexin V staining) indicated by the white arrow. Cells treated additionally with compound 9 still display apoptotic nuclei and plasma membrane flipping, whereas cells treated additionally with compound 22 do not and are comparable to control untreated cells. All fluorescent pictures were taken using an inverted stage fluorescence microscope (Magnification: 400x).

Figure 4.9.2B: Viability of SHSY-5Y cells 48h post-100μM H₂O₂ treatment

48h following 100μM H₂O₂ treatment, cultures were stained with Hoechst. Healthy and apoptotic nuclei from three separate experiments were counted using 5 fields/treatment group/experiment, and the number of healthy cells was plotted as a percentage of all the cells counted as Cell Viability. SHSY-5Y cells that were treated with compound 22 show strong resistance to apoptosis, with cell viability values close to those of the untreated control cells (~80% cell viability).
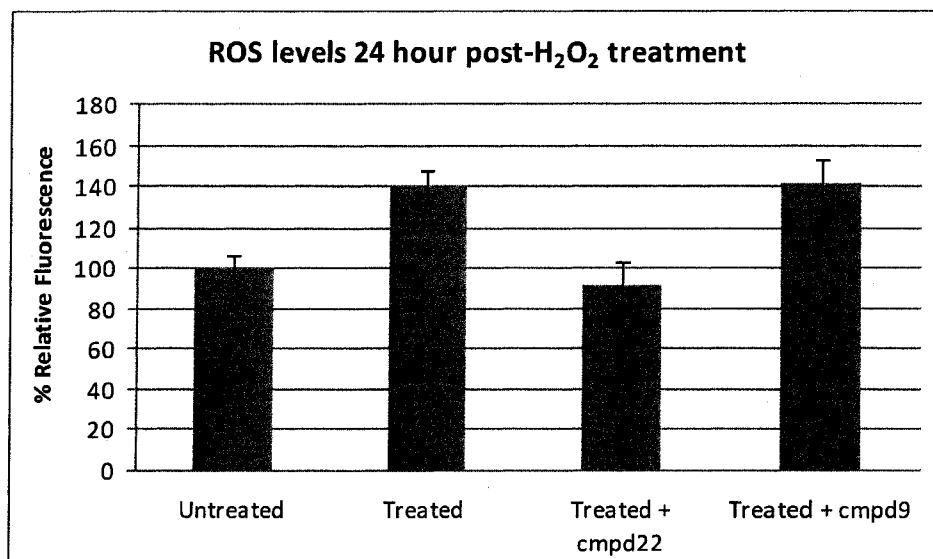
Figure 4.9.3: Mitochondrial ROS levels are lowered by compound 22 24h post-100µM H₂O₂ treatment

SHSY-5Y cells treated with 100µM H_2O_2 were harvested 24h later and the mitochondria were isolated. Levels of ROS were measured and expressed relative to the untreated control mitochondria. Compound 22 lowered mitochondrial ROS caused by 100µM H_2O_2 to levels comparable to the untreated control mitochondria (~ 100% relative fluorescence).

4.9.4 Active Caspase 3 levels are Lowered by Compound 22 24h Post-100μM H₂O₂ Treatment

In order to further examine the role of compound 22 in halting H₂O₂-induced apoptosis, the levels of Caspase 3 were monitored 24h following treatment. Caspase 3 is a pro-apoptotic protease involved primarily in the execution phase of apoptosis. As mentioned previously, it can be activated following release of Cytochrome c from the mitochondria, or through cleavage by Caspase 8. An assay based on the use of DEVD-AFC substrate can be used to determine the levels of active Caspase 3 fluorimetrically, as active Caspase 3 will cleave at the carboxy-terminal of aspartic acid residues, thus releasing the AFC fluorophore which can be picked up by a fluorescence plate reader. Cells that are undergoing apoptosis will have increased levels of active Caspase 3; this result was noted fluorimetrically in the post-nuclear cytosolic fractions harvested form cells treated with 100μM H₂O₂ (figure 4.9.4A). There was an increase of 66.54% in active Caspase 3 relative to the control untreated post-nuclear cytosol. This was reflected in the western blot of the post-nuclear cytosol for active Caspase 3 as seen in figure 4.9.4B, where there is an increase in intensity versus the control untreated.

4.9.5 Cell Viability in Differentiated SHSY-5Y Cells treated with 100μM H₂O₂

SHSY-5Y cells were differentiated as described in the methods section and challenged with 100μM H₂O₂ for 1h and monitored for signs of apoptosis 24h later. Since SHSY-5Y cells are neuronal precursor cells, it is important to observe the effects of compound 22 on fully differentiated neurons in determining its potential as a stroke therapeutic. Cells were monitored for signs of apoptosis by observing complete cellular morphology, nuclear morphology, the status of plasma membrane lipids, and lastly, $\Delta\Psi_m$.

4.9.5.1 Cellular Morphology of Differentiated Cells 24h Post-Treatment

Differentiated SHSY-5Y cells that were challenged with $100\mu M$ H_2O_2 were monitored for changes in their cellular morphology 24h post treatment. Healthy, differentiated neurons have cell bodies clustered together, with neurites projecting from them as seen in the untreated cells of figure 4.9.5.1. Differentiated cells that were observed 24 post-$100\mu M$ H_2O_2 treatment appeared to have shrunken in size, have membrane blebbing, and apoptotic bodies; all hallmarks of apoptosis (figure 4.9.5.1). Next, compound 22 and nonspecific compound 9 were tested for their ability to halt apoptotic events 24h following $100\mu M$ H_2O_2. Cells that were treated alone with compound 9 do not display any morphological signs of apoptosis; however, when challenged with H_2O_2, the morphological signs of apoptosis are seen as in figure 4.9.5.1. Cells that were treated with compound 22 alone do not display cellular morphology associated with apoptosis, and in contrast to cells treated with compound 9 and $100\mu M$ H_2O_2, those treated with compound 22 and $100\mu M$ H_2O_2 display healthy cellular morphology comparable to the control untreated cells.

4.9.5.2 Nuclear Morphology and Plasma Membrane Flipping of Differentiated Cells 24h Post-treatment

Following the observation of the cellular morphology, differentiated SHSY-5Y cells were monitored by nuclear morphology and plasma membrane flipping. As noted with the undifferentiated SHSY-5Y cells, differentiated SHSY-5Y cells that were untreated display healthy nuclei indicated by lighter Hoechst staining and an oval shape (figure 4.9.5.2A). Differentiated cells that were challenged with $100\mu M$ H_2O_2 exhibit brightly stained condensed
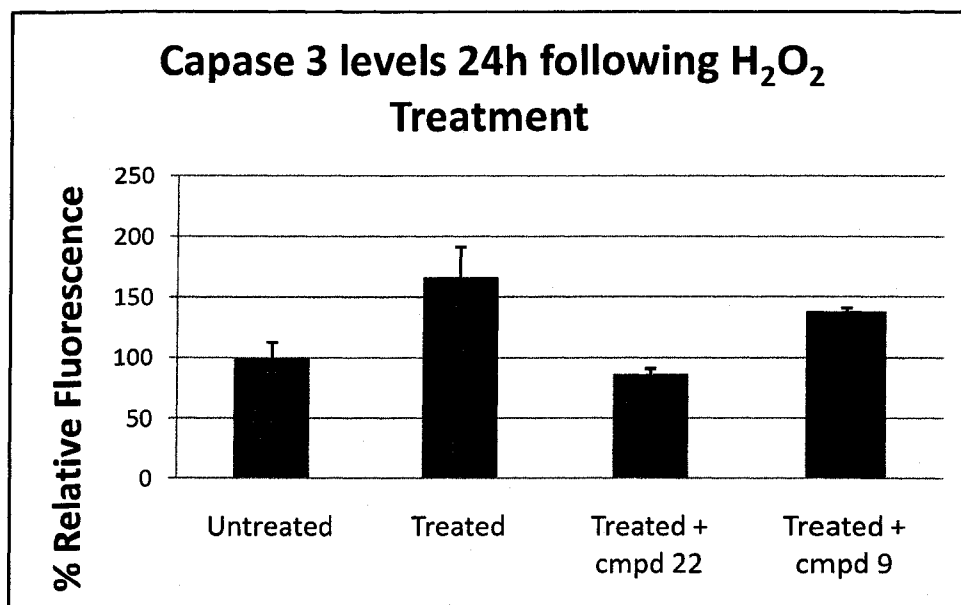
Figure 4.9.4: Post-nuclear cytosol isolated from cells challenged with 100μM H_2O_2 and treated with compound 22 display lower levels of active Caspase 3 similar to control, untreated cells

SHSY-5Y cells treated with 100μM H_2O_2 were harvested 24h later and the post-nuclear cytosol was isolated. Levels of active Caspase 3 were measured and expressed relative to the untreated control cytosol. Cytosol from cells that were treated with compound 22 displayed lower levels of active Caspase 3 (comparable to untreated control) than cytosol from cells treated with 100μM H_2O_2 alone.

nuclei indicative of apoptosis, as well as plasma membrane flipping highlighted by Annexin V staining. As shown before, as well as in this case, cells challenged with 100μM H_2O_2 and treated with compound 9 still have apoptotic nuclei and plasma membrane flipping, whereas those treated with compound 22 demonstrate healthy nuclei and a lack of plasma membrane flipping as visible in figure 4.9.5.2A.

Cell viability was again quantified by counting dead and alive apoptotic nuclei with the population of untreated cells having a percent viability of 84.02% and those treated with 100μM H_2O_2 possessed a cell viability of 50.83%. Cells that were challenged with 100μM H_2O_2 and treated with compound 9 had a cell viability of 46.45%, whereas those treated with compound 22 had 76.35% viable cells (figure 4.9.5.2B).

4.9.5.3 Nuclear Morphology and Mitochondrial Membrane Potential of Differentiated Cells 24h Post-treatment

Another method of detecting apoptosis is by monitoring mitochondrial membrane permealization, utilizing JC-1 dye, which was performed in tandem with Hoechst staining. This will reveal whether cells that have lost their $\Delta\Psi_m$, also possess apoptotic nuclei. As previously discussed, IM permeabilization involves the formation of pores or channels that cause the dissipation of the $\Delta\Psi_m$ established across the IM. Lipophilic cations accumulate in the mitochondrial matrix, driven by $\Delta\Psi_m$. Since the $\Delta\Psi_m$ ranges from 120 to 180mv in physiological conditions (the intramitochondrial side is electronegative), the concentration of cations is normally 2 to 3 logs higher in the mitochondrial matrix than in the cytosol. Due to this, different cationic flurochromes can be utilized to measure the $\Delta\Psi_m$ (Castedo, et al., 2002; Metivier et al., 1998).

Untreated

Treated 100μM H₂O₂

Untreated, treated cmpd 9

Treated 100μM H₂O₂, treated cmpd 9

Untreated, treated 20μM cmpd 22

Treated 100μM H₂O₂, treated 20μM cmpd 22
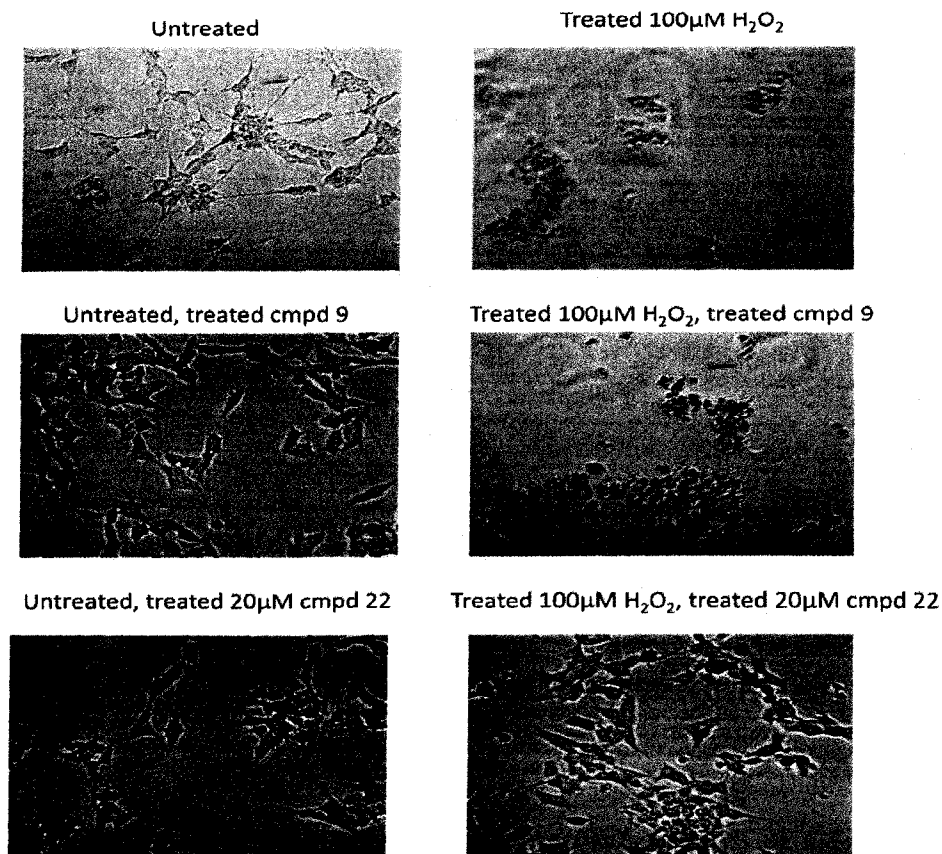
Figure 4.9.5.1: Differentiated SHSY-5Y cells treated with 20μM compound 22 display healthy cellular morphology following exposure to 100μM H₂O₂

SHSY-5Y cells were differentiated into neurons as described in Methods and cell morphology was monitored 24h following 100μM H₂O₂ treatment. Untreated cells, cells treated with compound 9 or 22 alone, or a combination of 100μM H₂O₂ and compound 22, show healthy morphology and neurites. Cells that were treated with 100μM H₂O₂, or a combination of 100μM H₂O₂ and compound 9 display condensed, shrunken morphology with membrane blebbing consistent with apoptosis. (Magnification: 400x).
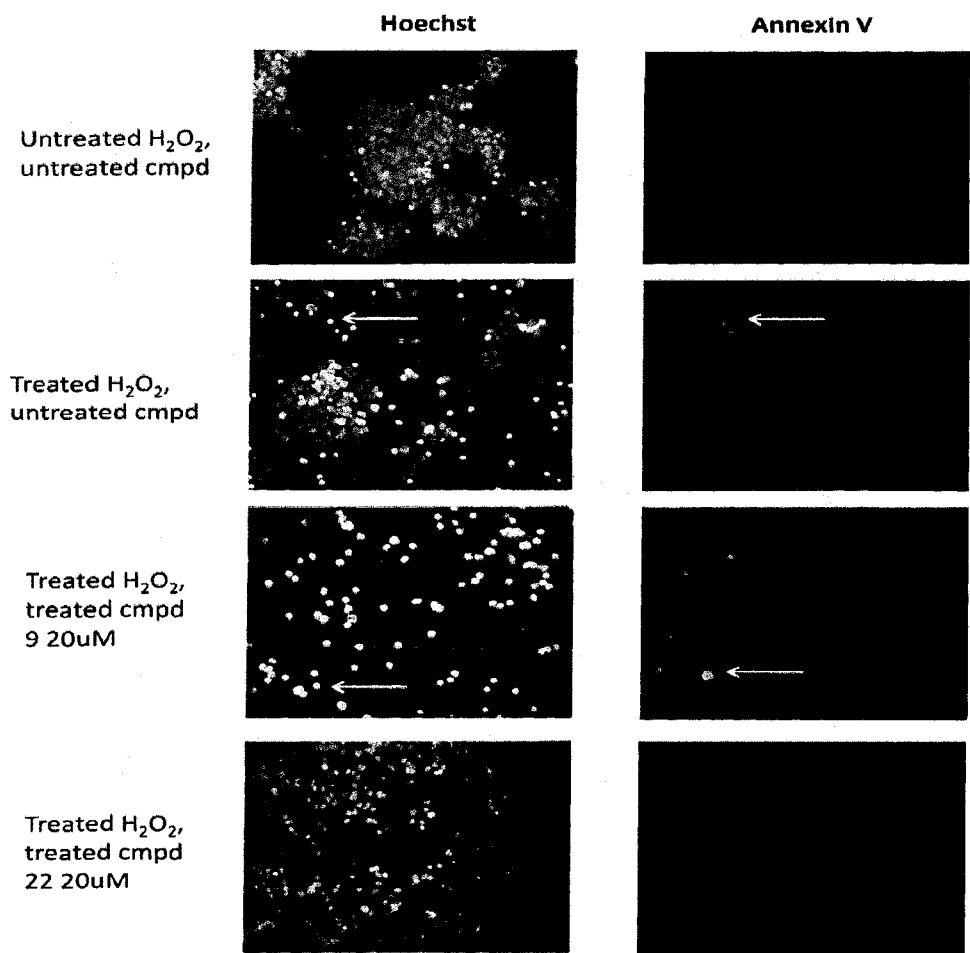
Figure 4.9.5.2A: Differentiated SHSY-5Y cells treated with 20µM compound 22 display healthy nuclear morphology and lack plasma membrane flipping 24h following exposure to 100µM H_2O_2.

Untreated control cells show predominantly healthy nuclear morphology, with minimal plasma membrane flipping. Control cell lines treated with 100µM H_2O_2 show many brightly stained condensed nuclei made visible by Hoechst staining (white arrow) and significant plasma membrane flipping (Annexin V staining) indicated by the white arrow. Cells treated additionally with compound 9 still display apoptotic nuclei and plasma membrane flipping, whereas cells treated additionally with compound 22 do not and are comparable to control untreated cells. All fluorescent pictures were taken using an inverted stage fluorescence microscope (Magnification: 400x).

Viability of Differentiated SHSY-5Y Cells 24h post-treatment

% Cell Viability

100
80
60
40
20
0

untreated   treated 100µM H2O2   treated 100µM H2O2, treated cmpd 9   treated 100µM H2O2, treated cmpd 22
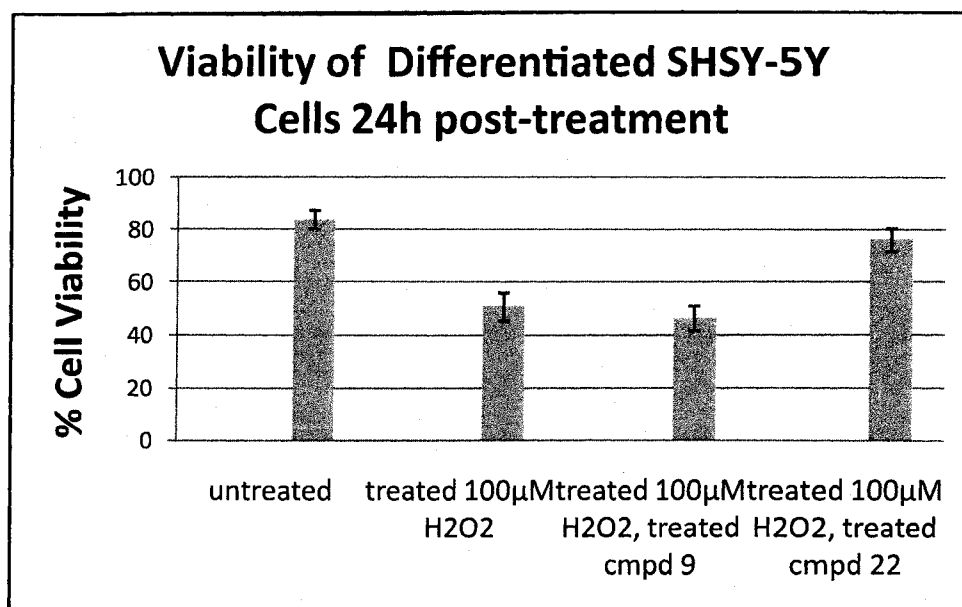
Figure 4.9.5.2B: Quantifying cell viability of differentiated SHSY-5Y cells 24h following 100µM H_2O_2 treatment.

24h following 100µM H_2O_2 treatment, cultures were stained with Hoechst. Healthy and apoptotic nuclei from three separate experiments were counted using 5 fields/treatment group/experiment, and the number of healthy cells was ᵖlotted as a percentage of all the cells counted as Cell Viability. SHSY-5Y cells that were treated with compound ... show strong resistance to apoptosis, with cell viability values close to those of the untreated control cells (~80% cell viability).

One such fluorochrome, 5, 5′, 6, 6′-tetrachloro-1, 1′, 3, 3′-tetraethylbenzimidazolcarbocyanine iodide (JC-1), emits green and/or red according to its oligomerization status. JC-1 incorporates into mitochondria where it either forms monomers (emitting green, at 527nm), or at higher dye concentrations (indicating a high $\Delta\Psi_m$), forms aggregates (emitting red, at 590nm). Thus, the ratio between green and red JC-1 fluorescence provides an estimate of $\Delta\Psi_m$ that is (relatively) independent of the mass of mitochondria. Mitochondria that have lost their $\Delta\Psi_m$, will not be able to form aggregates and will not stain brightly red, but will only fluoresce green.

As seen in figure 4.9.5.3, cells that were not subjected to 100μM H_2O_2 treatment retain the red JC-1 stain indicating the presence of $\Delta\Psi_m$ in addition to having a healthy nuclear morphology indicated by Hoechst staining. Cells that were challenged with 100μM H_2O_2 still show some green JC-1 staining, however the red aggregate staining was significantly diminished (figure 4.9.5.3), indicating a loss of $\Delta\Psi_m$; Hoechst staining indicates these cells possess apoptotic nuclei. The same outcome is seen with cells that were treated with 100μM H_2O_2 as well as with nonspecific compound 9: there is a decrease in red JC-1 staining, and positive apoptotic nuclei. Lastly, cells treated with both 100μM H_2O_2 and compound 22 display red punctate JC-1 fluorescence, indicating maintenance of $\Delta\Psi_m$, and healthy nuclear morphology shown by Hoechst staining.

4.9.6   Cell Viability of NT-2 Cells Treated with 100μM H_2O_2

To further characterize the ability of compound 22 to interact with Bax inside the cell and halt oxidative stress-induced apoptosis, it was important to observe the effects of compound 22 in an alternative cell line. The NT-2 (or N Tera 2) cell line is a neuronally-committed human teratocarcinoma, and like the the SHSY-5Y cell line, possesses the ability to be differentiated

into neurons. NT-2 cells challenged with 100μM H_2O_2 and treated with 20μM compound 22 were monitored for changes to nuclear morphology and plasma membrane composition for signs of apoptosis.

4.9.6.1 Nuclear Morphology of NT-2 Cells 24h Post-100μM H_2O_2 Treatment

The NT-2 cells that were monitored 24h post-100μM H_2O_2 treatment displayed similar nuclear morphology as the SHSY-5Y cells under the same conditions. NT-2 cells treated with 100μM H_2O_2 and compound 9 display no resistance to apoptosis, having brightly stained condensed nuclei, whereas those treated with 100μM H_2O_2 and compound 22 show significant resistance to apoptosis and display healthy nuclei (figure 4.9.6.1A).

Additionally, the NT-2 cell viability 24h following treatment was comparable to that of the SHSY-5Ys, with cell viabilities of untreated, 100μM H_2O_2-treated, 100μM H_2O_2 and compound 9 treated, and 100μM H_2O_2 and compound 22 treated were determined to be 82.20%, 54.53%, 54.40%, and 78.64% respectively (figure 4.9.6.1B).

4.9.6.2 Nuclear Morphology of NT-2 Cells 48h Post-100μM H_2O_2 Treatment

The NT-2 cells that were monitored 48h post-100μM H_2O_2 treatment displayed similar nuclear morphology as the SHSY-5Y cells under the same conditions. Those treated with 100μM H_2O_2 and compound 9 display no resistance to apoptosis, having brightly stained condensed nuclei, whereas those treated with 100μM H_2O_2 and compound 22, show resistance to apoptosis and display healthy nuclei (figure 4.9.6.2A).
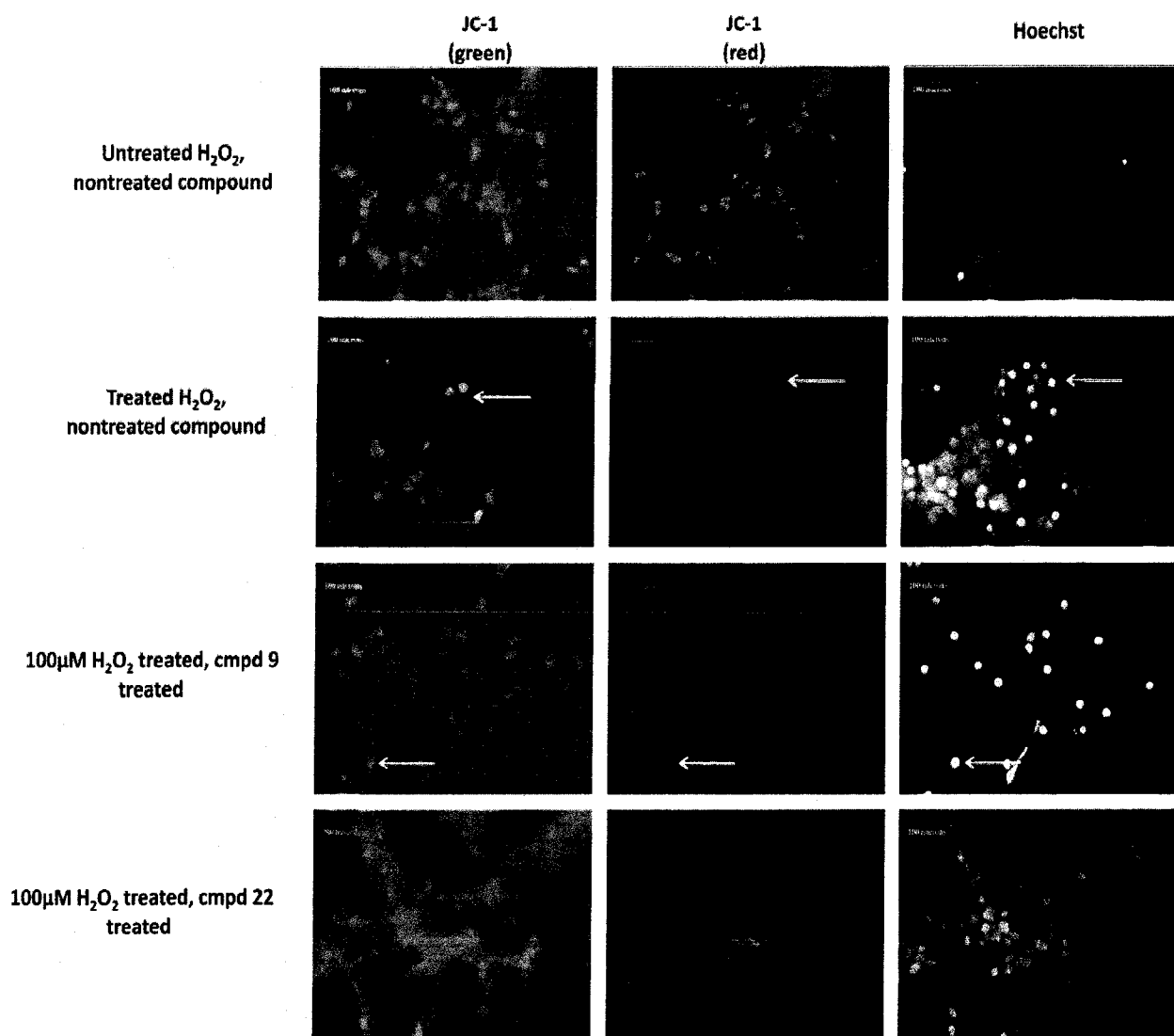
Figure 4.9.5.3: Mitochondrial membrane potential and nuclear morphology of differentiated SHSY-5Y cells 24h following 100μM H₂O₂ treatment

SHSY-5Y cells were differentiated as described in the Methods and subjected to 1h of 100μM H₂O₂ treatment. 24h following treatment, cells treated with 100μM H₂O₂ and compound 9, display a loss of $\Delta\Psi_m$ indicated by the loss of red staining (white arrow) combined with apoptotic nuclear morphology. Cells treated with 100μM H₂O₂ and compound 22 retain $\Delta\Psi_m$ indicated by the red JC-1 staining, and possess healthy nuclei made visible by the Hoechst staining. (Scale unit: 100 microns).

102

| Untreated H₂O₂, untreated cmpd | Treated H₂O₂, untreated cmpd | Treated H₂O₂, treated 20μM cmpd 9 | Treated H₂O₂, treated 20μM cmpd 22 |
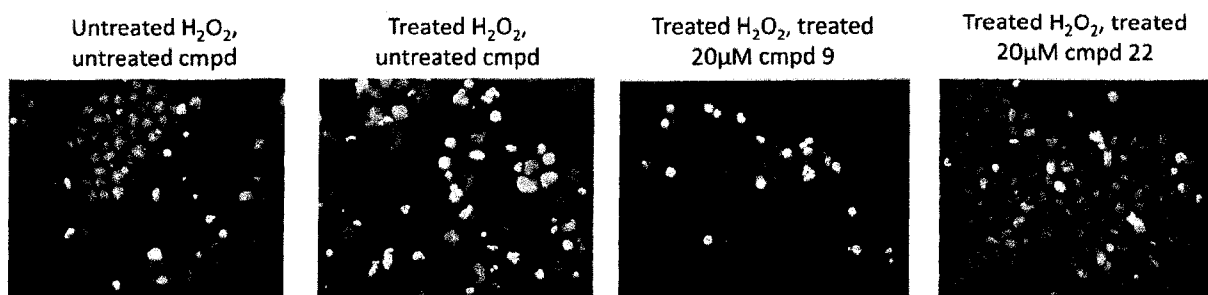
Figure 4.9.6.1A: Nuclear morphology of NT-2 cells 24h following 100μM H₂O₂ treatment

NT-2 cells treated with 100μM H₂O₂ and compound 9 display apoptotic nuclei, whereas NT-2 cells treated with 100μM H₂O₂ compound 22 have healthy nuclei comparable to control untreated cells. All fluorescent pictures were taken using an inverted stage fluorescence microscope (Magnification: 400x).
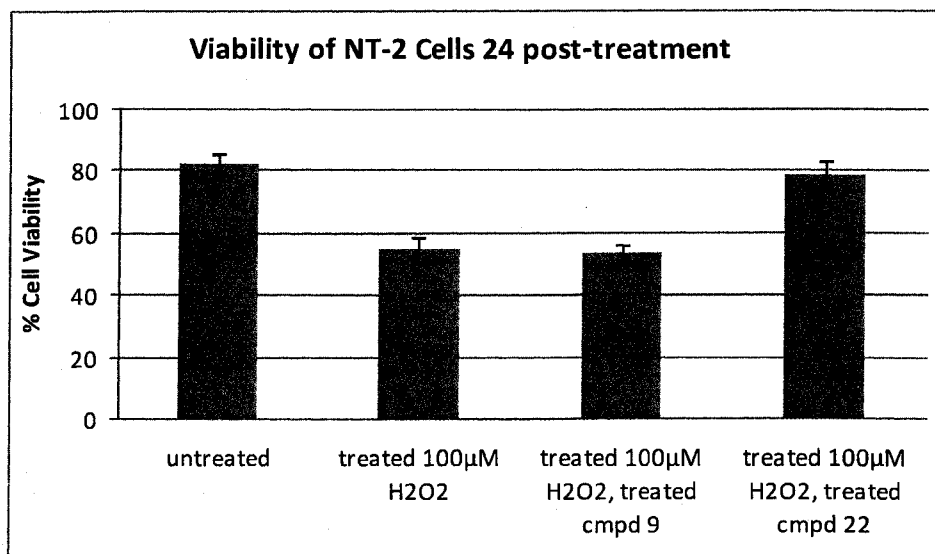
Figure 4.9.6.1B. Quantifying viability of NT-2 cells 24h following 100μM H₂O₂ treatment.

24h following 100μM H₂O₂ treatment, NT-2 cultures were stained with Hoechst. Healthy and apoptotic nuclei from three separate experiments were counted using 5 fields/treatment group/experiment, and the number of healthy cells was plotted as a percentage of all the cells counted as Cell Viability. NT-2 cells that were treated with compound 22 show strong resistance to apoptosis, with cell viability values close to those of the untreated control cells (~80% cell viability).

Additionally, the NT-2 cell viability 48h following treatment was comparable to that of the SHSY-5Ys, with cell viabilities of untreated, 100μM H_2O_2-treated, 100μM H_2O_2 and compound 9 treated, and 100μM H_2O_2 and compound 22 treated were determined to be 82.10%, 47.85%, 49.20%, and 79.84% respectively (figure 4.9.6.2B).

4.9.7 Monitoring Cell Viability of SHSY-5Y Cells Following Hypoxia/Hypoglycemia-Induced Oxidative Stress

Hypoxia/hypoglycemia was induced in cells treated with either non-specific compound 9 or compound 22 for 12h as described in the Methods section. After 12h, the cells were rescued by culturing them in nutrient-supplemented media and re-exposing them to oxygen. The cells were then monitored for signs of apoptosis by observing their nuclear morphology via Hoechst staining and plasma membrane flipping via Annexin V staining (figure 4.9.7A). Cell viability was again determined by counting Hoechst-stained nuclei and determining the total percent viability.

This hypoxia/hypoglycemia experiment was assumed to be a close model for investigating the damage caused by reperfusion of blood after suffering a stroke. As discussed, there is a marked increase in ROS during reperfusion, which can spread to surrounding healthy neurons, leading to over-activation of Bax, ultimately leading to inappropriate induction of apoptosis in these cells. Thus, we monitored the ability of compound 22 to inhibit Bax under similar conditions in order to prevent apoptosis.
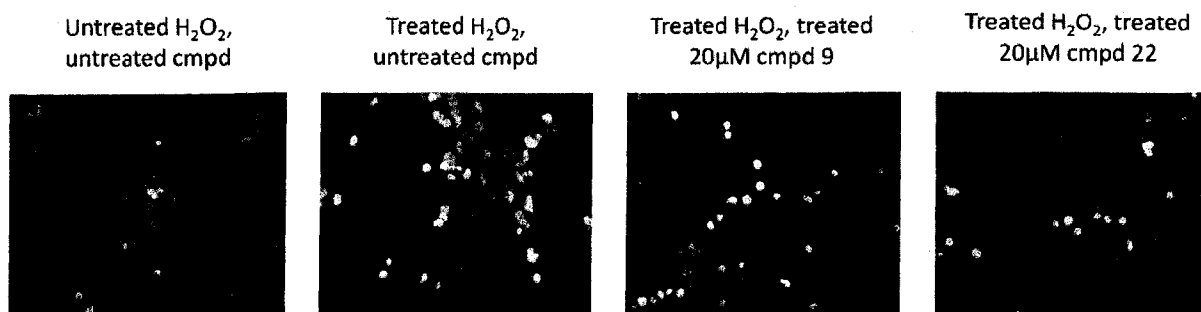
Figure 4.9.6.2A: Nuclear morphology of NT-2 cells 48h following 100μM H₂O₂ treatment.

NT-2 cells treated with 100μM H₂O₂ and compound 9 display apoptotic nuclei, whereas NT-2 cells treated with 100μM H₂O₂ compound 22 have healthy nuclei comparable to control untreated cells. All fluorescent pictures were taken using an inverted stage fluorescence microscope (Magnification: 400x).
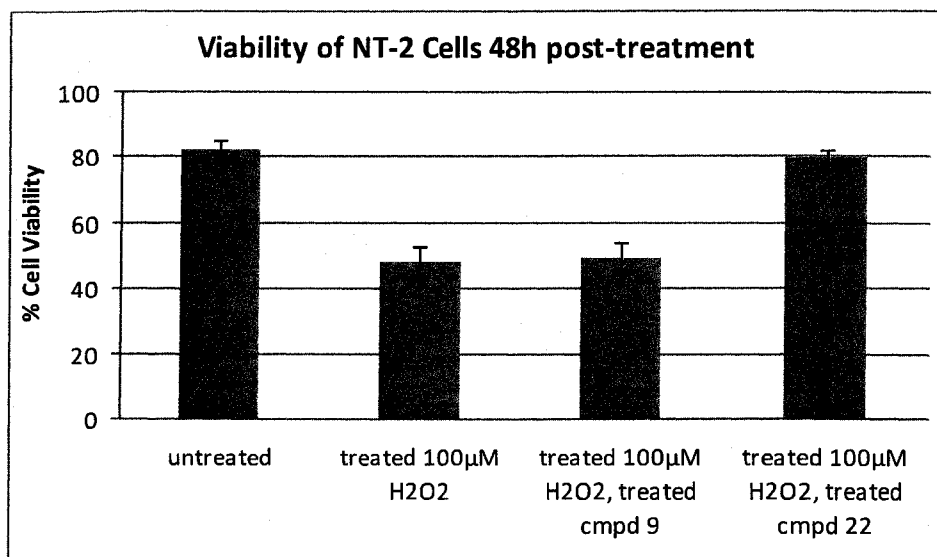
Figure 4.9.6.2B: Quantifying viability of NT-2 Cells 48h following 100μM H₂O₂ treatment.

48h following 100μM H₂O₂ treatment, NT-2 cultures were stained with Hoechst. Healthy and apoptotic nuclei from three separate experiments were counted using 5 fields/treatment group/experiment, and the number of healthy cells was plotted as a percentage of all the cells counted as Cell Viability. NT-2 cells that were treated with compound 22 show strong resistance to apoptosis, with cell viability values close to those of the untreated control cells (~80% cell viability.

It was observed after 12h of hypoxia/hypoglycemia, that cells that were additionally treated with 20μM of compound 9, still display brightly stained condensed nuclei and plasma membrane flipping indicative of apoptosis. Conversely, cells that were additionally treated with 20μM of compound 22 display healthy nuclei and lack plasma membrane flipping (figure 4.9.7A). The determined cell viability was in accordance with the observed nuclear morphology and plasma membrane flipping; cells additionally treated with compound 22 had a percent viability close to that of the untreated control (figure 4.9.7B).

4.9.8 Proliferation of SHSY-5Y Cells Following 100μM H_2O_2 Treatment

We observed that cells treated with 20μM compound 22 were resistant to apoptosis induced by exposure to 100μM H_2O_2 through cellular staining techniques and measurement of active Caspase 3 and ROS level, so we wanted to ensure that this resistance to apoptosis was not at the expense of other cellular mechanisms like cell division. Thus, we monitored SHSY-5Y cells for up to 10 days following 100μM H_2O_2 exposure. Cells were divided into four treatment groups: untreated, treated 100μM H_2O_2, treated 100μM H_2O_2 and compound 9, and treated 100μM H_2O_2 and compound 22. The four groups were split evenly from a common stock of cells to ensure that each group started with approximately the same cell number. Once the cells reached 70-80% confluence, the appropriate treatments were performed. Forty-eight hours following treatment, the cells were counted using Trypan Blue, replated and then counted again on day 5, and on day 10 to record a growth curve for each treatment group. In figure 4.9.8, it can be noted that the untreated cells and those treated with both 100μM H_2O_2 and compound 22 had comparable rates of proliferation with a population doubling of slightly less than 48h (the normal population doubling time for SHSY-5Y cells). Cells that were treated with 100μM H_2O_2 or
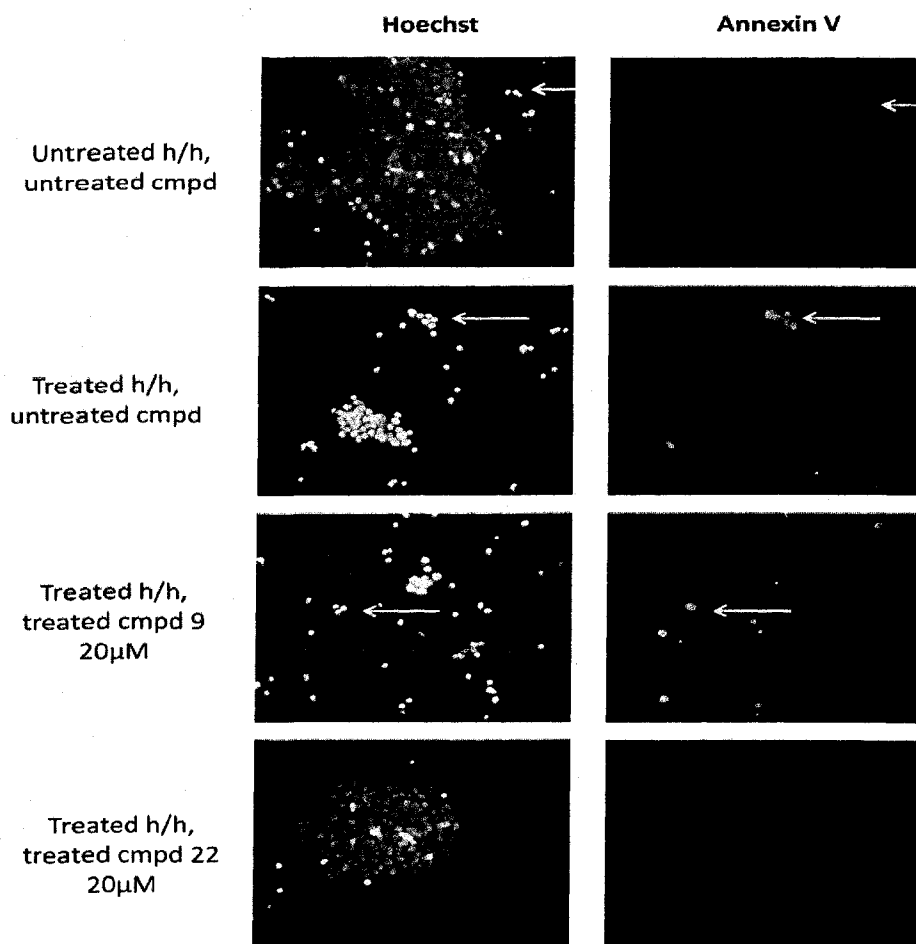
Figure 4.9.7.1A: Nuclear morphology and plasma membrane flipping in SHSY-5Y cells following hypoxia/hypoglycemia (h/h)

Control cell lines that were untreated show predominantly healthy nuclear morphology, with no plasma membrane flipping. Control cell lines placed under hypoxia/hypoglycemia show many brightly stained condensed nuclei made visible by Hoechst staining (white arrows) and significant plasma membrane flipping (Annexin V staining) indicated by the white arrows.   Cells treated additionally with compound 9 still display apoptotic nuclei and plasma membrane flipping, whereas cells treated additionally with compound 22 do not and are comparable to control untreated cells. All fluorescent pictures were taken using an inverted stage fluorescence microscope (Magnification: 400x).

107

Viability of SHSY-5Y Cells Following Hypoxia/Hypoglycemia
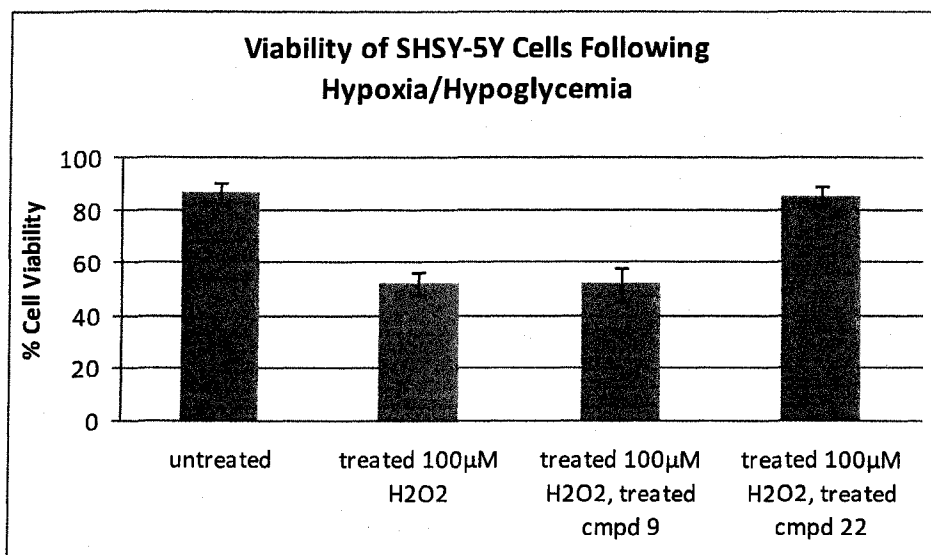
Figure 4.9.7.1B: Quantifying viability of SHSY-5Y cells following hypoxia/hypoglycemia

12h following hypoxia/hypoglycemia, cell cultures were stained with Hoechst. Healthy and apoptotic nuclei from three separate experiments were counted using 5 fields/treatment group/experiment, and the number of healthy cells was plotted as a percentage of all the cells counted as Cell Viability. Cells that were treated with compound 22 show strong resistance to apoptosis, with cell viability values close to those of the untreated control cells (~80% cell viability).

Cellular Proliferation

Legend:
- untreated
- 100uM H2O2
- 100uM H2O2 + cmpd 9
- 100uM H2O2 + cmpd 22
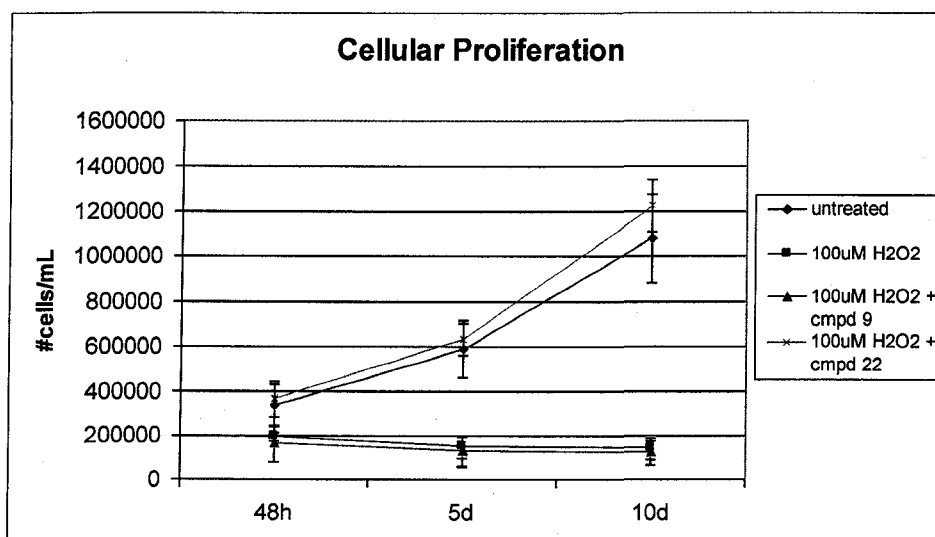
Figure 4.9.8: Proliferation of SHSY-5Y cells following 100μM H₂O₂ exposure.

Cell division was monitored by counting live cells using Trypan Blue, starting at 48h after 100μM H₂O₂ (1h) treatment. Cells treated additionally with compound 22 underwent slightly under two division cycles from 5d to 10d, which is in agreement with the doubling rate of SHSY-5Y. Cells additionally treated with compound 9 were not able to divide normally following 100μM H₂O₂ exposure, and the population of cells slightly decreased between ⁵d to 10d.
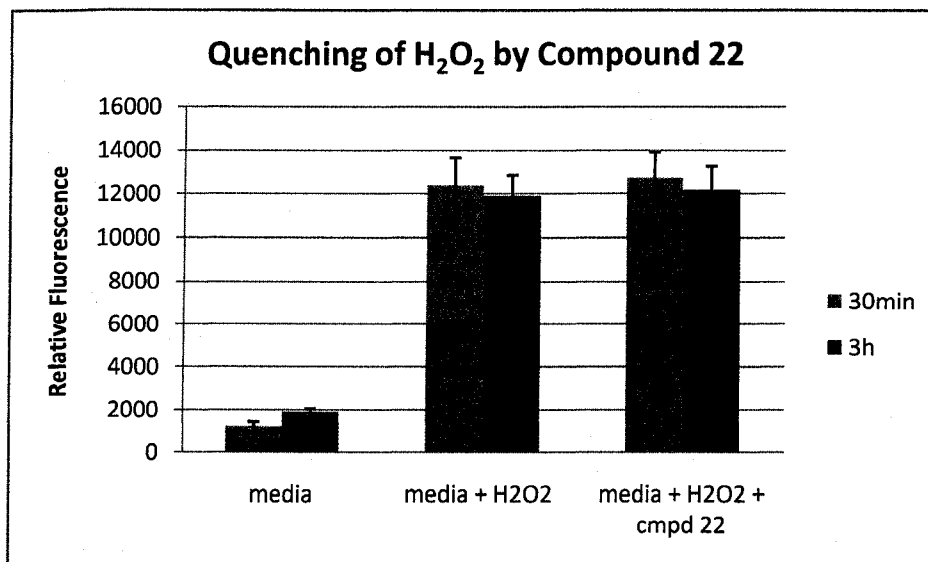
Figure 4.9.9: Levels of H_2O_2 are not directly quenched by compound 22

When 100μM H_2O_2 was incubated alone with SHSY-5Y cell media, there was a 6 fold increase in relative fluorescence intensity when compared to media alone (measured using Amplex Red). When compound 22 was added, there was no change in relative fluorescence after 30min and 3h of incubation. This means that compound 22 itself is not directly quenching H_2O_2 before it can enter the cell and cause oxidative stress.

4.9.10 Preliminary Study of the Cellular Uptake of Compound 22

To investigate the cellular uptake of compound 22, its unique absorbance peak in the visible spectra was taken advantage of. Following a wavelength scan beginning a 250nm and going to 700nm, compound 22 was found to have an absorbance peak at 425nm (see figure 4.9.10A). The media that was used to grow the SHSY-5Y cells was found to have an absorbance peak at around 230nm, and so the presence of compound 22 could be monitored in the media. Additionally, a standard concentration curve was developed for compound 22 so that the specific concentration found in the media following predetermined incubation times could be calculated (figure 4.9.10B) and the molar extinction coefficient was also found to be on average, $22,070M^{-1}cm^{-1}$.

It was found after 18h of incubation that media incubated with 20μM of compound 22 alone had 10.9μM left. This meant that perhaps there was some degradation of compound 22 or its absorbance was quenched by binding to serum proteins of the media over the 18h. However, when SHSY-5Y cells were present in the dish, only 2.46μM of compound 22 remained in the media, indicating that some could be entering the cell over 18h (figure 4.9.10C).

Lastly, when a wavelength scan from 400nm-500nm was performed on isolated post-nuclear cytosol, it was noted that there was no significant absorbance peak (it hovered around 0.100). However, when 20μM of compound 22 was incubated with the post-nuclear cytosol, a clear absorbance peak could be seen around 425nm with a value of 0.649. This could be useful in the future for determining the relative amount of compound 22 in particular subcellular components of the cell; however this work is still preliminary.

Absorption Peak of Compound 22
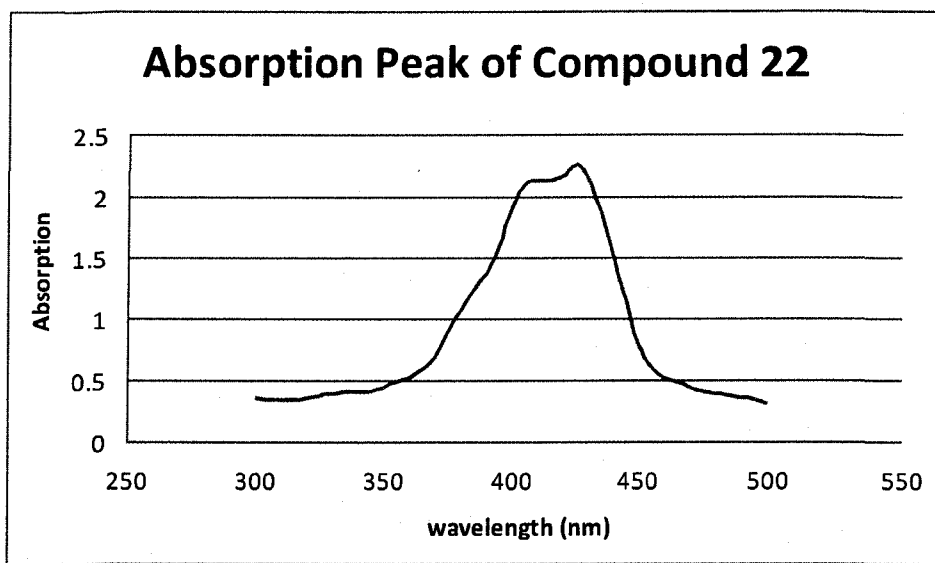
Figure 4.9.10A: Absorption profile of compound 22

By performing a wavelength scan of absorption from 250nm-700nm (only 250-550nm is shown here), we determined that the absorption peak of compound 22 occurs at 425nm. In this case 80µm of compound 22 was used for the scans and the Genesys 10 UV-Vis Spectrophotometer was utilized to perform the scans.
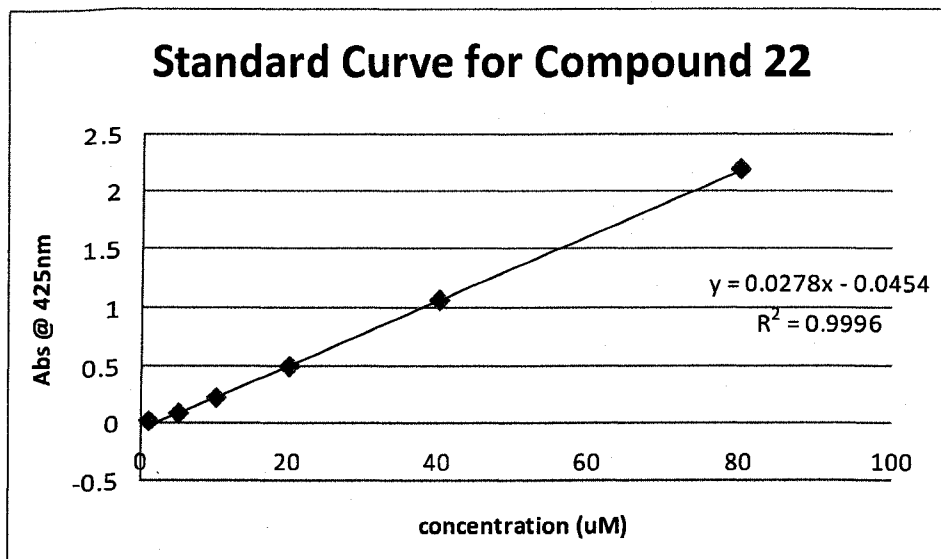
Figure 4.9.10B: Absorption at 425nm of varying concentrations of compound 22

The relationship between absorption and concentration of compound 22 was found to be linear and can be used to determine various concentrations of compound 22 present in the media surrounding cells. This can be used to see how much compound 22 is taken into the cell over a specified time period.

114
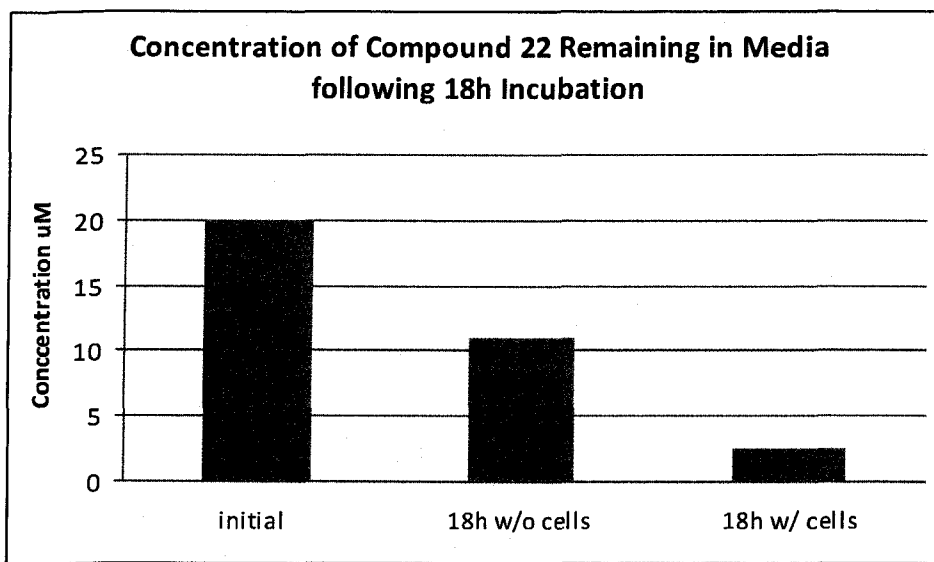
Figure 4.9.10C: Concentration of compound 22 remaining in the media following 18h incubation

Initially, 20μM of compound 22 was added to both media alone, and media surrounding SHSY-5Y cells. Eighteen hours later there was a decrease in the concentration of compound 22 in both the media alone and the media with cells. However, the decrease in compound 22 was significantly more in the media surrounding cells than in the media incubated with compound 22 alone. This indicated that perhaps the cells are indeed taking in compound 22.
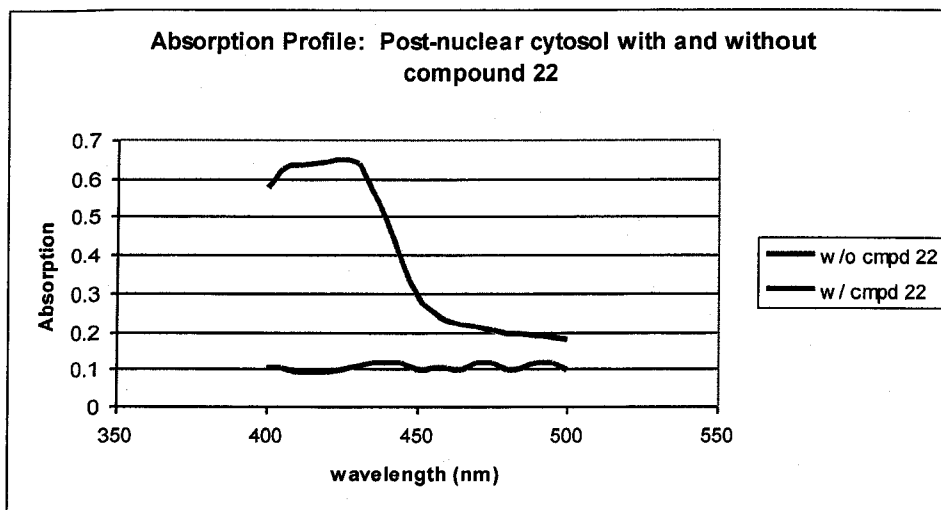
Figure 4.9.10D: Absorption profile of post-nuclear cytosol incubated with and without compound 22

An absorbance scan between 400nm-500nm was performed on 10μg/mL of post-nuclear cytosol alone or incubated with 20μM compound. It was noted that only post-nuclear cytosol incubated with compound 22 had a significant peak at 425nm.

4.9.11 Preliminary Investigation of the effect of Compound 22 on the Interaction of Bax with VDAC

We observed that compound 22 was capable of protecting mitochondria from Bax-induced permealization, so we wanted to understand if perhaps compound 22 was binding to Bax at its VDAC interaction site, and preventing Bax-induced opening of the mitochondrial PTP. Using mitochondria isolated from untreated SHSY-5Y cells, $100\mu M$ H_2O_2-treated cells, and $100\mu M$ H_2O_2-treated cells treated with either compound 9 or 22, we performed immunoprecipitation using anti-VDAC antibodies and protein G-Sepharose beads as described in the methods. From previously published results as well as work performed in our laboratory, Bax is known to interact with VDAC, and can be co-precipitated using anti-VDAC or anti-Bid antibodies bound to protein G-Sepharose resin (Gueorguieva *et al.,* 2006). Utilizing this information, we hypothesized that if compound 22 was interacting with Bax at the VDAC binding site, the presence of compound 22 would prevent Bax-VDAC interaction, which could be monitored by immunoprecipitation, followed by SDS-PAGE and Western Blot. Indeed, a decrease in Bax was observed by preliminary Western blot analysis in mitochondrial fractions isolated from cells that were treated with $100\mu M$ H_2O_2 and compound 22 versus compared to those treated with $100\mu M$ H_2O_2 alone (data not shown).

Chapter 5: Discussion

Part 1

In this study we have identified a novel manner of both quenching and increasing the activity of Caspase 3. This study considered the ability of two Caspase 3-specfic V_HHs to modulate the activity of isolated Caspase 3 as well as within SHSY-5Y cells via transient transfections. The VhhCasp31 was capable of inhibiting the activity of Caspase 3, whereas VhhCasp32 enhanced Caspase 3 activity. Moreover, VhhCasp31 and VhhCasp32, respectively, inhibited and accelerated apoptosis when expressed as intrabodies in mammalian cells. These anti-Caspase 3 V_HHs have important potential as models for identifying small molecular weight modulators that can mimic the action of the V_HHs described above. These small molecular weight mimetics could be used for possible treatment of neurodegenerative diseases or cancer involving Caspase 3 activation.

5.1 Targeting Caspase 3 as a mean of inhibiting oxidative stress induced apoptosis

Caspase 3 was chosen as a target for to modulate apoptosis, as it is one of the most common executioners of apoptosis (Denault, *et al.*, 2002). Caspase 3 is also activated by both intrinsic and extrinsic pathways of apoptosis, with the ability to be cleaved by both Caspase 8 and the Caspase 9-APAF-1 complex, meaning that it can become activated by ligand signalling from the plasma membrane as well as signalling from the mitochondria. Caspase 3, as an executioner caspase, plays a role in mediating the cleavage of ICAD, the inhibitor of CAD, which is responsible for DNA degradation and Caspase 3 is one of the last checkpoints in the pathway toward DNA degradation, and subsequent apoptosis, thus making it an important target for modulating of the apoptotic pathway (Lee, *et al*, 2000a).

Caspase 3 has been shown to be important for survival, as Caspase 3 knockout mice are born at low frequency and die after only a few weeks. A striking characteristic of these mice are skull defects with ectopic masses of supernumerary cells that represent the failure of apoptosis during the development of the brain, but surprisingly, not in other organs or tissues (Kuida et al., 1996 and Woo et al., 1998). Thus, Caspase 3 acts in a tissue selective manner early in development with two possible explanations. There may be a shortage of crucial caspase 3-like proteases that can substitute for Caspase 3 at a crucial stage in the neuronal apoptosis program, or Caspase 3 may lie at the heart of an essential neuronal apoptotic pathway.

The pivotal role of caspase 3 in neuronal apoptosis is highlighted again when examining cell death mechanisms in neurodegeneration. Particularly, it has been found that Caspase 3 activity is induced by reperfusion in the ischemic core and penumbra after stroke in neonates (Manabat et al., 2003). Recent evidence has suggested that although some Caspase 3-dependent cell death occurs in the adult brain after ischemia, caspase-dependent death is quite prominent in the neonatal brain after hypoxia and ischemic insults, including hypoxia-ischemia (Cheng et al., 1997; Ferrer et al., 1997; Han et al., 2000). This presents an interesting, relevant focus for therapeutic targeting of Caspase 3 following ischemic stroke.

The role of Caspase 3 has been studied thoroughly in cancer models, in particular breast cancers, and other caspase-3 deficient cancer cell lines such as certain ovarian and cervical cell lines. Approximately 75% of the tumour as well as morphologically normal peritumoral tissue samples lacked the caspase3 transcript and caspase 3 protein expression. Additionally, the caspases3 mRNA levels in commercially available total RNA samples from breast, ovarian, and cervical tumours were either undetectable (breast and cervical) or substantially decreased (ovarian). Despite the complete loss of caspase-3, the expression levels of other caspases, such

as caspase 8 and caspase 9, were normal in all the tumour samples studied (Devarajan *et al.,* 2002). These results suggest that the loss of caspases3 expression may represent an important cell survival mechanism in patients with these forms of cancer and highlights the importance of normal caspase 3 expression in proper cell homeostasis. Although, a caspase 3-targeting therapeutic would not be of much use in caspase 3-deficient cancers, it has a relevant role in targeting cancers where caspase 3 is present but not activated properly from upstream modulators.

5.2 Using Single domain antibodies to modulate Caspase 3 activity

As previously discussed, unlike the larger human antibodies such as IgG, the camelid species such as llamas camels have antibodies that consist of only variable heavy chains (V_HHs). The absence of the light chains allow researchers to isolate a smaller antigen binding active complexes termed single domain antibodies (sdAbs), which are at least half the size of the scFvs isolated from conventional IgGs. These particular antibodies are advantageous for intracellular studies, compared to the scFvs due to their smaller size and greater solubility. Additionally, sdAbs have antigen combining sites that consist of only the three CDRs of the heavy chain variable domain (Tanha *et al*, 2002). The CDR3, however, makes the most antigen contacts and molecular interactions in the antibody combining sites (Padlan, 1994). Through isolation and amplification of only these specific antigen binding regions, we can select a low molecular weight peptide fragment that possess very specific and strong bindng affinities for the antigen of interest, such as caspase 3.

In addition, by utilizing a llama phage display library, the specific gene for the antibody against the antigen is individually cloned into a phage which will express the desired antibody on its surface. Thus by panning, we can isolate both the specific sdAb for a particular antigen

(displayed on the phage surface) as well as the gene. Utilizing this particular panning assay, we have isolated two unique sdAbs against Caspase 3 as well as their respective genes. Subsequently, this allowed us to study the sdAbs in two ways: *in vitro* to test their efficacy at modulating Caspase 3 activity and intracellularly via transient transfection. The former *"in vivo"* approach allowed us to study the sdAbs as intrabodies, and observe if they can modulate apoptosis.

5.3   Specificity and efficacy of anti-Caspase 3 V_HHs in modulating Caspase 3 function *in vitro*

We were able to show *in vitro* that Vhhcasp31 was capable of lowering the activity of Caspase 3 and VhhCasp32 was able to increase the activity in a concentration-dependent manner. Importantly, when Caspase 3 was treated with an irrelevant V_HH, Vhh5.2, under both concentration conditions, Caspase 3 demonstrated negligible changes in activity, thus ruling out the possibility that the modulating effects of VhhCasp31 and VhhCasp32 might be non-specific. The initial Caspase 3 concentration of 4.7μM was chosen because this was the lowest concentration of active Caspase 3 that produced a significant amount of fluorescence when compared to a control well contain buffer and DEVD-AFC peptide alone. In the future, the effect VhhCasp31 and VhhCasp32 on Caspase 3 binding could be monitored kinetically to determine, for example, the saturation point, rate of reaction, K_m, and K_i.

A previous study performed by Lee *et al.* in 2000 identified selective inhibitors for both Caspase 3 and 7, and have suggested that blocking these two caspases alone within the cell is sufficient for blocking apoptosis (Lee *et al.*, 2000a). Thus, it was important in our study to not only consider the effects of VhhCasp31 and VhhCas32 *in vitro*, but extend this approach to the cellular level in order to evaluate the efficacy of the antibodies in halting apoptosis *in vivo*.

5.4 Anti-Caspase 3 V_HHs are specific inhibitors of the Caspase 3-associated apoptotic pathway

Transient transfections were performed to evaluate the ability of the V_HHs to quench the activity of Caspase 3 (activated by oxidative stress) by VhhCasp31 and to increase the activity of Caspase 3 by VhhCasp32 within the cells. Applying the V_HHs directly to active Caspase 3 isolated from cellular lysate does allow for observation into the modulating abilities of the V_HHs, however, expression of the V_HHs intracellularly takes into account factors present in the cell that may affect the ability of the V_HHs to modulate Caspase 3 activity. The V_HHs may have different effects within the cells when compared with their actions outside of the cell. For example, the V_HHs could prove to be toxic to the cell, may not be expressed at all, and may either show prevention of apoptosis, acceleration of apoptosis, or no protection from apoptosis. Even though the V_HHs may show specificity toward Caspase 3, it may not show beneficial alterations within the cell, or even cause problems with other metabolic pathways within the cell.

The V_HHs may have altered the activity of Caspase 3 by binding to (i) the active site of Caspase 3, preventing its catalytic function, (ii) different subunits, preventing them from dimerizing, hence preventing procaspase 3 from becoming active, (iii) a site on procaspase 3 that enhances the cleavage and subsequent dimerization, thus boosting activity and (iv) a site on Caspase 3 that results in conformational changes leading to inactivation (by VhhCasp31) or enhancement (by VhhCasp32) of Caspase 3 activity.

SHSY-5Y cells were used as a model in this study to show prevention of cell death in regards to neurodegenerative disease. SHSY-5Y cells have the ability to be differentiated into neuronal cells, making them a good choice for qualitatively observing the effects of oxidative

stress, and the abilities of the V_HHs to affect cell death via transient transfections (McCarthy *et al.*, 2004; Gueorguieva *et al.*, 2006); this "transient"model, however, provides only qualitative data. Using stably transfected, SHSY-5Y cell lines which permanently express the V_HH genes one could obtain quantitative data such as apoptotic index. Additionally, stably-transfected, V_HH-expressing SHSY-5Y cells could be differentiated into neuronal cells which are closer a model to neurons in neurodegenerative disease.

Part 2

In this study, we screened a 34-member pharmacaphore library of biologically active low molecular weight compounds for those that could bind to Bax in the same manner as an anti-Bax V_HH (sdAb) previously identified by our group to block Bax function under oxidative stress. We found one particular compound, "compound 22," that was capable of binding to and blocking Bax function *in vitro* (thus lowering levels of mitochondrial ROS) as well *in vivo* (using a neuronal cell-based model). Neuronal cells treated with compound 22 are virtually resistant to oxidative-stress-induced apoptosis and are able to divide normally following oxidative stress. Additionally, compound 22 was found to be taken in by the cells through spectrophotometric analysis and does not quench H_2O_2 before it can enter the cell and initiate oxidative stress. This finding has important implications in the development of therapies for neurodegenerative diseases.

5.5 Targeting Bax as a means to inhibit oxidative stress induced apoptosis

When considering methods of blocking oxidative-stress-induced apoptosis, particularly in the post-mitotic neurons of the brain, we chose to target Bax protein due to the important role it plays in intrinsic apoptotic signal transduction via the mitochondria (Wolter *et al.*, 1997).

Following activation, Bax is understood to translocate from the cytosol to the MOM, where is inserts itself and interacts with the permeability transition pore. In particular, Bax is thought to associate with VDAC, a component of the PTP, causing the rupturing of the mitochondrial outer membrane (MOM) and release of various pro-apoptotic proteins such as Cyt c, which can lead to subsequent cell death.

Bax becomes an important target for development of treatments for neurodegeneration, as the activity of Bax is increased in the presence of ROS, leading to the inappropriate induction of apoptosis due to oxidative damage. Specifically, in ischemia/reperfusion, levels of ROS become elevated causing DNA damage and in turn rapid p53 upregulation, which in turn can mediate apoptosis through transcription of Bax (Culmsee *et al.*, 2007).

In a study by Chi-Hsin *et al.*, in 2005, it was shown that Bax translocation could be blocked by an anti-apoptotic drug furosemide, and neuronal cell death due to ischemia could be prevented (Chi-Hsin *et al.*, 2005). Furthermore, elevated levels of Bax have also been shown to be present in the 1-Methyl-4-phenyl-1,2,3,6-tetrahydropyridine (MPTP)-induced Parkinson's model. MPTP causes damages dopaminergic neurons in the substantia nigra pars compacta (SNpc) as seen in Parkinson's disease. This group showed that Bax was highly expressed in the SNpc and in adult mice, and there was an up-regulation of Bax in the SNpc after MPTP administration and a decrease in Bcl-2. Additionally, they found that mutant mice lacking Bax were significantly more resistant to MPTP than their wild-type littermates (Vila *et al.*, 2000). This study demonstrates that Bax plays a critical role in the MPTP neurotoxic process and suggests that targeting Bax may provide protective benefit in the treatment of Parkinson's disease.

Additionally, it has been shown that the deletion of Bax in mice increases the resistance to ischemic insults (Hertz *et al.,* 2005). Further evidence for the crucial role of Bax in neuronal cell death was provided by a study showing that cerebellum granule neurons are protected against prion-induced apoptosis in Bax$^{-/-}$ mice (Chiesa *et al.,* 2005). Bax$^{-/-}$ mice/gerbils are viable (as compared to Caspase 3$^{-/-}$ mice) and provide a valuable means to study the specificity of a particular inhibitor for Bax. For example, in a study by Hertz *et al.,* (2005), neurons from Bax$^{-/-}$ gerbils that were treated with a Bax channel inhibitor show no protection from ischemia. Alternatively, neurons from wildtype litermates treated with the Bax channel inhibitor display protection from ischemia (Hertz *et al.,* 2005). However, this inhibitor of Bax channel formation would only be administered temporarily to reduce tissue damage following ischemic injuries in the brain. Either Bax or Bak protein is required for MOMP to occur, however, permanent inhibition of Bax function in the adult brain could lead to a reduction in overall desirable apoptosis to eliminate damaged cells that are required to die (Wei, *et al.,* 2001). This is turn could tip the balance of cell death survival in favour of the development of cancer. In particular, endogenous Bax inhibitors such as Bax Inhibitor-1 have been shown to be upregulated in aggressive cancers such as prostate (Grzmil *et al.,* 2003).

5.6 Using a pharmacaphore library of small molecular weight compounds to inhibit Bax activity

In the search for avenues of modulating the activity of a protein of interest, an area that has recently received much focus is the utilization of small molecular-weight compounds capable of modulating protein-protein interaction, and subsequently protein activity. The Bcl-2 family of proteins has been given much attention of the last several years as targets for small-molecule

modulators (Becattini *et al.*, 2006; Degterev *et al.*, 2001; Enyedy *et al.*, 2001; Oltersdorf *et al.*, 2005; and Wang *et al.*, 2000). Small-molecule inhibitors are more stable than peptide inhibitors, are cell peremeable, and less immunogenic than their peptide counterparts. This is an important consideration when in search for possible therapeutics for neurodegeneration, as passage through the blood-brain barrier is tightly regulated.

When looking for small-molecule inhibitors that could bind to Bax, there are two specific regions that could be considered for targeting. One such region is the BH3 domain (helix α2), which is used for both homodimerization and heterodimerization with other members of the Bcl-2 family. Another region to consider is a portion C-terminal hydrophobic region of Bax, the putative transmembrane domain, which composes helix α9. The helix α9 of Bax is located in the hydrophobic pocket, bound to the BH3 domain, when present in the cytosol. Upon activation, the helix α9 disengages from the BH3 domain and is thought to insert into the MOM (Nechushtan *et al.*, 1999).

In our present study of screening pharmacaphore libraries for small molecular weight compounds that can bind to pro-apoptotic Bax in the same manner as the labelled anti-Bax sdAb and block its function, we screened 34 small molecules from the same commercial library that was utilized by a group that found inhibitors of the Bcl-x_L/Bak-BH3 interaction One of these compounds was the BH3I-1 inhibitor itself, and the remaining 33 were derivatives of BH3I-1. Since Bax has a BH3 domain, and BH3I-1 disrupts the BH3 domain of Bak from interacting with the hydrophobic cleft formed by the BH1, BH2 and BH3 domains of Bcl-x_L (Degterev *et al.*, 2001), we proposed that perhaps these derivatives of BH3I-1 could bind to the BH3 domain of Bax, thus blocking its homodimerization or heterodimerization with other Bcl-2 family members,

or preventing the disengagement of αhelix 9 from the BH3 domain, thus preventing subsequent loss of $\Delta\Psi_m$ and apoptosis.

5.7 Specificity of the binding of compound 22 to Bax protein and lowering of ROS levels

Of the 34 small molecular weight compounds, nine were found to be capable of competitively binding to Bax protein in the presence of cy5.5-labelled sdAb5.2. The sdAb5.2 was selected from six previously screened anti-Bax sdAbs that were all capable of preventing Bax-induced mitochondrial ROS as well as protecting cells from oxidative-stress induced apoptosis. However, sdAb 5.2 was found to have the greatest ability to lower levels of Bax-induced ROS and inhibit oxidative-stress-induced apoptosis, and thus was chosen for fluorescent cy5.5 labelling (Gueorguieva *et al.*, 2006). We performed a competitive binding assay because we wanted to find a small molecular weight compound that was able to bind to Bax in the same manner as the labelled anti-Bax sdAb, meaning that it would be highly specific. We found that compound 22 was quite effective at competitively bind to Bax in the presence of labelled sdAb5.2, and thus tested compound 22, along with a non-specific compound, compound 9 on their ability to competitively bind to Bax through an alternative binding assay. In this second binding assay, Bax was immobilized on nitrocellulose paper, thus ensuring that Bax would not be dislodged from the bottom of a coated well and float in the supernatant where labelled sdAb could still be binding to Bax, thus skewing the fluorescence reading of the supernatant. It was shown again through this method that compound 22 was able to competitively bind to Bax in the presence of labelled sdAb5.2, whereas nonspecific compound was again unable to competitively bind to Bax.

While the specificity for binding to Bax was determined for each compound, the compounds were also tested on their ability to lower the levels of Bax-induced ROS in isolated mitochondria.

Although the exact mechanism of Bax-induced mitochondrial membrane permealization is still under debate, it has been well documented that presence of Bax does indeed cause $\Delta\Psi_m$ collapse resulting in elevated ROS generation and release (Adachi *et al.*, 2004; Halestrap *et al.*, 2002; Naderi *et al.*, 2006; Narita *et al.*, 1998). By incubating mitochondria isolated from SHSY-5Y cells with Bax and the compound of interest, we could monitor the ability of the compounds to modulate the level of Bax-induced ROS. There were a number of compounds that either moderately or significantly lowered Bax-induced ROS but were not specific for Bax (meaning they did not competitively bind to Bax in the presence of cy5.5-labelled sdAb5.2). These compounds may actually bind to Bax, but not in the same manner as the labelled anti-Bax sdAb5.2, thus not dislodging the labelled sdAb in the competitive binding assay, but still lowering Bax-induced ROS. Previous work completed by our group suggests that the anti-Bax sdAbs may be binding to the VDAC binding site on Bax (specifically the transmembrane, α9 helix) (Gueorguieva *et al.*, 2006). Perhaps these compounds may not bind directly to the transmembrane α9 helix, but could interfere with homodimerization of Bax, or interaction with other members of the Bcl-2 family required for translocation of Bax to the mitochondria (such as tBid) by binding to the BH3 domain. An alternative theory is that these compounds could be protecting the mitochondria in a Bax-independent fashion; for example, by binding to components of the mitochondria such as members of the permeability transition pore, thus blocking Bax from binding and initiating mitochondrial dysfunction. These compounds could be studied further in a cellular model to observe if they offer any protection *in vivo*.

There was one compound (compound 25) that elevated Bax-induced mitochondrial ROS. This compound could be binding to Bcl-2 protein that is normally associated with the

mitochondria, preventing it from sequestering Bax at the mitochondria, thus permitting increased amounts of Bax to interact with the mitochondria and causing dysfunction.

Compound 17 and 22 were the only compounds that were found to competitively bind to Bax in the presence of labelled sdAb and lower Bax-induced ROS. However, the competitive binding of compound 17 to Bax was very weak, and thus compound 22 was selected to study in further detail. Compound 22 was shown to lower Bax-induced ROS in a concentration-dependent manner and did so at a lower concentration than known anti-oxidant CoQ_{10}, although, it was important to observe if compound 22 had similar effects inside the cell (*in vivo*).

In the future, gel filtration could be performed to see if compound 22 directly interferes with either the homodimerization of Bax, heterodimerization of Bax to other members of the Bcl-2 family such as Bid, or the Bax-VDAC interaction. Through gel filtration we would be able to see first what the elution profile would be for the dimers alone, and then dimers incubated with compound 22. The protein dimers would have a higher molecular weight than the proteins separately and thus would elute first from the column. If we were to see a decrease in the peak associated with the protein dimer, and an appearance of a lower molecular weight peaks, the elution volume of these smaller molecular weight peaks could be used to determine the actual molecular weight of the protein could give us some indication of the Bax interaction that compound 22 is interfering with.

Since compound 22 is from a targeted library of potential BH3 domain binders, there is a possibility that it could target other Bcl-2 family members besides Bax. To analyze other potential binders of compound 22, compound 22 could be cross-linked to beads in a column and used to pull out potential suspect binding partners such as Bak and Bid.

5.8 Specificity and efficacy of compound 22 in preventing oxidative-stress-induced apoptosis

By testing compound 22 on neuronal mammalian cell lines we can monitor its ability to halt oxidative-stress-induced apoptosis from inside the cell. As previously mentioned, it was important to see if compound 22 could inhibit Bax *in vivo* in the same manner as was shown *in vitro*. The concentration of compound 22 used in treating the mammalian cell lines was 20μM; 10μM and 40μM concentrations were also tried in the beginning, however there was greater protection seen using 20μM when compared to 10μM, and 40μM appeared to be slightly toxic to the cells when tested on its own (data not shown). Other studies that tested small molecule inhibitors of the Bcl-2 family on cellular models have used concentrations in the micromolar range. For example, in the study by Degterev *et al.*, concentrations of BH3I-1 that were use in the cellular model ranged from 15μM to 100μM (Degterev *et al.*, 2001). We have also seen in our study that there is a diminished absorbance peak of compound 22 incubated in the media alone, indicating potential degradation or binding to serum proteins that mask the absorbance prior to cellular uptake.

When cells were monitored five different fields of view were taken of each group, and the % viability was averaged between them. In the future, viable/apoptotic cells could be quantified via flow cytometry using Annexin V. Post-nuclear cytosolic Caspase 3 levels and mitochondrial ROS levels were also lowered by 20μM of compound 22 following treatment to levels comparable to untreated control fractions, indicating that compound 22 is indeed exerting its effects upstream of mitochondrial dysfunction and subsequent Caspase 3 activation. In the future, isolated post-nuclear cytosol and mitochondria should be monitored for purity by

checking for the presence of β-actin (in cytosolic fractions) and succinate dehydrogenase (in mitochondrial fractions).

5.9 Preliminary study of the cellular uptake of compound 22

Through the spectrophotometric analysis of compound 22 in solution, we have established a preliminary method of analyzing the cellular uptake of compound 22 from the surrounding media. We found that compound 22 has an absorbance peak of 425nm that is distinct from both the supplemented media used to grow SHSY-5Y cells, as well as post-nuclear cytosolic fractions of SHSY-5Y cells. It was also revealed that perhaps there was some degradation of compound 22 in the media over an 18h period or perhaps compound 22 was binding to a serum protein present in the media. However, there did appear to be some cellular uptake of compound 22 indicated by the lower absorbance at 425nm of compound 22 incubated with media and cells, however there could still be further degradation of compound 22. When the absorbance spectrum of post nuclear cytosol was taken between 400-500nm, there was very minimal absorbance (~0.1) which should be examined further as it is quite surprising that there is nothing in the cytosol absorbing in this range. Ideally, compound 22 could be radio-labelled (i.e. with ^{14}C) and its presence in subcellular components/organelles could be traced more effectively.

5.10   Preliminary elucidation of a potential binding site on Bax for compound 22

Bax permealization of the MOM has been shown to happen through the formation of the PTP when Bax binds to the MOM component of the PTP, VDAC (Narita, M *et al.*, 1998). Since we observed that mitochondrial ROS was lowered and $\Delta\Psi_m$ was maintained in cells treated with compound 22 (under oxidative stress conditions), we believed that the Bax-VDAC interaction

may be prevented in these cells. This theory was evaluated by comparing the level of Bax which is co-precipitated with VDAC in control 100μM H_2O_2-treated cells to100μM H_2O_2, compound 22-treated cells. We found that the level of Bax binding to VDAC was indeed decreased in cells treated with compound 22, which suggests that it may be binding to the VDAC binding site on Bax (specifically the transmembrane, α9 helix), or binding to the BH3 domain in a manner that does not allow α9 helix to disengage and interact with VDAC. However, this experiment would need to be repeated with proper controls in order to be meaningful (thus why the data is not shown). Compound 22 could also be interfering with Bax's homerdimerization or its interaction with other modulators upstream of MOMP such as Bid (by binding to its BH3 domain). This would mean that less Bax translocates to the mitochondria to interact with VDAC, and thus less Bax would be pulled down by VDAC.

Chapter 6   Conclusions and Future Work

In this two-part study we were able to identify modulators of two pro-apoptotic proteins Caspase 3 and Bax. In the first half of the study we identified anti-Caspase 3 V_HHs capable of binding to Caspase 3 and either blocking its action (VhhCasp31) or accelerating its activity (VhhCasp32). These two V_HHs could have applications in the study of cellular mechanisms involving Caspase 3 activation as well as in the development of therapeutics for neurodegeneration (VhhCasp31) or cancer (VhhCasp32). Importantly, a cell line stably-expressing the sdAbs would be important in monitoring their behaviour inside the cell.

The application of the anti-Caspase 3 intrabodies as direct therapeutics against neurodegenerative disease and cancer is limited by the difficulty in crossing the blood brain barrier. As we have done with the anti-Bax sdAb5.2, the anti-Caspase 3 V_HHs could be used in screening a pharmacaphore library for small molecular weight compounds that could competitively bind to Caspase 3 in the presence of the V_HHs as well as modulate the activity of Caspase 3 *in vitro* as well as *in vivo*.

In the second half of our study, we screened a small pharmacaphore library for small molecular weight compound that could competitively bind to Bax in the presence of a labelled anti-Bax sdAb (sdAb5.2) and inhibit the activity of Bax both *in vitro* and *in vivo*. We found one such compound, compound 22, that was capable of lowering Bax-induced ROS in isolated mitochondria, and halted oxidative-stress-induced apoptosis in a neuronal cell model.

In the future we would like to confirm the preliminary cellular uptake studies and potentially have compound 22 radio-labelled to explore its intracellular distribution. Additionally, further immunoprecipitations could confirm the role of compound 22 in interfering

with Bax-VDAC interactions, and potential interactions with other Bcl-2 family member. Currently, our collaborators at the NRC-IBS in Ottawa are engaged in NMR studies looking at the potential docking site of compound 22 on Bax. This would aid us in determining with greater certainty; the protein-protein interaction compound 22 could be interfering with

We would also like to study the ability of compound 22 to protect neuronal cells following oxidative stress. In this study, we administered compound 22 at the same time as the oxidative stress as well as after. It would be interesting to see the effects of compound 22 on cells that were first challenged with oxidative stress and then rescued up to 3h following.

Furthermore, a future goal would be to observe the effects of compound 22 in blocking apoptotic cell death in mouse model of ischemia/reperfusion. Mice could be administered compound 22 both before and after middle cerebral artery occlusion and subsequent reperfusion, and apoptosis could be monitored up to 48h following. This would provide us with further insight as to whether compound 22 is well-tolerated within a living organism, and whether it is useful as a potential therapeutic in neurodegenerative disease, particularly ischemic stroke.

References

Adachi M, Higuchi H, Miura S, Azuma T, Inokuchi S, Saito H, Kato S and H. Ishii (2004).Bax interacts with the voltage-dependent anion channel and mediates ethanol-induced apoptosis in rat hepatocytes. *Am J Physiol Gastrointest Liver Physiol* **287**: G695-705.

Adams JM and Cory S. (1998).The Bcl-2 family: arbiters of cell survival. *Science* **281**: 1322-1326.

Adhihetty P J and Hood D A. (2003).Mechanism of Apoptosis in Skeletal Muscle. *Basic App. Myol.* **13**: 171-179.

Alexandrova ML and Bochev PG. (2005).Oxidative stress during the chronic phase after stroke. *Free Radical Biology & Medicine* **39**: 297-316.

Arbabi GM, Desmyter A, Wyns L, Hamers R, and Muyldermans S. (1997).Selection and Identification of Single Domain Antibody Fragments from Camel Heavy-Chain Antibodies. *FEBS Let* **414**: 521-526.

Arafat W. (2000).Antineoplastic effect of anti-erbB-2 intrabody is not correlated with scFv affinity for its target. *Cancer Gene Ther.* **7**: 1250-1256.

Baiping L, Xiujuan T, Hongwei C, Qiming X & Quling G. (1994).Effect of moderate hypothermia in lipid peroxidation in canine brain tissue after cardiac arrest and resuscitation. *Stroke* **25**: 147-152.

Becattini B. (2004).Rational design and real time, in-cell detection of the proapoptotic activity of a novel compound targeting Bcl-X$_L$. *Chem. Biol.* **11**: 389-395.

Becattini B, Culmsee C, Leone M, Zhai D, Zhang X, Crowell KJ, Rega MF, Landshamer S, Reed JC, Plesnila N, and Pellecchia M. (2006).Structure-activity relationships by interligand NOE-based design and synthesis of antiapoptotic compound targeting Bid. *Proc. Natl. Amer. Soc.* **103**:12602-12606.

Berg T. (2003).Modulation of Protein-Protein Interactions with Small Organic Molecules. *Angew. Chem.* **42**: 2462-2481.

Bouchier-Hayes L, Lartigue L and Newmeyer DD (2005).Mitochondria: phamacological manipulation of cell death. *The Journal of Clinical Investigations* **115**: 2640 - 2647.

Bredesen DE, Rao RV, and Mehlen P. (2006).Cell death in the nervous system. *Nature* **443**: 796-802.

Cain K, Bratton SB, and Cohen GM. (2002).The Apaf-1 apoptosome: a large caspase-activating complex. *Biochemie* **84**: 203-214.

Castedo M, Ferri K, Roumier T, Metivier D, Zamzani N, Kroemer G. (2002).Quantitation of mitochondrial alterations associated with apoptosis. *J Immunol Methods* **265**: 39-47.

Cheng Y, Gidday JM, Yan Q, Shah AR, Holtzman DM. (1997).Marked age dependent neuroprotection by brain-derived neurotrophic factor against neonatal hypoxic-ischemic brain injury. *Ann Neurol.* **41**: 521–529.

Chiesa R, Piccardo P, Dossema S, Nowoslawski I, Roth KA, Ghetti B, and Harris DA. (2005). *Bax* deletion prevents neuronal loss but not neurological symptoms in a transgenic model of inherited prion disease. *Proc. Natl. Acad. Sci. U.S.A.* **102**: 238-243.

Chi-Hsin L, Yen-Zhen L, Fu-Chou C, Lan-Feng C and Chi-Mei H (2005).Bax-regulated mitochondria-mediated apoptosis is responsible for the in vitro ischemia induced neuronal cell death of Sprague Dawley rat. *Neuroscience Letters* **387**: 22-27.

Chipuk JE, Bouchier-Hayes L, Kuwana T, Newmeyer DD, and Green DR. (2005).PUMA couples the nuclear and cytoplasmic proapoptotic function of p53. *Science* **309**: 1732-1735.

Choi DW. (1988).Calcium-mediated neurotoxicity: relationship to specific channel types and role in ischemic damage. *Trends Neurosci.* **11**: 465-469.

Chung HT, Pae HO, Choi BM, Billiar TR, and Kim YM. (2001).*Biochem. Biophys. Res. Commun.* **282**: 1075-1079.

Clarke DD and Sokoloff L. (1999).Circulation and energy metabolism of the brain. *Baisic Neurochemistry: Molecular, Cellular and Medical Aspects.* Lippincott-Raven, Philadelphia, pp. 637-669.

Clement T. (2006).It's your health: Stroke, Health Canada (cited June 25th 2008) (http://www.hc-sc.gc.ca/hl-vs/iyh-vsv/diseases-maladies/stroke-vasculaire-eng.php)

Cohen GM. (1997).Caspases: the executioners of apoptosis. *Biochem. J.* **326**: 1-16.

Colby DW, Chu Y, Cassady JP, Duennwald M, Zazulak H, Webster JM, Messer A, Lindquist S, Ingram VM, and Wittrup KD. (2004).Potent inhibition of huntingtin

137

aggregation and ctotoxicity by a disulfide bond-free single domain intracellular antibody. *Proc Natl. Amer. Sci.* **101**: 17616-17621.

Conclaves J. (2002).Functional neutralization of HIV-1 Vif protein by intracellular immunization inhibits reverse transcription and viral replication.

Cooper AJL. (1997).Glutathione in the brain: disorders of glutathione metabolism. *The Molecular and Genetic Basis of Neurological Disease*. Butterworth-Heinemann, Boston, pp. 1195-1230.

Criesa R, Piccardo P, Dossema S, Nowoslawski I, Roth KA, Ghetti B, and Harris DA. (2005). *Bax* deletion prevents neuronal loss but not neurological symptoms in a transgenic model of inherited prion disease. *Proc. Natl. Acad. Sci. U.S.A.* **102**: 238-243.

Crochet. (1998).Intracellular expression of an antibody fragment-neutralizing p21 ras promotes tumor regression. *Cancer Res.* **58**: 1170-1176.

Crompton M. (1999).The mitochondrial permeability transition pore and its role in cell death. *Biochem. J.* **341**: 233-249.

Cryns V and Yuan J. (1998).Proteases to die for. *Genes Dev.* **12**: 1551-1570.

Culmsee C and Krieglstein J. (2007).Ischaemic brain damage after stroke: new insights into efficient therapeutic strategies. *EMBO reports* **8**: 129-133.

De Giorgi F, Lartigue L, Bauer MK, Schubert A, Grimm S, Hanson GT, Remington SJ Youl RG, and Ichas F. (2002).The permeability transition pore signals apoptosis by directing Bax translocation and multidimerization. *FASEB J* **16**: 607-609.

Degterev A, Lugovskyoy A, Cardone M, Mulley B, Wagner G, Mitchison T, and Yuan J. (2001).Identification of small-molecule inhibitors of interaction between the BH3 domain and Bcl-x$_L$. *Nature Cell Biology* 3:173-182.

DeLano WL, Ultsch MH, de Vos AM, and Wells JA. (2000).Convergent Solutions to Binding at a Protein-Protein Interface. *Science* 287: 1279-1283.

Denault J-B, Salveson GS. (2002).Caspases: Keys in the Ignition of Cell Death. *Chemical Reviews.* 102: 4489-4499.

Devarajan E, Sahin AA, Chen JS, Krishnamurthy RR, Aggarwal N, Brun A-M, Sapino A, Zhang F, Sharma D, Yang X-H, Tora AD, and Mehta K. (2002).Down-regulation of caspase 3 in breast cancer: a possible mechanism for chemoresistance. *Oncogene* 21: 8843-8851.

Dietrich WD, Busto R, Valdes I & Loor Y. (1990).Effects of normothermic versus mild hyperthermic forebrain ischemia in rats. *Stroke* 21: 1318-1325.

Dringen R. (2000).Metabolism and functions of glutathione in brain. *Progress in Neurobiology* 62: 649-671.

Dröge W. (2002).Free Radicals in the Physiological Control of Cell Function. *Physiol. Rev.* 82: 47-95.

Enari MS, Sakahira H, Yokoyama H, Okawa K, Iwamatsu A, and Nagata S. (1998).A caspase-activated DNase that degrades DNA during apoptosis and its inhibitor ICAD. *Nature* 391: 43-50.

Enyedy IJ. (2001).Discovery of small-molecule inhibitors of Bcl-2 through structure-based computer screening. *J. Med. Chem.* 44: 4313-4324.

Fadeel B and Orrenius S. (2005).Apoptosis: a basic biological phenomenon with wide-ranging implications in human disease. *Journal of Internal Medicine* **258**: 479-517.

Fernández-Checa JC. (2003).Redox regulation and signaling lipids in mitochondrial apoptosis. *Biochemical and Biophysical Research communications* **304**: 471-479.

Ferrer I, Pozas E, Lopez E, Ballabriga J. (1997).Bcl-2, Bax, and Bcl-x$_L$ expression following hypoxia-ischemia in the infant rat brain. *Acta Neuropathol (Berl)*. **94**: 583–589.

Fleury C, Mignotte B, and Vayssière J-L. (2001).Mitochondrial reactive oxygen species in cell death signaling. *Biochimie* **84**: 131-141.

Fridovich L. (1998).The biology of oxygen radicals. *Science* **201**: 875-880.

Friedlander RM. (2003).Apoptosis and Caspases in Neurodegenerative Diseases. *N Engl J Med* **348**: 1365-1375.

Ginsberg MD, Graham DI & Busto R. (1985).Regional glucose utilization and blood flow following graded forebrain ischemia in the rat: correlation with neuropathology. *Ann Neurol* **18**: 470-481.

Goping LS, Gross A, Lavoie JN, Nguyen M, Jemmerson R, Roth K, Korsmeyer SJ, and Shore GC. (1998).Regulated targeting of BAX to mitochondria. *J. Cell Bio.* **143**: 207-215.

Green DR and Reed JC. (1998).Mitochondria and apoptosis. *Science* **281**: 1309-1312.

140

Green DR and Kroemer G. (2004).The pathophysiology of mitochondrial cell death. *Science* **305**: 626-629.

Gross A, Jockel J, Wei MC, and Korsmeyer SJ. (1998).Enforced dimerization of BAX results in its translocation, mitochondrial dysfunction and apoptosis. *EMBO J* **17**: 3878-3885.

Groves JT. (1999).Peroxynitrite: reactive, invasive and enigmatic. *Curr. Opin. Chem.Biol.* **3**: 226-235.

Grzmil M, Thelen P, Hemmerlein B, Schweyer S, Voigt S, Mury D, and Burfeind P. (2003). Bax Inhibitor-1 Is Overexpressed in Prostate Cancer and Its Specific Down-Regulation by RNA Interference Leads to Cell Death in Human Prostate Carcinoma Cells. *American Journal of Pathology* **163**: 543-552.

Gueorguieva D, Li S, Walsh N, Mukerji A, Tanha J, and Pandey S. (2006).Identification of single-domain, Bax-specific intrabodies that confer resistance to mammalian cells against oxidative-stress-induced apoptosis. *FASEB J* **20**: E2-E11.

Halliwell B and Gutteridge JMC. (1989).Free Radicals in Biology and Medicine 2nd ed. Clanderdon Press, Oxford, London.

Halliwell B and Gutteridge JM. (1990).Role of free radicals and catalytic metal ions in human disease: an overview. *Methods Enzymol.* 1-85.

Halliwell B. (1992).Reactive oxygen species and the central nervous system. *J. neurochem.* **59**: 1609-1623.

Halestrap AP. (2002).The mitochondrial permeability transition: a pore way to die. *J. Clin. Basic Cardiol.* **5**: 29-41.

Han BH, D'Costa A, Back SA, Parsadanian M, Patel S, Shah AR, Gidday JM, SrinivasanA, Deshmukh M, Holtzman DM. (2000).BDNF blocks caspase-3 activation in neonatal hypoxia-ischemia. *Neurobiol Dis.* **7**: 38–53.

Heng BC, Kemeny DM, Liu H and Cao T. (2005).Potential applications of intracellular antibodies (intrabodies) in stem cell therapeutics. *J. Cell. Mol. Med.* **9**(1): 191-195.

Hengartner MO. (2000).The biochemistry of apoptosis. *Nature* **407**: 770-776.

Hertz C, Vitte P-A, Bombrun A, Rostovtseva TK, Montessuit S, Hiver A, Schwartz MK, Church DJ, Korsmeyer SJ, Martinou JC, and Antonsson B. (2005).Bax Channel Inhibitors Prevent Mitochondrion-mdiated Apoptosis and Protect Neurons in a Model of Global Brain Ischemia. *J Biol Chem* **280**: 42960-42970.

Hsu H, Shu H-B, Pan M-G, and Goeddel DV. (1996). TRADD–TRAF2 and TRADD–FADD Interactions Define Two Distinct TNF Receptor 1 Signal Transduction Pathways. *Cell* **84**: 99-308.

Hsu YT and Youle RJ. (1997).Nonionic detergents induce dimerization among members of the Bcl-2 family. *J. Biol. Chem.* **272**: 13829-13834.

Huh PW, Belayev L, Zhao W, Koch S, Busto R, and Ginsberg MD. (2000).Comparative neuroprotective efficacy of prolonged moderate intraischemic and postischemic hypothermia in focal cerebral ischemia. *J Neurosurg* **92**: 91-99.

Humke EM, Ni J, and Dixit VM. (1998).ERICE, a novel FLICE-activated caspase. *J. Biol. Chem.* **273**: 15702-15707.

Ichas F and Mazat JP. (1998).From calcium signalling to cell death: two conformations for the mitochondrial permeability transition pore. Switching from low-to-high-conductance state. *Biochim. Biophys. Acta.* **1366**: 33-50.

Karibe H, Chen J, Zarow GJ, Graham SH, Weinstein PR. (1994).Delayed induction of mild hypothermia to reduce infarct volume after temporary middle cerebral artery occlusion in rats. *J Neurosurg* **80**: 112-119.

Kerr JFR, Wyllie AH and Currie AR. (1972).Apoptosis: a basic biological phenomenon with wide-ranging implications in tissue kinetics. *Br.J.Cancer* **26**: 239-257.

Kil HY, Zhang J, and Piantadosi CA. (1996). Brain Temperature Alters Hydroxyl Radical Production During Cerebral Ischemia/Reperfusion in Rats. *Journal of Cerebral Blood Flow & Metabolism* **16**: 100-106.

Kontermann RE. (2004).Intrabodies as therapeutic agents. *Methods* **34**: 163-170.

Krieger DW, De Georgia MA, Abou-Chebl A, Andrefsky JC, Sila CA, Katzan IL, Mayberg MR, and Furlan AJ. (2001).Cooling for Acute Ischemic Brain Damage (COOL AID). *Stroke* **32**: 1847-1854.

Kroemer G and Martin SJ. (2005).Caspase-independent cell death. *Nat Med* **11**: 725-730.

Kroemer G, Galluzzi L, and Brenner, C. (2007).Mitochondrial membrane Permealization in Cell Death. *Physiol Rev* **87**: 99-163.

Kuida K, Zheng TS, Na S, Kuan C-Y, Yang D, Karasuyama H, Rakic P, and Flavell RA. (1996).Decreased apoptosis in the brain and premature lethality in CPP32-deficient mice. *Nature* **384**: 368-372.

Kuwana T, Mackey MR, Perkins G, Ellisman MH, Latterich M, Schneiter R, Green DR, and Newmeyer DD. (2002).Bid, Bax, and lipids cooperate to form supramolecular openings in the outer mitochondrial membrane. *Cell* **111**: 331-342

Lancaster JR, Laster SM, and Gooding LR. (1989).Inhibition of target cell mitochondrial electron transfer by tumor necrosis factor. *FEBS Lett.* **248**: 169-174.

Lecerf JM. (2001).Human single-chain Fv intrabodies counteract *in situ* huntingtin aggregation in cellular models of Huntington's disease. *Proc. Natl. Acad. Sci.USA* **98**: 4764-4769.

Lee D, Long SA, Adams JL, Chan G, Vaidya KS, Francis TA, Kikly K, Winkler JD, Sung CM, Debouck C, Richardson S, Levy MA, DeWolf WE, Keller PM, Tomaszek T, Had MS, Ryan MD, Haltiwanger RC, Liang PH, Janson CA, McDevitt PJ, Johanson K, Concha NO, Chan w, Abdel-Meguid SS, Badger AM,

Lark MW, Nadeau DP, Suva LJ, and Gowen M, Nuttall ME. (2000a).Potent and Selective Nonpeptide Inhibitors of Caspase 3 and 7 Inhibit Apoptosis and Maintain Cell Functionality. *J. Biol. Chem.* **275**: 16007-16014.

Lee JM, Zipfel GJ and Choi DW. (2000b).The challenging landscape of ischaemic brain injury mechanisms. *Nature* **399**: A7-A14.

Li F, Srinivasan A, Wang Y, Armstrong RC, Tomaselli KJ, and Fritz LC. (1997). Cell-specific induction of apoptosis by microinjection of cytochrome c. *J. Biol. Chem.* **272**: 30299-30305.

Li LY, Luo X, and Wang X. (2001).Endonuclease G is an apoptotic DNase when released from mitochondria. *Nature* **412**: 95-99.

Li N, Ragheb K, Lawler G, Sturgis J, Rajwa B, Melendez JA and Robinson JP. (2003).Mitochondrial complex-I inhibitor rotenone induces apoptosis through enhancing mitochondrial reactive oxygen species production. *J Biol.Chem* **278**: 8516-8525.

Lin MT and Beal MF. (2006).Mitochondrial dysfunction and oxidative stress in neurodegenerative diseases. *Nature* **443**: 787-795.

Linnuk MD, Zobrist RH, and Hartfield MD. (1993).Evidence supporting a role for programmed cell death in focal cerebral ischemia in rats. *Stroke* **24**: 2002-2009.

Maher J and Hachinski V. (1993).Hypothermia as a potential treatment for cerebral ischemia. *Cerebrovasc Brain Metab Rev* **5**: 277–300.

Manabat C, Han BH, Wendland M, Derugin N, Fox CK, Choi J, Holtzman DM, Ferriero DM, and Vexler ZS. (2000).Reperfusion Differentially Induces Caspase-3 Activation in Ischemic Core and Penumbra After Stroke in Immature Brain. *Stroke* **34**: 207-213.

Margaill I, Plotkine M, and Leroet D. (2005).Antioxidant strategies in the treatment of stroke. *Free Radical Biology & Medicine* **39**: 429-443.

Martin SJ and Green DR. (1996).Protease Activation during Apoptosis: Death by a Thousand Cuts? *Cell* **82**: 349-352.

McCarthy, S., Somayajulu, M., Sikorska, M., Borowy-Borowski, H., Pandey, S. (2004).Paraquat Induces Oxidative Stress and Neuronal Cell Death: Neuroprotection by Water Soluble Coenzyme Q_{10}. *Toxicol Appl Pharmacol.* **201**: 21-31.

Meldrum B. (1985).Possible therapeutic applications of antagonists of excitatory amino acid neurotransmitters. *Clin Sci.* **68**: 113-122.

Metivier D, Dallaporta B, Zamzani N, Larochette N, Susin SA, Marzo I, Kroemer G. (1998).Cytofluorometric detection of mitochondrial alterations in early CD95/Fas/APO-1-triggered apoptosis of Jurkat T lymphoma cells. Comparison of seven mitochondrion-specifice fluorochromes. *Immunol Lett* **61**: 157-163.

Mhashilkar AM. (2002).Intrabody-mediated phenotypic knockout of major histocompatibility complex class I expression in human and monkey cell lines and in primary human keratinocytes. *Gene Ther.* **9**: 307-319.

Miller TW and Messer A. (2005).Intrabody Applications in Neurological Disorder: Progress and Future Prospects. *Molecular Therapy* **12**: 394-401.

Mittl PRE, Di Marco S, Krebs JF, Bai X, Karanewsky DS, Preiestle JP, Tomaselli KJ, and Grutter MG. (1997).Structure of Recombinant Human CPP32 in Complex with the Tetrapeptide Acetyl-Asp-Val-Ala-Asp Fluoromethyl Ketone. *J. Biol. Chem.* **272**: 6539-6547.

Moore RS, Wielgosz AT, Johansen HL and Taylor GW. (1993). The cost of cardiovascular diseases in Canada. L. C. f. D. C. Internal document. Ottawa: Health Canada, 1998.

Moro MA, Almeida A, Bolaños JP, Lizasoain I. (2005).Mitochondrial respiratory chain and free radical generation in stroke. *Free Radical Biology & Medicine* **39**: 1291-1304.

Muchmore SW, Sattler M, Liang H, Meadows RP, Harlan JE, Yoon HS, Nettesheim D, Chang BS, Thompson CB, Wong SL. (1996).X-ray and NMR structure of Bcl-x_L, an inhibitor of programmed cell death. *Nature* **381**: 335-341.

Naderi J, Somayajulu-Nitu M, Mukerji A, Sharda P, Sikorska M, Borowy-Borowski H, Antonsson B, and Pandey S. (2006).Water-soluble Coenzyme Q10 inhibits Bax-induced destabilization of mitochondria in mammalian cells. *Apoptosis* **11**: 1359-1369.

Narita M, Shimizu S, Ito T, Chittenden T, Lutz RJ, Matsuda H and Tsujimoto Y. (1998).Bax interacts with the permeability transition pore to induce permeability

transition and cytochrome c release in isolated mitochondria. *PNAS* **95**: 14681-14686.

Nechushtan A, Smith CK, Hsu YT, and Youle RJ. (1999).Conformation of the Bac C-terminus regulates subcellular location and cell death. *EMBO J.* **18**: 2330-2341.

Newmeyer DD and Ferguson-Miller S.(2003).Mitochondria: releasing power for life and unleashing the machineries of death. *Cell* **112**: 481-490.

Nicholson DW and Thornberry NA. (1997).Caspases: Killer Proteases. *Trends Biochem Sci.* **22**: 299-306.

Oltavai ZN, Millman CL, and Korsmeyer SJ. (1993).Bcl-2 Heterodimerizes In Vivo with a Conserved Homolog, Bax, That Accelerates Programmed Cell Death. *Cell* **74**: 609-619.

Oltersdorf, T, Elmore SW, Shoemaker AR, Armstrong RC, Augeri DJ, Belli BA, Bruncko M, Deckwerth TL, Dinges J, Hajduk PJ, Joseph MK, Kitada S, Korsmeyer SJ, Kunzer AR, Letai A, Li C, Mitten MJ, Nettesheim DG, Ng S, Nimmer PM, O'Connor JM, Oleksijew A, Petros AM, Reed JC, Shen W, Tahir SK, Thompson CB, Tomaselli KJ, Wang B, Wendt MD, Zhang H, Fesik SW, Rosenberg SH. (2005).An inhibitor of Bcl-2 family proteins induces regression of solid tumours. *Nature* **435**: 677-681.

Padlan EA. (1994).Anatomy of the Antibody Molecule. *Mol. Immunol.* **31**: 169-217.

Papa S and Skulachev VP. (1997).Reactive oxygen species, mitochondria, apoptotis and aging. *Mol Cell. Chem.* **174**: 305-319.

Persengiev SP, Zhu X, and Green MR. (2004). Nonspecific, concentration-dependent stimulation and repression of mammalian gene expression by small interfering RNAs (siRNAs). *RNA* **10**: 12-18.

Pinkus R, Weiner lm, and Daniel V. (1996).Role of oxidants and antioxidants in the induction of AP-1, NF-κB, and glutathione S-transferase gene expression. *J. Biol. Chem.* **271**: 13422-12429.

Pollack M and Leeuwenburgh C. (2001).Apoptosis and Aging: Role of the Mitochondrial. *Journal of Gerontology* **11**: 475-482.

Porter AG and Janicke RU. (1999).Emerging roles of caspase-3 in apoptosis. *Cell Death and Differentiation* **6**: 99-104.

Precht TA, Phelps RA, Linseman DA Butts BD, Le SS, Laessig TA, Bouchard RJ, and Heidenrech KA. (2005).The permeability transition pore triggers Bax translocation to mitochondria during neuronal apoptosis. *Cell Death Differ* **12**: 255-265.

Reed DJ. (1990).Glutathione: toxological implications. *Annu. Rev. Pharmacol. Toxicol.* **30**: 603-631.

Reed JC. (1997).Cytochrome *c*: Can't live with it – can't live without it. *Cell* **91**: 559-562.

Rothman SM and Olney JW. (1986).Glutamate and the pathophysiology of hypoxic-ischemic brain damage. *Ann. Neurol.* **19**: 105-111.

Salvesen GS and Dixit VM. (1999).Caspase activation: The induced-proximity model. *Proc. Natl. Acad. Sci* **96**: 10964-10967.

Scaller B, Graf R, and Jacobs AH. (2003).Ischemic tolerance: a window to endogenous neuroprotection? *Lancet* **362**: 1007-1088.

Schaller B. (2004).Introduction to serial reviews on free radicals and stroke. *Free Radical Biology & Medicine* **38**: 409-410.

Schreiber SL. (1998).Chemical genetics resulting from a passion for synthetic organic chemistry. *Bioorg. Med. Chem.* **6**: 1127-1152.

Scorrano L, Ashiya M, Buttle K, Weiler S, Oakes SA, Mannella CA, and Korsmeyer SJ. (2002).A distinct pathway remodels mitochondrial cristae and mobilizes cytochrome *c* during apoptosis. *Dev. Cell* **2**: 55-67.

Shimin H, Snipas SJ, Vincenz C, Salvesen G, and Dixit VM. (1998).Caspase-14 Is a Novel Developmentally Regulated Protease. *J. Biol. Chem.* **273**: 29648-29653.

Shimizu S, Matsuka Y, Shinohara Y, Yoneda Y, and Tsujimoto Y. (2001).Essential role of voltage-dependent anion channel in various forms of apoptosis in mammalian cells. *J Cell Biol* **152**: 237-250.

Shoji Y, Uedono Y, Ishikura H, Takeyama N, and Tanaka T. (1995).DNA damage induced by tumour necrosis factor-alpha in L929 cells is mediated by mitochondrial oxygen radical formation. *Immunology* **84**: 543-548.

Shulze-Osthoff K, Bakker AC, Vanhaesebroeck B, Beyaert R, Jacob WA, and Fiers W. (1992).Cytotoxic activity of tumour necrosis factor is mediated by early damage of mitochondrial functions.   Evidence for the involvement of mitochondrial radical generation. *J. Biol. Chem.* **267**: 5317-5323.

Sidoti-de Fraisse C, Rincheval V, Risler Y, Mignotte B, and Vayssière JL. (1998).TNF-α activates at least two apoptotic signaling cascades. *Oncogene* **17**: 1639-1651.

Sies H. (1991). Oxidative stress: from basic research to clinical application. *Am. J. Med.* **91**: 31S-38S.

Stavrovskaya IG and Kristal BS. (2004).The powerhouse takes control of the cell: Is the mitochondrial permeability transition a viable therapeutic target against neuronal dysfunction and death? *Free Radical Biology & medicine* **38**: 687-697.

Strasser A, O'Connor L, Dixit VM. (2000).Apoptosis Signaling. *Annu. Rev. Biochem.* **69**: 217-245.

Susin, SA, Lorenzo HK, Zamzani N, Marzo I, Snow BE, Brothers GM, Mangion J, Jactot E, Costantini P, Loeffler M, Larochette N, Goodlett DR, Aebersold R, Siderovski DP, Peninger JM, and Kroemer G. (1999).Molecular characterization of mitochondrial apoptosis-inducing factor. *Nature* **397**: 441-446.

Suzuki M, Youle R and Tjandra N (2000).Structure of Bax: Coregulation of dimer formation and intracellular localization. *Cell* **103**: 645-654.

Tahna J, Dubuc GJ, Hirama T, Narang SA, and MacKenzie CR. (2002).Selection by Phage Display of llama Conventional V$_H$ Fragments with Heavy Chain Antibody V$_H$H Properties. *J Immunol. Methods.* **263**: 97-109.

Tanha J, Muruganandam A and Stanimirovic D. (2003).Phage display technology for identifying specific antigens on brain endothelial cells. *Methods in molecular medicine* **89**: 435-439.

Tsujimoto Y, and Shimizu S. (2000).VDAC regulation by the Bcl-2 family of proteins. *Cell Death Differ* **7**: 1174-1181.

Turrens JF, Alexandre A, and Lehinger AL.(1985).Ubisemiquinone is the electron donor for superoxide formation by complex III of heart mitochondria. *Arch. Biochem. Biophys.* **237**: 408-414.

Van de Craen M, Vandanbeele P, Declereq W, Van den Brande I, Van Loo G, Molemans F, Schotte P, Van Criekinge W, Beyaert R, and Fiers W. (1997).Characterization of seven murine caspase family members. *FEBS Lett.* **403**: 61-69.

Varadhachary AS, Edidin M, Hanlon AM, Peter ME, Krammer PH, and Salgame P.(2001).Phosphatidylinositol 3*-Kinase Blocks CD95 Aggregation and Caspase-8 Cleavage at the Death-Inducing Signaling Complex by Modulating Lateral Diffusion of CD951. *The Journal of Immunology* **166**: 6564-6569.

Vila M, Jackson-Lewis V, Vukosavic S, Djaldetti R, Liberatore G, Offen D, Korsmeyer SJ, and Przedborski S. (2000).Bax ablation prevents dopaminergic neurodegeneration in the 1-methyl-4-phenyl-1,2,3,6-tetrahydropyridine mouse model of Parkinson's disease. *Proc Natl Acad Sci* **98**: 2837–2842.

Walker NPC, Talanian RV, Brady KD, Dang LC, Bump NJ, Ferenz CR, Franklin S, Ghayur T, Hackett MC, Hammil LD, Herzog L, Hugunin M, Houy W, Mankovich JA, McGuiness L, Oriewicz E, Paskind M, Pratt CA, Reis P, Summani A, Terranova M, Welch JP, Xiong L, Moller A, Tracey DE, Kamen R, and Wong WW. (1994).Crystal structure of the cysteine protease interleukin-1β-converting enzyme: A (p20/p10)₂ homodimer. *Cell* **78**: 343–352.

Wang J-L, Liu D, Zhang Z-J, han S, Han X, Srinivasula SM, Crose CM, Alnemri ES, and Huang Z. (2000).Structure-based discovery of an organic compound that binds Bcl-2 protein and induces apoptosis of tumor cells. *Proc. Natl. Acad. Sci.* **97**: 7124-7129.

Weaver JG, Tarze A, Moffat TC, Lebras M, Deniaud A, Brenner C, Bren GD, Morin MY, Phenix BN, Doug L, Jiang SX, Sim VL, Zurakowski B, Lallier J, Hardin H, Wettstein P, van Heeswijk RP, Douen A, Kroemer RT, Hou ST, Bennett SA, Lynch DH, Kroemer G, and Badley AD. (2005).Inhibition of adenine nucleotide translocator pore function and protection against apoptosis in vivo by an HIV protease inhibitor. *J Clin Invest* **115**: 1828-1838.

Wei MC, Zong WX, Cheng EH, Lindsten T, Panoutsakopoulou V, Ross AJ, Roth KA, MacGregor GR, Thompson CB, and Korsmeyer SJ. (2001).Proapoptotic BAX and BAK: a requisite gateway to mitochondrial dysfunction and death. *Science* **292**: 727-730.

Weil M, Jacobson M, Coles H, Davies T, Gardner R, Raff K, and Raff M. (1996).Constitutive expression of the machinery for programmed cell death. *J. Cell Biol.* **133**: 1053-1059.

Wellington CL, Ellerby LM, Hackam AS, Margolis RL, Trifiro MA, Singaraja R, McCtcheon K, Salvesen GS, Propp SS, Bromm M, Rowland KJ, Zhang T, Rasper D, Roy S, Thornberry N, Pinsky L, Kakizuka A, Ross CA, Nicholson DW, Bredesen DE, and Hayden MR. (1998).Caspase Cleavage of Gene Products Associated with Triplet Expansion Disorders Generates Truncated Fragments Containing the Polyglutamine Tract. *J. Biol. Chem.* **273**: 9158-9167.

Wigdal S, Kirkland R, Franklin J, and Haak-Frendscho M. (2002).Cytochrome *c* release precedes mitochondrial membrane potential loss in cerebellar granule neuron apoptosis: lack of mitochondrial swelling. *J Neurochem* **82**: 1029-1038.

Wilson KP, Black JF, Thomson JA, Kim EE, Griffith JP, Navia MA, Murko MA, Chambers SP, Aldape RA, Raybuck SA, and Livingston DJ. (1994).Structure and mechanism of interleukin-1_β converting enzyme. *Nature* **370**: 270-275.

Wolf BB and Green DR. (1999).Suicidal Tendencies: Apoptotic Cell Death by Caspase Family Proteinases. *J. Biol. Chem.* **274**: 20049-20052.

Wolozin B, Iwasaki K, Vito P, Ganjei JK, Lacan E, Sunderland T, Zhao B, Kusiak JW, Wasco W, and D'Adamio L. (1996).Participation of Presenilin 2 in Apoptosis: Enhanced Basal Activity Conferred by an Alzheimer Mutation. *Science* **274**: 1710-1713.

Wolter KG, Hsu YT, Smith CL, Nechushtan A, Xi XG, and Youle RJ. (1997).Movement of Bax from the cytosol to mitochondria during apoptosis. *J Cell Biol* **139**: 1281-1292.

Woo M, Hakem R, Soengas MS, Duncan GS, Shahinian A, Kagi D, Hakem A, McCurrach M, Khoo W, Kaufman SA, Senaldi G, Howard T, Lowe SW, and Mak TW. (1998).Essential contribution of caspase-3/CPP32 to apoptosis and its associated nuclear changes. *Genes Dev.* **12**: 806-819.

Xin M and Deng X. (2006).Protein phosphatise 2A enhances Bax's proapoptotic function through dephosphorylation. *J. Biol. Chem.* **281**: 18859-18867.

Yin XM, Oltavai ZN, and Korsmeyer SJ. (1994).BH1 and BH2 domains of Bcl-2 are required for inhibition of apoptosis and heterodimerization with Bax. *Nature* **369**: 321-323.

Young K. (1998).Identification of a calcium channel modulator using a high throughput yeast two-hybrid screen. *Nature Biotechnol.* **16**: 946-950.

Yuan J and Yankner BA. (2000).Apoptosis in the nervous system. *Nature* **407**: 802-809.

Zamzani N and Kroemer G. (2001).The mitochondrion in apoptosis: how Pandora's box opens. *Nat. Rev. Mol. Cell. Biol.* **2**: 67-71.

Zha H, Aime-Sempe C, Sato T and Reed JC. (1995).Proapoptotic protein Bax heterodimerizes with Bcl-2 and homodimerizes with Bax via a novel domain (BH3) distinct from BH1 and BH2. *The Journal of Biological Chemistry* **271**: 7440-7444.

Zhu Q, Zeng C, Huhalov A, Yao J, Turi TG, Danley D, Hynes T, Cong Y, DiMattia D, Kennedy S, Daumy G, Schaeffer E, Marasco WA, and Huston JS. (1999).Extended half-life and elevated steady-state level of a single-chain Fv intrabody are critical for specific intracellular retargeting of its antigen, caspase-7. *J Immunol. Methods* **231**: 207-222.

Name: Katrina McGonigal

Place of Birth: Edmonton, Alberta

Year of Birth: 1983

Education: St. Anne Catholic High School, Tecumseh, ON

         1997-2002

         University of Windsor, Windsor, ON

         2002-2006 B.Sc.

         University of Windsor, Windsor, ON

         2006-2008 M.Sc.

Published Research Article:

Katrina McGonigal, Jamshid Tanha, Elitza Palazov, Shenghua Li, Deyzi Gueorgeiva, and Siyaram Pandey.Isolation and functional characterization of single domain antibody modulators of Caspase-3 and apoptosis. *Applied Biochemistry and Biotechnology*, 2008.

Published Abstract:

Katrina McGonigal, Jamshid Tanha, Elitza Palazov, Shenghua Li, Deyzi Gueorguieva, and Siyaram Pandey. Apoptosis 2008: From mechanisms to applications, January 2008.

Conference Presentation:

McGonigal, K., Gueorguieva, D., Tanha, J., Pandey, S. 34th Annual Southern Ontario Undergraduate Student Chemistry Conference, March 18th, 2006, York University, North York, Ontario

Poster Presentations:

Katrina McGonigal, Jamshid Tanha, Elitza Palazov, Shenghua Li, Deyzi Gueorgeiva, and Siyaram Pandey. Apoptosis 2008: From mechanisms to applications, January 23rd to 26th 2008, European Conference Center, Luxembourg-Kirchberg.

Gueorguieva, D., Walsh, N., McGonigal, K., Kis, O., Pandey, S., Tanha, J. University of Windsor Health Fair, November 2005.

Honors Thesis:

McGonigal, K. (2006). Identification and Characterization of Single Domain Antibodies against the Pro-apoptotic Protein Caspase 3 in Prevention of Neurodegenerative Disease. University of Windsor.